Use of South African Spent Pulping Liquor to Synthesise Lignin Phenol Formaldehyde Resins

by

Priyashnie Govender

Thesis presented in partial fulfilment
of the requirements for the Degree

of

MASTER OF ENGINEERING
(CHEMICAL ENGINEERING)

in the Faculty of Engineering
at Stellenbosch University

Supervisor
Prof Johann Görgens

Co-Supervisor
Dr Luvuyo Tyhoda

March 2020

Declaration

By submitting this thesis electronically, I declare that the entirety of the work contained therein is my own, original work, that I am the sole author thereof (save to the extent explicitly otherwise stated), that reproduction and publication thereof by Stellenbosch University will not infringe any third party rights and that I have not previously in its entirety or in part submitted it for obtaining any qualification.

Date: *March 2020*

Plagiarism Declaration

1. Plagiarism is the use of ideas, material and other intellectual property of another's work and to present is as my own.

2. I agree that plagiarism is a punishable offence because it constitutes theft.

3. I also understand that direct translations are plagiarism.

4. Accordingly all quotations and contributions from any source whatsoever (including the internet) have been cited fully. I understand that the reproduction of text without quotation marks (even when the source is cited) is plagiarism.

5. I declare that the work contained in this assignment, except where otherwise stated, is my original work and that I have not previously (in its entirety or in part) submitted it for grading in this module/assignment or another module/assignment.

Initials and surname: *P. Govender*

Date: *March 2020*

Abstract

The probable scarcity of petroleum-based products, the resultant price fluctuations, and environmental concerns have driven the need for a total or partial phenol replacement in phenol-based products. Lignin, a biopolymer found in plant biomass, has great potential as a phenol substitute due to its phenolic structure, abundance as a by-product of the paper and pulp industry, and relatively lower cost and toxicity compared to phenol. However, despite its benefits and availability, lignin is rarely exploited for higher-value applications, largely due to its structural complexity and resultant low reactivity. This study aims to investigate the potential of using lignin derived from South African spent pulping liquor as a phenol substitute in phenol formaldehyde resins (PFRs). Six South African pulping-based lignins were investigated. They were characterized in terms of structural, compositional and thermal properties. Thereafter, they were used to synthesize lignin-phenol formaldehyde resins at 100% phenol substitution, labelled as LPF100 resins. These resins were characterized according to structural, curing and shear bonding strength properties. Direct use (unmodified) of the LPF100 resins as adhesives was labelled as R_0 LPF100 adhesives. To improve the shear strength properties of the unmodified LPF100 adhesives, the LPF100 resins were modified via the addition of a crosslinker (hexamine) as well as the hardener glyoxal (R_1) or the hardener epichlorohydrin (R_2). They were labelled as R_1 LPF100 and R_2 LPF100 adhesives, respectively. The objective of this study was to investigate/determine the extent to which various South African pulping lignins were suitable for replacement of phenol in PFRs for use in the wood industry, specifically plywood boards. The LPF100 resins produced in this study are not expected to fulfil commercial requirements. Instead the intent is to determine the potential of these South African pulping lignins, and show that further research is needed to elevate it to a viable level. Ultimately, from the modified LPF100 adhesives, the best performing were the R_1 KF2-P-N LPF100 adhesive and the R_2 SL-E-T LPF200 adhesive, both recording 1.4 MPa of shear strength, thus exceeding the GB/T 17657-2013 plywood standard of $\geq$0.7 MPa. The curing temperature of these two resins are 71°C and 126°C, respectively. Thus, considering both curing and bonding properties, KF2-P-N lignin is a more promising phenol substitute. However, the S-SCB-S resin was a consistent performer, even recording the highest shear strength from the unmodified adhesives (0.5 MPa). Additionally, the S-SCB-S resin had the highest curing rate from all resins samples, and the lowest curing temperature of 68°C. Thus, both the KF2-P-N (pine kraft) and S-SCB-S (bagasse soda) lignins show great potential as a phenol substitute in phenol formaldehyde resins.

Opsomming

Die waarskynlike skaarsheid van petroleum-gebaseerde produkte, die resultante prysfluktuasies, en omgewingskommer, het die nood vir ’n totaal of gedeeltelike fenolvervanging in fenol-gebaseerde produkte gedryf. Lignien, ’n biopolimeer gevind in plantbiomassa, het groot potensiaal as ’n fenolplaasvervanger as gevolg van sy fenoliese struktuur, oorvloed as ’n byproduk van die papier-en-pulp-industrie, en relatiewe lae koste en toksisiteit in vergelyking met fenol. Maar ongeag sy voordele en beskikbaarheid, word lignien selde ontgin vir hoër-waarde toepassings, grootliks as gevolg van sy strukturele kompleksiteit en resulterende lae reaktiwiteit. Hierdie studie beoog om die potensiaal vir die gebruik van lignien, verkry uit Suid-Afrikaanse gebruikte pulploog, as ’n fenolplaasvervanger in fenolformaldehiedharpuis, te ondersoek. Ses Suid-Afrikaanse pulp-gebaseerde ligniene is ondersoek. Hulle is gekarakteriseer in terme van strukturele, komposisionele en termiese eienskappe. Daarna is hulle gebruik om lignien-fenolformaldehiedharpuis te sintetiseer by 100% fenolvervanging, gemerk as LPF100-harpuis. Hierdie harpuis is gekarakteriseer na aanleiding van strukturele, droging- en skuifverbindingkrageienskappe. Direkte gebruik (onveranderd) van die LPF100-harpuis as kleefstof is gemerk as R0 LPF100-kleefstowwe. Om die skuifkrageienskappe van die onveranderde LPF100-kleefstowwe te verbeter, is die LPF100-harpuis ongemodifiseer via die toevoeging van ’n kruisskakel (heksamien) sowel as die verharder glioksaal (R1) of die verharder epichloorhedrien (R2). Hulle is gemerk as R1 LPF100- en R2 LPF 100-kleefstowwe, onderskeidelik. Die doelwit van hierdie studie was om die omvang te ondersoek/bepaal waartoe Suid-Afrikaanse pulpligniene gepas is vir vervanging van fenol in fenolformaldehiedharpuis vir die gebruik in die houtindustrie, spesifiek vir saamgeperste planke. Daar word nie verwag dat die LPF100-harpuis geproduseer in hierdie studie aan kommersiële vereistes gaan voldoen nie. Die doel is eerder om die potensiaal van hierdie Suid-Afrikaanse pulpligniene te bepaal, en te wys dat verdere navorsing nodig is om dit tot ’n lewensvatbare vlak op te hef. Eindelik, uit die veranderde LPF100-kleefstowwe, was die wat die beste gedoen het die R1 KF2-P-N LPF100-kleefstof en die R2 SL-E-T LPF200-kleefstof, waar beide 1.4 MPa van skuifkrag opgeteken het, en dus die GB/T 17657-2013-saamgeperste plank standaard van >0.7 MPa oorskry. Die drogingtemperatuur van hierdie twee harpuis is 71 °C en 126 °C, onderskeidelik. Dus, as albei droging- en verbindingeienskappe oorweeg word, is KF2-P-N-lignien ’n meer belowende fenolvervanger. Die S-SCB-S-harpuis was ’n konstante presteerder, wat selfs die hoogste skuifkrag van die onveranderde kleefstowwe (0.5 MPa) aangeteken het. Daarby, het die S-SCB-S-harpuis die hoogste droogtempo van al die harpuissteekproewe gehad, en die laagste droogtemperatuur van 68 °C. Dus, beide die KF2-P-N (dennekraft) en S-SCB-S (bagasse soda)-ligniene het groot potensiaal as ’n fenolvervanger in fenolformaldehiedharpuise aangetoon.

Acknowledgments

This research was financially sponsored by the Paper Making Association of South Africa (PAMSA) in conjunction with Sappi Ltd as an industry partner. The opinions, findings, conclusions and recommendations made are that of the author and not necessarily attributed to the sponsors.

The author would like to acknowledge the input and assistance of the following people for their contribution to this piece of work:

- Prof. Görgens for the opportunity to do this study, and the guidance and feedback for this study.
- Dr Tyhoda (Department of Forestry and Wood Sciences) for the guidance and feedback for this study.
- The abovementioned sponsors for the opportunity to pursue a Masters' degree at Stellenbosch University.
- Sanet Minaar and Nelson Sefara (Sappi Technology Centre) for their support and assistance during this study.
- Dr Alawode (formerly of the Department of Forestry and Wood Sciences) for his invaluable input and assistance during the experimental phase of this study.
- Dr Iraola-Arregui (formerly of the Department of Process Engineering) for her invaluable input and assistance during the experimental phase of this study.
- Mr Soloman and Mr Hendrikse (Department of Forestry and Wood Sciences) for their assistance.
- Mr Petersen and the rest of the technical staff at the Department of Process Engineering for their assistance.
- Staff of the Chemical Sciences and Biorefinery departments at the Sappi Technology Centre for their assistance during the experimental phase of this study.
- My family and friends for their support and belief in me.
- And last, but not least, my parents and sister for their continued support and love, and being a pillar of strength to me.

List of Abbreviations

DSC	Differential scanning calorimetry
FTIR	Fourier transform infrared
GPC	Gel permeation chromatography
HCHO	Formaldehyde
KF2-P-N	Pine kraft lignin
KF3-E-N	Eucalyptus kraft lignin
LPF	Lignin phenol formaldehyde
LPFR	Lignin phenol formaldehyde resin
MDF	Middle density fibreboard
MF	Melamine formaldehyde
M_N	Number average molecular weight
M_W	Weighted average molecular weight
NMR	Nuclear magnetic resonance
NSSC	Neutral sulphite semi-chemical
OSB	Orientated strand board
PAMSA	Paper Manufacturers Association of South Africa
PCA	Principal component analysis
PF	Phenol formaldehyde
PFR	Phenol formaldehyde resin
PI	Polydispersity index
pMDI	Polymeric diphenylmethane diisocyanate
PVA	Polyvinyl acetate
SCB	Sugarcane bagasse
SE-SCB	Sugarcane bagasse steam explosion lignin
SL-E-T	Eucalyptus (Sappi) sodium lignosulphonate

SL-M-PR	Mixed origin (MPact) sodium lignosulphonate
S-SCB-S	Sugarcane bagasse soda lignin
TGA	Thermogravimetric analysis
UF	Urea formaldehyde

Table of Contents

List of Figures

List of Tables

Chapter 1: Introduction

1.1. Background of Investigation

Phenol formaldehyde (PF) resins are commonly used as wood adhesives in wood construction and in the production of wood composites. This is because they exhibit excellent resistance properties and are known to produce high bonding strengths (Ferdosian, et al., 2017). However, there are problems associated with the use of PF resins, the most significant of which is that phenol is derived from petrochemicals such as benzene and propylene. As a result, the cost of phenol is heavily influenced by the cost of crude oil (Gravitis, et al., 2010), which itself is subject to dwindling reserves and price fluctuations (Alonso, et al., 2005; Yang, et al., 2014). These factors, coupled with growing environmental concerns over the impact of fossil fuels (Effendi, et al., 2008), have driven the need for a total or partial phenol replacement in phenol-based products.

Lignin, a biopolymer found in plant biomass, has great potential as a phenol substitute due to its phenolic structure, thermoplastic nature, and abundance as a by-product of the paper and pulp industry. It also has high resistance to water and biodegradation, and is relatively cheaper and less toxic than phenol (Hu, et al., 2011; Siddiqui, 2013). However, despite its benefits and availability, lignin is rarely exploited for higher-value applications. Instead, it is largely used as fuel for paper and pulp mills, and commercial applications of lignin is limited to additives and fillers, albeit to a smaller extent (Laurichesse & Avérous, 2014). This underutilization of lignin is largely attributed to its structural complexity and resultant low reactivity (Hu, et al., 2011), which is further aggravated by its structural diversity according to biomass origin, separation and fragmentation processes (Laurichesse & Avérous, 2014). Thus, partial incorporation of lignin into a resin system usually results in decreased reactive functionalities within the polymeric structure (Podschun, et al., 2015). As a result, most research has found that only lignin substitution up to 50% is capable of producing good bonding strengths, although other important resin properties like curing and dimensional stability remain problematic (Effendi, et al., 2008).To address these issues, a number of modification methods have been developed to enhance lignin's chemical reactivity, as well as increase its solubility in organic solvents, improve its processability, and reduce its brittleness as lignin-based polymers (Laurichesse & Avérous, 2014). However, these methods have not yet reached commercialization, primarily due to low viability and ineffectiveness across different lignin feedstocks (Hu, et al., 2011). Nonetheless, gradual progress in this field of research, ongoing environmental concerns, and the probable scarcity of petrochemicals has sustained the interest in developing economically feasible lignin valorization processes, particularly with regards to production of bio-based polymers (Effendi, et al., 2008; Laurichesse & Avérous, 2014; Yang, et al., 2014).

1.2. Context of Study

Efforts by key organizations and industry partners has positioned the South African paper and pulp industry as a sector that is aware and conscientious of its role in the economy, in society, and in the environment. The South African paper and pulp industry contributes R28 billion value-add to the economy per year, adding R7.3 billion to the country's balance of trade in 2018. The sector also develops the remote rural communities in which plantations and pulp mills are operated, with the forestry-pulp-paper-recycling value chain employing over 157 000 people as of 2018 (PAMSA, 2018; PAMSA, 2019). In terms of sustainability, environmental stewardship is a priority in the paper and pulp industry, with organizations like the Paper Manufacturers Association of South Africa (PAMSA) engaging in various practices to respond to climate change, and efficiently use resources such as water, energy, and fibers (PAMSA, 2019).

Black liquor, or spent pulping liquor, is a term used to describe the waste by-product stream that exits pulping processes. This spent pulping liquor is comprised largely of lignin, spent cooking chemicals, as well as other dissolved wood constituents (Gellerstedt & Henriksson, 2008). Since spent pulping liquor is considered to be renewable and carbon neutral, it is mostly burned as fuel to generate energy for the mills and recover cooking chemicals. This combination of using both fossil fuels and renewable resources to generate energy allows the paper and pulp industry to reduce their reliance and pressure on the national power grid, as well as lower their carbon footprint (PAMSA, 2019). However, conventional pulping mills often experience difficulties at the recovery unit whereby excess black liquor causes a bottleneck at the recovery boilers which ultimately limits pulp production (Siddiqui, 2013; Namane, 2016). In an attempt to remedy the situation, many mills store the excess black liquor in tanks or dams. In addition to environmental concerns, the disadvantages of this is that storage often diminishes the heating value, and resultant utility, of the liquor. Thus, an alternative option would be to divert the excess black liquor from the recovery unit, and potentially find a different but sustainable and viable use for it. One proposed solution could be extraction of the lignin from the liquor. Whilst this lignin could still be used as fuel for energy generation in the mill, the global paper and pulp industry has come to view that as a waste of resource, considering the potential applications of lignin as a biomaterial and biochemical (Namane, 2016). Currently, the only commercial application of lignin derived from South African spent pulping liquor is the sale of lignosulphonates as binders, dispersants and emulsifiers (Sappi Ltd, 2019). However, as discussed previously, there is potential of utilizing lignin for higher-end applications. Recent years have seen the South African paper and pulp industry become more interested in lignin derived from spent pulping liquor, particularly as a phenol substitute in phenol-formaldehyde resins and polyurethanes.

As a result, this project was commissioned to investigate the potential of using lignin derived from South African spent pulping liquor as a phenol substitute in phenol formaldehyde resins.

The overall aim was to develop lignin-phenol formaldehyde (LPF) resins at 100% phenol substitution and subsequently investigate the impact of total phenol replacement by lignin on adhesive properties, particularly curing properties and bonding strength. This was done using locally available lignins from various pulping processes (soda, kraft, NSSC, and steam explosion), with various biomass origins (Eucalyptus, Pine, and Sugarcane Bagasse). These lignins were sourced from the spent pulping liquor of local paper mills, namely those of Sappi Ltd and MPact Ltd (South Africa). The use of lignin derived from South African spent liquor is an important factor since, to the best of our knowledge, no study in recent times have made use of pulping lignins from the South African paper and pulp industry.

1.3. Thesis Layout

This thesis is structured as follows:

Chapter 1 provides an introduction to the study, giving a background on the concepts explored and the context in which this project was started.

Chapter 2 reviews literature on the topics of lignin and adhesives in the wood industry, after which the focus is shifted to phenol-formaldehyde resins and lignin-phenol-formaldehyde resins. This chapter concludes with a brief analysis of the gaps in literature, and a list of project objectives.

Chapter 3 presents results on the characterization of the various lignin samples, focusing on the various compositional, structural and thermal analyses that were conducted.

Chapter 4 describes the synthesis of resins using the various lignins as a feedstock. Results on resin characterisation are also presented, with a particular focus on curing behaviour and shear bonding strength.

Chapter 5 contains general conclusions based on the previous chapters, and recommendations for future work are also provided.

Chapter 2: Literature Review

2.1. Lignin

Lignin is a complex, irregular biopolymer. It is one of three main organic polymers found in lignocellulosic biomass; the other two being cellulose and hemicellulose (Hu, et al., 2011). With the exception of cellulose, lignin is the most abundant biopolymer on earth, with an estimated bio-production of 20 billion tonnes per year (Matsushita, 2015).

The primary function of lignin in plants is to provide biomechanical support, specifically by stiffening and fortifying the secondary cell walls within the vascular and support tissues (Martone, et al., 2009). The lignin polymers, mixed with hemicelluloses, create a dense matrix that binds the cellulose microfibrils, and crosslinks other wall components (Argyropoulos & Menachem, 1997; Martone, et al., 2009). This imparts strength and rigidity to the cells, thereby providing support to the stem, preventing the collapse of conductive vessels, and allowing the plant to grow vertically (Martone, et al., 2009). Lignin also contributes to the hydrophobic nature of the cell walls of vascular tissue, thus aiding in the transport of water and nutrients (Tian, et al., 2016). Furthermore, lignin plays a vital role in seed dispersal and plant defence (Welker, et al., 2015). Lignified cell walls add to the recalcitrance of wood, thereby enabling the plant to resist biodegradation (Argyropoulos & Menachem, 1997) (Haygreen & Bowyer, 2007). It also allows the plant to protect itself against abiotic stresses such as changes in water balance or humidity (Argyropoulos & Menachem, 1997; Welker, et al., 2015).

Lignin's complexity as a polymer arises from the fact that it occurs naturally in various forms (Haygreen & Bowyer, 2007), i.e. its structure, linkages and composition can vary between species, environmental conditions, and even between parts of the same plant (Chen, 2014). Furthermore, its high stability as a compound, and close association to cellulose, makes it difficult to isolate from the rest of the plant biomass (Haygreen & Bowyer, 2007). As a result, various separation methods are employed, all of which alter the structure and properties of native lignin to some degree (Argyropoulos & Menachem, 1997). In fact, lignins isolated from the same plant via different separation methods would have different functional group compositions and different categories of linkages, thus resulting in further structural complexities (Chen, 2014). Due to these challenges, the complete structure and exact composition of native lignin remains uncertain (Haygreen & Bowyer, 2007), however decades of research on the topic has yielded many structural models (Chen, 2014). These models are not intended to be taken as the true standard structure of native lignin, but rather a guideline and example that illustrates the types of structural constituents and linkages in a particular lignin source, as well as the proportions in which they exist (Ozmen, 2000).

Industrially, lignin is predominantly obtained in the paper and pulp sector. A key component in paper production is cellulosic fibres, which are separated from woody biomass via chemical or mechanical methods (Argyropoulos & Menachem, 1997). Processes involved in the liberation of cellulose generate large quantities of liberated/solubilised lignin as a by-product (Gellerstedt & Henriksson, 2008), with an annual lignin production of 40-50 million tonnes (Welker, et al., 2015). However, most of this lignin is burned to generate energy and recover chemicals (Hu, et al., 2011). These lignin by-products, often called technical lignins, are still thermoplastic and polymeric in nature. Thus, there is an opportunity to develop these technical lignins into useful, higher-value products that can be used in adhesives, thermosets, thermoplastics, etc. (Argyropoulos & Menachem, 1997). This is an especially desirable option given the current "green movement" towards more sustainable and renewable chemical products, as well as the added benefit of increasing resource and waste efficiency in the paper and pulp industry. However, challenges with this include the complex structure of native lignin, its reactions and structural changes during delignification and bleaching (Argyropoulos & Menachem, 1997), as well as its low reactivity.

2.1.1. Chemical Structure

Lignin is an amorphous, cross-linked heteropolymer, a fragment of which is shown in Figure 2.1. Its elemental building blocks, called monomers, consists of phenylpropane units that are linked together by various carbon-carbon or carbon-oxygen bonds in a random, non-linear fashion (Chen, 2014).

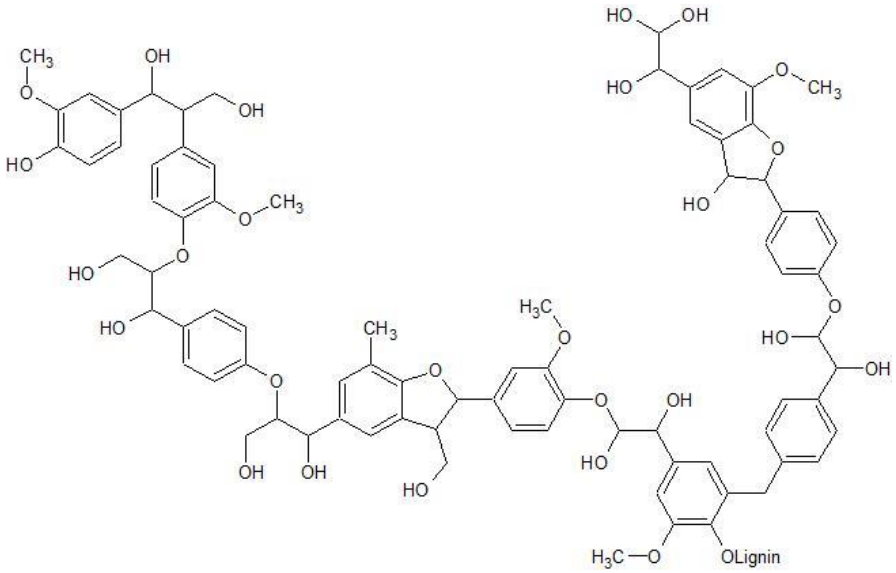

Figure 2.1: Representative fragment of proposed general structure of lignin. Redrawn from Xu, et al (2014).

A basic lignin monomer comprises of a phenol ring with a propane side chain. The principal structural difference that can arise between lignin monomers is the presence or absence of a methoxyl group (-OCH_3) at positions 3' or 3'-5' of the phenol ring. As a result, there are three primary precursors of

lignin, namely p-coumaryl alcohol, coniferyl alcohol, and sinapyl alcohol (Ozmen, 2000). These lignin monomers, also called monolignols, are named after their aromatic moieties, i.e. p-coumaryl alcohol after its p-hydroxyphenyl (H) moiety, coniferyl alcohol after its guaiacyl (G) moiety, and sinapyl alcohol after its syringyl (S) moiety (Pfungen, 2015). As such, they are usually referred to as H, G or S monomers, the likes of which are illustrated in Figure 2.2. If lignin from a particular source is found to contain mostly G monomers, for example, it can then be referred to as guaiacyl or G lignin, and so forth.

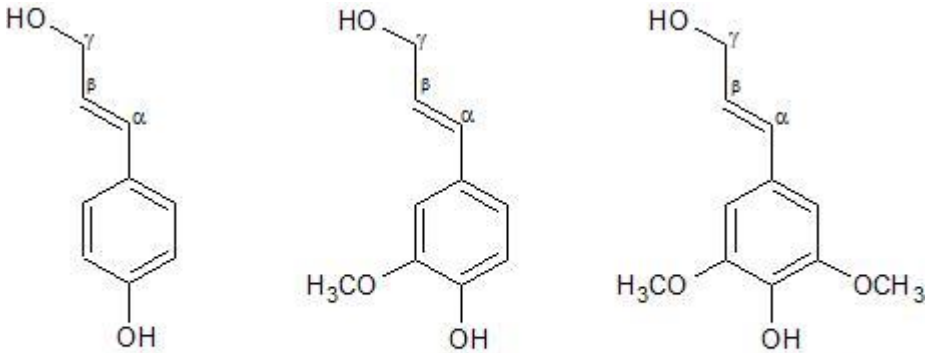

Figure 2.2: Structure of Lignin Monomers. Redrawn from Pfungen (2015).

Lignin monomers are essentially synthesised via the shikimic acid pathway, after which they undergo enzymatically induced radical polymerization to form the lignin macromolecule (Pfungen, 2015). A more detailed explanation of the biosynthesis process will follow on in Section 2.1.3. During polymerization, a variety of ether (C-O-C) and carbon-carbon (C-C) bonds are formed. The most prominent of these linkages include the ether bonds β-O-4, α-O-4, and 4-O-5; and the C-C bonds 5-5, β-5, and β-β (Pfungen, 2015).

2.1.2. Primary Sources and Distribution of Native Lignin

At a cellular level, lignin is found in the various layers of the cell wall, i.e. the primary wall, the secondary wall, and the middle lamella. The secondary wall is further divided into the S_1, S_2, and S_3 layers, with the S_2 layer having the greater wall thickness, and consequently housing 80-90% of the cell wall material. As a result, although the middle lamella possess an extremely high lignin content, it is the S_2 layer of the secondary wall that contains about 70% of the overall lignin in a plant, due to its relatively larger volume (Argyropoulos & Menachem, 1997).

Within the plant kingdom, lignin is predominantly found in vascular plants (tracheophytes), however a recent discovery revealed the presence of minor amounts of syringyl lignin in the intertidal red alga,

Calliarthron cheilosporioides (Martone, et al., 2009). Lignin content varies between plant divisions, plant species, growth stages of a plant, and according to environmental conditions (Welker, et al., 2015; Tian, et al., 2016). Amongst tracheophytes, trees are the most abundant sources of lignin (Ozmen, 2000), with the lignin content of woody plants (lignophytes) in the range of 15-40% (Gellerstedt & Henriksson, 2008). Non-woody plants, specifically grasses (monocotyledonous angiosperms), also have significant lignin contents in the range of 15-20% (Chen, 2014). Sugar cane bagasse (SCB), straw, bamboo, and flax are of particular importance in the grass family (Lora, 2008; Pfungen, 2015). Other herbaceous plants usually have lignin contents that are less than 15% (Gellerstedt & Henriksson, 2008). Important lignophytes include hardwood trees (dicotyledonous angiosperms) and softwood trees (gymnosperms). Temperate softwoods have a lignin content of 15-35%, with tropical and subtropical softwoods not exceeding this range. Temperate hardwoods contain 18-26% lignin, however, hardwoods found in tropical or subtropical climates can boast higher lignin contents, e.g. 43% in *Eucalyptus marginata* or 35% in *Adenanthera intermedia* (Pfungen, 2015).

Monomer distribution can also vary between divisions and species. Softwoods have high proportions of guaiacyl and smaller amounts of p-hydroxyphenyl. Hardwoods contain significant amounts of both guaiacyl and syringyl, with smaller amounts of p-hydroxyphenyl (Pfungen, 2015). Thus, softwoods generally have a higher lignin content, whilst hardwoods have a greater variability in lignin composition (Ozmen, 2000). Grasses typically show an equal distribution between the three lignin monomers (Pfungen, 2015). Based on composition, softwoods can be referred to as G lignins, hardwoods as GS lignins (Ozmen, 2000), and grasses, like most monocotyledons, are GHS lignins (Chen, 2014). A summary of monomer distribution between lignin-rich plants is given in Table 2.1.

Table 2.1: Distribution of H/G/S units in selected plant groups. Adapted from Pfungen (2015).

Division	% H-Monomer (p-Hydroxyphenyl)	% G-Monomer (Guaiacyl)	% S-Monomer (Syringyl)	Reference
Softwoods	5 <5	94 >95	1 None/Trace	(Gellerstedt & Henriksson, 2008; Pfungen, 2015)
Hardwoods	0-8	25-50	45-75	(Gellerstedt & Henriksson, 2008)
Grasses	15-35 5-35	50-70 35-80	15-35 20-55	(Gellerstedt & Henriksson, 2008; Pfungen, 2015)

With regards to bond type, the β-O-4 linkage dominates in softwoods, hardwoods, and grasses (Chen, 2014). This particular ether bond comprises 35-60% and 40-70% of all interunit linkages in softwoods and hardwoods, respectively (Pfungen, 2015). The amount of β-O-4 linkages in grasses is similar to

that of softwood, although it should be noted that most of its H monomers are connected in the form of their esters (Chen, 2014).

2.1.3. Biosynthesis

The biosynthesis of lignin can be divided into two major steps; the synthesis of monolignols and the radical polymerization of these monolignols to form lignin.

Synthesis of monolignols occur in the cell cytoplasm (Gellerstedt & Henriksson, 2008) and proceeds via the phenylpropanoid pathway (Chen, 2014). This biosynthetic pathway is not only responsible for the production of monolignols, but also for the production of other aromatic compounds such as flavonoids and anthocyanins, both of which have considerable economic importance (Welker, et al., 2015). Looking specifically at monolignol synthesis, the process begins with the conversion of glucose to L-phenylalanine and L-tyrosine via the shikimic acid pathway. Phenylalanine then undergoes deamination via the cinnamic acid pathway, after which the resultant cinnamic acid is hydroxylated to coumaric acid (Chen, 2014). The deamination reaction is catalysed by the phenylalanine ammonia lyase (PAL) enzyme, the likes of which is only found in lignin-synthesising plants (Argyropoulos & Menachem, 1997). Meanwhile, tyrosine is directly converted to *p*-coumaric acid under the enzymatic influence of tyrosine ammonia lyase (TAL) (Chen, 2014). Interestingly, TAL is only found in grasses, which may account for the substantial amount of H monomers found in this plant division (Argyropoulos & Menachem, 1997). Hereafter, *p*-coumaric acid is either hydroxylated to caffeic acid, or it is reduced to *p*-coumaryl alcohol (H monomer) by reductase enzymes. The caffeic acid is then methylated to ferulic acid by the caffeic acid-O-methyltransferase (COMT) enzyme, after which it is reduced to coniferaldehyde (Chen, 2014). It should be noted that beyond this stage, the biosynthetic pathways for hardwoods and softwoods diverge, primarily due to the COMT enzyme. It was found that softwoods possessed COMT enzymes with different functionalities and substrate specificities to that of hardwoods. These COMT enzymes are thought to be one of the reasons for the difference in monomer composition between softwoods and hardwoods (Argyropoulos & Menachem, 1997). As the synthesis process continues, coniferaldehyde is either hydroxylated to 5-hydroxy-coniferaldehyde, or it is further reduced to coniferyl alcohol (G monomer). The hydroxylated form is subsequently methylated to sinapaldehyde by COMT, after which it is reduced to sinapyl alcohol (S monomer) (Gellerstedt & Henriksson, 2008). In softwoods, the mono-functional COMT enzyme is inhibited by caffeic acid, thus preventing the methylation of 5-hydroxy-coniferaldehyde and the subsequent formation of S monomers. This results in the exclusive formation of G monomers. In hardwoods, the COMT enzyme is di-functional, thus allowing the formation of both G and S monomers. Researchers have further found that reductase enzymes in

softwoods are inactive towards sinapic acid and sinapoyl-CoA. Additionally, ferulic acid-5-hydroxylase (F5H), an enzyme that catalyses the conversion of ferulic acid to S monomers, was also found to be absent in gymnosperms. This contributes to the exclusive presence of G monomers in softwoods (Argyropoulos & Menachem, 1997).

Once the synthesis of the monolignols are complete, they are transported across the plasma membrane to the apoplastic space within the cell wall. Thus far, only the transporter involved in the translocation of *p*-coumaryl alcohol is known, i.e. adenosine triphosphate (ATP)-binding (ABC) cassette transporter. Transporters involved with the other monolignols have yet to be discovered (Welker, et al., 2015). In the cell wall, the monolignols are oxidized to resonance-stabilized phenoxy radicals by laccase and peroxidase enzymes (Gellerstedt & Henriksson, 2008). These free radicals form the lignin polymer via a random coupling reaction, the likes of which occurs predominantly in the cell wall and middle lamellae (Welker, et al., 2015). The reactivity of these radicals, as well as the tendency that a specific resonance form will form a particular linkage, depends on β electron spin density (Argyropoulos & Menachem, 1997), and spatial constraints imposed by the surrounding polymer (Welker, et al., 2015). Studies have determined that free electron spin densities are highest at the aliphatic β-carbon, the phenolic oxygen, and the C_1 and C_5 positions of the aromatic ring. The latter becomes less reactive when the C_1 or both the C_1 and C_5 positions are occupied in coniferyl and sinapyl alcohol, respectively. Consequently, the phenoxy oxygen and the β-carbon are the most reactive species, and readily couple into aryl ether linkages. This may account for the high frequency of β-O-4 interunit linkages found in lignin (Argyropoulos & Menachem, 1997).

2.1.4. Physical Properties

When subjected to any mechanical, enzymatic or chemical action, the physical properties of lignin can change (Chen, 2014). As a result, most physical properties of native lignins have been deduced by inference of isolated lignin properties (Goring, 1971). Accordingly, there is a degree of variability in the properties between native lignins and isolated lignins, as well as between lignins isolated by different methods. Important physical properties of lignin that have been identified include solubility, molecular weight and polydispersity, and glassy transition temperatures.

It is generally accepted that native lignin is an insoluble (Chen, 2014), high molecular weight biopolymer (Haygreen & Bowyer, 2007). Early literature indicates that its insolubility is due to its existence as a network polymer within wood or plant biomass (Goring, 1971). Explicitly, the presence of hydroxyls and other polar groups in the lignin structure result in strong intra- and intermolecular hydrogens bonds which render native lignin insoluble in most solvents (Chen, 2014). Thus, the goal

of all isolation processes is to sufficiently degrade the polymeric structure, such that the resultant fragments become soluble in the pulping media (Upton & Kasko, 2015).

Subsequently, the solubilised lignin fragments are of various sizes and molecular weights (Goring, 1971). As a result, there is a distribution of molecular weights from which the average molecular weight can be determined (Mathias, 2016). Various techniques are used to measure molecular weight, thus different types of averages exist. Of particular significance is the weighted average molecular weight (M_W), and the number average molecular weight (M_N). The ratio of these two mean values, M_W/M_N, is called the polydispersity index (PI). This index is a measure of the distribution of the molecular weight in a given polymer sample (Atkins & Paula, 2006). In general, linear polymers display narrow molecular weight distributions with smaller PI values, whereas the converse is true for nonlinear polymers. For example, glycogen, a branched polysaccharide, has been found to be highly polydisperse in both its native and degraded states, with some PI values exceeding 100. On the other hand, xylan, a linear biopolymer, has been reported to have a PI of 1.2 thus indicating its low polydispersity (Goring, 1971). Some biopolymers, such as pure proteins, have a PI of 1, and are thus monodisperse. This indicates that it has a single, definite molar mass. Synthetic polymers are polydisperse and usually have a PI of about 4. However, should they display polydispersity indices less than 1.1, they are then classified as monodisperse (Atkins & Paula, 2006). Lignins isolated from pulping processes usually display high molecular weights in the range of 100-300 000, and consequently can have a high degree of polydispersity (Gellerstedt & Henriksson, 2008). Lignosulphonates usually have molecular weights in the range of 10^3-10^5, however some studies have reported values in the range of 10^6 and above (Chen, 2014). Similarly alkali lignins usually have molecular weights in the range of 1000-10^6. Hardwood lignins have also shown lower molecular weights than softwood lignins, but both are still polydisperse (Goring, 1971).

Regarding its thermal behaviour, lignin is classified as a thermosoftening plastic or thermoplastic. This means that it becomes soft and pliable at high temperatures, and hardens again as it cools down (Haygreen & Bowyer, 2007). The temperature at which it starts to soften is known as the softening temerature (T_s), or the glassy transition temperature (T_g). Below the glassy transition temperature, lignin is in a solid glass state. Above this temperature, it softens and becomes sticky, thereby exhibiting an adhesive force. Softening temperatures for isolated lignins can vary with plant origins, isolation processes, water content, and molecular weight. Lignins with high molecular weights often have higher softening points. For instance, lignins with a molecular weight of 4300 display a glassy transition temperature of 127°C, whilst a molecular weight of 85000 corresponds to a temperature of 176°C. Incidently, this relation between molecular weight and softening temeprature is also observed with synthetic polymers (Goring, 1971). Dried lignins exhibit softening temperatures in the range of

127°C - 129°C. However, it was found that increasing the water content of these dried lignins decreased the softening temperatures, thereby proving that water acts as a plasticizer to lignin (Chen, 2014). Another important thermal property is the thermal degradation of lignin which, due to the complex structure of lignin, is a relatively complex process as well, consisting of competing and/or successive reaction steps. The various oxygen-based functional groups within the lignin structure have different thermal stability with scissions happening at different temperatures. As a result, thermal decomposition of lignin occurs over a wide temperature range. The first step of dehydration occurs at fairly low temperatures of 150-275°C, and is attributed to the dehydration of hydroxyl groups located on benzyl groups. Additionally, cleavage of α- and β-aryl-alkyl-ether linkages occurs from 150-300°C. Aliphatic side chains start splitting off from the aromatic ring at about 300°C, after which cleavage of C-C linkages between lignin units occurs at 370-400°C. Lastly, at temperatures of 500-700°C, complete rearrangement of the lignin backbone occurs, resulting in 30-50 wt. % char and volatiles like CO, CO_2, CH_4 and H_2 (Laurichesse & Avérous, 2014).

2.1.5. Pulping as a Source of Technical Lignins

Many softwood and hardwood species, along with certain grass species, are of commercial significance in the paper and pulp industry (Gellerstedt & Henriksson, 2008). They contain appreciable amounts of cellulose fibres, which are key components in the production of textile fibres and paper products. These cellulose fibres are separated from the rest of the biomass, particularly lignin and hemicellulose, by various pulping processes, which employ a series of mechanical and/or chemical methods (Argyropoulos & Menachem, 1997). Due to the high content of lignin in trees, as well as its close association to cellulose (Haygreen & Bowyer, 2007), the isolation and removal of lignin (delignification) is a vital part of the pulping process. Of even more importance is the removal of lignin without loss of or degradation to the cellulose product. The pulping liquor that exits the process is essentially a waste stream, and is often referred to as spent liquor. This spent liquor contains large quantities of lignin, together with pulping chemicals and other wood constituents like sugars (hemicelluloses) and ash (Gellerstedt & Henriksson, 2008). These lignins, frequently referred to as technical lignins, are often not isolated but rather burnt with the rest of the liquor to generate energy and recover the pulping chemicals (Hu, et al., 2011).

Commercial pulping methods are dominated by the sulphite, soda, and kraft processes, whilst the steam explosion and organosolv processes have recently garnered interest for commercialization (Lora, 2008; Pfungen, 2015). As discussed in previous sections, all separation processes alter the structure and properties of native lignin to some extent (Gellerstedt & Henriksson, 2008). Thus, a

high degree of variability can exist between native and technical lignin, and even across technical lignins from different pulping processes.

The soda process was one of the first chemical pulping methods to be developed, and was named after the cooking reagent used, i.e. caustic soda (Pfungen, 2015). Although traditionally used for non-woody biomass, such as grasses, it is also used to produce high-yield hardwood pulps. The biomass is digested at around 160°C using an aqueous caustic soda solution. Lower temperatures may be used if non-woody feedstock is processed, mainly due to the lower lignin content and relatively more accessible lignin structure. Under these conditions, various reactions take place, namely lignin depolymerization, cleavage of lignin-carbohydrate linkages, and lignin-lignin condensation (Lora, 2008). Depolymerization occurs principally by the hydrolysis of more than 95% of the β-O-4 linkages, as well as the partial modification/partial elimination of most of the phenylpropane side chains (Gellerstedt & Henriksson, 2008). These reactions generate moieties with free phenolic groups, the likes of which are soluble in the alkaline pulping solution (Lora, 2008). One of the more common methods of extracting the solubilised soda lignin from the spent pulping liquor is by acidification of the alkaline solution (Upton & Kasko, 2015) which decreases the solubility of soda lignin causing it to precipitate out of solution. This is then followed by separation techniques like filtration or centrifugation to remove the lignin precipitates. However, this method has yet to have widespread commercial implementation, most likely due to the large volumes of acid required, and the resultant downstream processing of the acid waste streams. Notable properties of soda lignin include low molecular weights, insolubility in water, and low ash and sugar contents (Table 2.2). A key advantage of soda pulping over other commercial pulping methods is that soda lignin is sulphur-free, thus they are considered to be closest to native lignin (Lora, 2008). Another attractive feature is that silicates, a major component of ash in non-woody species (Lora, 2008), can be removed in the form of sodium ammonium silicates. This is especially desirable when processing bamboo or cereal straw, both of which have high silica contents in the range of 1.5 – 3% and 3 – 7%, respectively (Pfungen, 2015).

The acid sulphite process was invented shortly after the soda process (Pfungen, 2015). The biomass is digested using an aqueous solution of a sulphite or bisulphite salt of calcium, sodium, ammonium, or magnesium. Process temperatures are in the range of 140-170°C, and the pH is determined by the type of salt as well as its solubility and dissociation characteristics. Reactions that take place include cleavage of lignin-carbohydrate linkages, scission of β-O-4 linkages, and the sulphonation of aliphatic side chains. The last reaction is particularly important in sulphite pulping, and as a result, sulphite lignins are predominantly referred to as lignosulphonates (Lora, 2008). Sulphonate groups on the lignin molecule increases its hydrophilicity (Pfungen, 2015), thereby making it highly water-soluble.

Furthermore, sulphonate groups also prevent condensation of lignin structures, the likes of which is a major competing reaction in sulphite pulping (Lora, 2008). Alternatively, condensation can be suppressed with a high concentration of bisulphite ions present in the pulping liquor (Gellerstedt & Henriksson, 2008). Other notable properties of lignosulphonates include a significantly high sugar content (Table 2.2), and insolubility in organic solvents (Lora, 2008). Currently, the most reported method of recovering lignosulphonates is by ultrafiltration of the spent liquor (Gellerstedt & Henriksson, 2008), however this method does not have widespread implementation in industry. This is most likely because the process has high production costs, and requires a special selection of membranes for each spent liquor in order to maximise product yield and purity (Fatehi & Chen, 2016).

In the kraft process, high temperatures of 170°C are used to digest the biomass with an aqueous solution of sodium hydroxide and sodium sulphide (Lora, 2008) at a pH of 14 (Pfungen, 2015). Since kraft pulping is an enhancement of the soda process (Pfungen, 2015), the same reactions take place, ultimately resulting in alkaline-soluble lignins (Lora, 2008). Notable properties of kraft lignin include low ash and sugar contents (Table 2.2). Although the lack of sulphur in soda lignins is advantageous, the presence of sulphur in kraft lignins can also be advantageous. This is because the sulphide and hydrosulphide ions are stronger nucleophiles than the hydroxyl ions in soda liquor (Pfungen, 2015), thus minimising the condensation of lignin fragments in kraft liquor (Lora, 2008). As a result, kraft pulping has more effective delignification, with a 90-95% dissolution of total lignin in the feedstock. Once again, one of the more common methods of recovering the dissolved lignin fragments is by acidification of the kraft pulping liquor (Gellerstedt & Henriksson, 2008). This is due to the decreasing water solubility of kraft lignin with decreasing pH of the spent liquor. As the pH is lowered, the ionisation of lignin molecules decrease, thereby causing self-aggregation. Meanwhile, the other components of black liquor, such as inorganic constituents and carbohydrates, are soluble over a wide pH range (Lora, 2008) and remain in solution. Due to the reliability and favourable economics of the acidification method, the LignoBoost and LignoForce technologies were developed to extract kraft lignin from spent kraft liquor. These technologies use the basic concept of acidification, coupled with other process steps such as oxidation, filtration, coagulation, etc. It should be noted that both these technologies have only been commercialised in North America thus far, and have yet to reach paper mills and lignin production plants in other parts of the world (Fatehi & Chen, 2016).

Table 2.2: Physical properties of technical lignins from commercial pulping processes. Extracted from Lora (2008).

Pulping Process	Soda	Sulphite	Kraft
Ash Content (%)	< 1[a]	NR	< 3.0
Sugars Content (%)	2.0 – 3.0	≤ 35	< 2.3
Acid Soluble Lignin Content (%)	NR	NR	3
Acid Insoluble Lignin Content (%)	NR	NR	90
Sulphur Content (%)	[-]	4.0-8.0	1.5 – 3.0
Weight Average Molecular Weight (M_W)	6900 -8500	1000-150000	2500-39000
Polydispersity Index (PI)	3	7	2.5-3.5[b]
Glass Transition Temperature (°C)	158 - 185	130[b]	140
Lignin Degradation Temperature (°C)	NR	450	452

* NR – not reported, [-] doesn't exhibit that property

[a] Refers specifically to the silica content

[b] Extracted from (Laurichesse & Avérous, 2014)

Organosolv pulping involves digestion of the biomass using organic solvents, such as alcohols and organic acids (Pfungen, 2015). The process usually runs at high temperatures of about 200°C, and can consist of more than one cooking cycle. Lignin from the resultant cooking liquor can be extracted using a liquid/solid separation system, after which the remaining liquor can be used to generate energy and recover solvents. Organosolv lignins are relatively pure, with low ash and sugar contents. They are also water-insoluble, and they have a low glassy transition temperature. Furthermore, they have low molecular weights and a narrow molecular weight distribution (Ozmen, 2000). Advantages of the organosolv process include the lack of sulphur and high pressures, as well as the ability to simultaneously isolate high purity yields of cellulose, hemicellulose, and lignin. However, a major downside is that the solvent recovery step has not been successfully optimized, thus organosolv is a comparatively higher cost pulping method (Upton & Kasko, 2015).

Steam explosion involves the treatment of biomass with high temperature steam followed by a rapid pressure release. This causes the material to 'explode', thereby liberating the biopolymer fibres. Temperatures of around 200°C are usually used, and the cooking liquor is weakly acidic due to the release of acetic acid from hemicellulose. Major reactions that occur include hydrolysis of polysaccharides, hydrolysis of lignin, and condensation of lignin fragments. Additionally, the use of high temperatures is also thought to cause homolytic cleavage of bonds, such as β-O-4 linkages. The degree of degradation of the biomass can be controlled by adjustment of temperature and reaction time. The lignin in the resultant cooking liquor can be extracted with either an aqueous alkali or organic solvent, thereby leaving behind a cellulose-rich pulp residue. These lignins are extremely heterogeneous in structure, with a high content of phenolic end-groups (Gellerstedt & Henriksson,

2008). It should be noted, however, that this pulping method is mainly utilized at lab and pilot plant scales (Upton & Kasko, 2015).

2.1.6. Potential as Biofuels & Bio-products

The ever-growing need for fuel, energy, and various chemical products has sparked the demand for more sustainable, cleaner and renewable sources of such commodities (Welker, et al., 2015). Lignin in general has great potential for utilization as a raw material for high-value products due to its polymeric structure, biodegradability, high thermal stability, thermoplasticity, and its antioxidant and antimicrobial properties. Additionally, it is carbon neutral, renewable and in high abundance (Upton & Kasko, 2015; Welker, et al., 2015).

The paper and pulping industry produces approximately 40-50 million tonnes of technical lignin per year. However, only 1.5% of this is currently used for purposes other than low-value energy generation (Welker, et al., 2015). This mainly includes lignosulphonates that are commercially used as dispersants in cement and gypsum blends (Welker, et al., 2015), and as super-plasticizers in concrete and gypsum (Matsushita, 2015). Additionally, sulphonated and aminated kraft lignins are commercially used as dispersants, emulsifiers, and surfactants (Lora, 2008), albeit to a smaller extent than lignosulphonates. Besides the paper and pulp industry, the cellulosic ethanol industry is the other relatively significant producer of technical lignin. This industry enzymatically hydrolyses lignocellulosic biomass to produce cellulosic ethanol, with an estimated 0.5-1.5kg of enzymatic lignin being co-generated for every litre of ethanol produced (Tian, et al., 2016). In 2015, reportedly 537.7 million litres of ethanol was produced in the USA alone (Tian, et al., 2016), which would mean that approximately 268 000 tonnes of lignin was produced as a by-product. This large volume of technical lignins have a vast range of potential applications.

As an energy source, lignin-rich pulping liquor can undergo thermochemical processing to produce combustible biogas, hydrogen, and bio-oil. Lignin char, produced by pyrolysis of lignin, can also be used as activated carbon (Tian, et al., 2016). Lignin itself can be used as an additive in synthetic polymers, such as polyethylene and polystyrene, to improve thermal stability. It can also be used as an additive in packaging bio-composites for reinforcement and water resistance, as a slow-release additive in fertilisers, and as an antioxidant and reinforcement additive in natural and synthetic rubbers (Tian, et al., 2016). Furthermore, lignin can be broken down into monolignols and lignin derivatives such as phenols, aldehydes, and aliphatics. These monolignols and derivatives, as well as lignin as a macromonomer, can be used as a feedstock for the synthesis of various high-value polymeric materials such as polyurethanes, polyamides, polyesters, graft co-polymers, epoxide resins, and phenolic resins (Upton & Kasko, 2015). There are also possibilities of using the carbon fibres

prepared from lignin for the manufacture of high energy super capacitors in the automotive industry (Welker, et al., 2015). Within the biomedical field, there is ongoing research into the use of lignins and lignosulphonate derivatives for the treatment of diabetes and obesity, and lignin-based nanoparticles are being developed for drug delivery systems. Lignin can be used as an anticoagulant, and is a promising candidate in the treatment of HIV and orally transmitted STDs due to its antiviral activity (Vinardell & Mitjans, 2017). Moreover, lignin can be used in the production of hydrogels which are used in drug and protein delivery systems, and as scaffolds in tissue engineering (Upton & Kasko, 2015). Other pharmacological applications include the use of calcium lignosulphonate as an encapsulating agent of functional ingredients in animal feed (Matsushita, 2015).

Despite the vast range of high-end applications and its relative success at research level, technical lignins still remain largely underutilized. This is partly because most of the aforementioned applications would prefer lignins with minimal impurities. Thus, some technical lignins would likely require some form of purification to ensure a low ash content. Common purification methods would include ultrafiltration of lignosulphonates (Fatehi & Chen, 2016), and dilute acidification of alkaline lignins (Thies & Klett, 2016). As discussed in the previous section, these methods are not easily implemented in industry. Lignin also suffers from low reactivity due to its complex chemical structure, thus, some lignins may need to be functionalized or modified to make it more reactive and suitable for a particular application. This adds further cost to the production of the potential lignin-based biomaterial, thus limiting its viability. Additionally, processes that isolate and degrade lignin to phenolic products or monolignols are usually energy intensive, and currently have higher production costs than its petroleum derived counterparts. Ultimately, any process that uses lignin products as feedstocks for synthesis of other materials would need to be efficient, energy and environmentally favourable, and cost-effective (Upton & Kasko, 2015). The same can be said for lignin extraction, purification and modification methods wishing to seek commercialisation. These are some of the reasons why lignin presently has greater commercial utilization as low-value fuel.

However, there is still ongoing research into the effective and feasible utilization of lignin as a source of chemical products and energy. Incidentally, most producers of low-ash lignin, specifically those of kraft lignin, predict that the largest markets for application of their products will be as partial phenol replacements in phenol formaldehyde resins, and as partial polyol replacements in the production of rigid polyurethane foams. Reportedly, the total annual world capacity of low-ash lignin is approximately over 100 000 tonnes, whilst the total annual market for phenols and polyols is around 10-15 million tonnes. Thus, there is a huge potential for breaking into this market and relieving the dependency on fossil fuels, if only by a small degree initially (Thies & Klett, 2016).

2.2. Adhesives in the Wood Industry

Adhesives are materials that use cohesive forces to bond two surfaces together under specified conditions of pressure, temperature and humidity (Siddiqui, 2013). The basic objective of any adhesive is to keep the bonded surfaces in a fixed position such that when an applied stress reaches a critical point, the failure would occur with the material and not the adhesive. To be a satisfactory adhesive, it must possess the dual ability of wetting the bonding surface (polar attraction) and converting to a rigid solid form, either through solvent evaporation, catalysed chemical reactions, or physical cooling (Ozmen, 2000). A major component in adhesives are the resins, which essentially contain all the relevant adhesive properties.

Wood adhesives can be classified into three main categories, namely natural, synthetic, and bio-based. Natural wood adhesives are typically derived from animals, proteins, and vegetables. Due to low moisture resistance, short working life, and relatively low bonding strengths (Siddiqui, 2013), they were eventually phased out and replaced with synthetic adhesives. Synthetic adhesives generally possess better economics (Ozmen, 2000), and exhibit better resistance and strength properties (Siddiqui, 2013). However, depletion of fossil fuels and growing environmental concerns dictated the need to move onto "greener' alternatives.

Bio-based adhesives are semi-synthetic and contain natural, renewable raw material components. These renewable resources usually serve as a substitution for the petroleum-derived components used in traditional synthetic adhesives, or they can be used in the formulation of a completely different bio-based adhesive. As a result, bio-based adhesives are biodegradable, have lower toxicity (Ferdosian, et al., 2017), are renewable, and have feedstocks that are usually abundant. However, in comparison to traditional synthetic adhesives, most bio-based adhesives suffer from poor water resistance (Ferdosian, et al., 2017), short pot life (Hemmila, et al., 2017), reduced reactivity, inferior bond strength, curing difficulties, and reduced thermal stability (Siddiqui, 2013). To improve these properties, modification of the natural resource is required (Hemmila, et al., 2017) which either adds to the production cost of the adhesive, or increases the feedstock price of the otherwise low cost natural resource. Alternatively suitable crosslinkers may be used in the adhesive formulation, but since there is a lack of economically viable bio-based crosslinkers, synthetic crosslinkers have to be used, some of which are expensive. Comparatively, synthetic adhesives are lower cost, and their properties are adjustable (Hemmila, et al., 2017). These factors hinder the widespread commercialisation of bio-based adhesives in the present day.

2.2.1. Natural Adhesives

Natural adhesives were used as far back as the Stone Age, where it was predominantly used as a glue in the making of weapons and living structures. Modern applications were also in the form of glues, with the first commercial glue plant supposedly founded in Holland in 1690 (Keimel, 2003). Common glues used in the wood industry include animal-based glues, starch-based vegetable glues, protein-based glues, and casein glues.

Animal-based glues are made from the bones of cattle, horses, and fish. These glues have high strength properties, however the strength is only realised when fully dried, and they lack proper resistance to moisture. Therefore, its usage becomes inconvenient and relatively expensive. As a result, animal-based glues have been replaced largely with synthetic polyvinyl acetate (PVA) emulsions, particularly in furniture applications (Siddiqui, 2013).

Starch-based glues are relatively inexpensive, have high strength and allegedly have a long pot life. However, like animal glues, they have poor moisture resistance properties, in addition to poor storage stability. Moreover, food competition is also a factor to consider since the starch used originates from food crops such as cassava, potatoes, maize, and rice. Thus, these glues have been displaced by synthetic urea formaldehyde (UF) resins, especially in the manufacture of hardwood plywood and furniture (Siddiqui, 2013).

Protein-based glues are generally derived from whole soybeans, protein from soybeans, or a blend of (animal) blood and soybeans. They exhibit low moisture resistance, moderate resistance to intermediate temperatures, and have a low to moderate dry strength. Hence, they have been replaced by phenol formaldehyde (PF) resins, particularly in softwood plywood production (Siddiqui, 2013).

Casein glues are derived from the precipitates of skim and butter milk. They exhibit moderate resistance to moisture and intermediate temperatures, have a short pot life, and have a relatively high dry strength. Due to these properties casein glues were used primarily for interior laminated timber applications. However, they require excessive amounts of milk for production, i.e. roughly 30 litres of milk is required to produce half a kilogram of dry casein. As a result of food competition, they have been phased out (Siddiqui, 2013).

2.2.2. Synthetic Adhesives

Due to important limitations with natural adhesives, synthetic adhesives were developed, with widespread use seemingly occurring after World War II. These adhesives are made from petroleum-based products which are, in turn, derived from fossil fuels such as natural gas and crude oil (Siddiqui, 2013). There are four major synthetic thermosetting resins used as wood adhesives, namely phenol

formaldehyde (PF), urea formaldehyde (UF), melamine formaldehyde (MF), and polymeric diphenylmethane diisocyanate (pMDI) resins (Ferdosian, et al., 2017). Additionally, thermoplastic resins such as polyvinyl acetate (PVA) emulsions are also commonly used as wood adhesives (Siddiqui, 2013).

PF resins are synthesized from the reaction of phenol and formaldehyde under alkaline conditions. They exhibit excellent thermal properties and moisture resistance, high adhesive and mechanical strength, and low initial viscosity (desirable for application purposes). They are mainly used for the production of orientated strand board (OSB), wood sidings that requires exterior exposure durability, and softwood plywood (Ferdosian, et al., 2017). These resins are fully elaborated on in Section 2.3.

UF resins are the most widely used synthetic resins, and are primarily used in the production of interior grade plywood, particle board (Siddiqui, 2013), and medium density fibreboard (MDF). Some advantages of UF resins over PF resins include a wide curing temperature range (i.e. 25-150°C), shorter pressing times and lower pressing temperatures, thus resulting in lower energy consumption and higher production rates. Additionally, their light colour make them suitable for use in decorative products (Ferdosian, et al., 2017). However, low to moderate moisture resistance, brittle adhesive layer and excessive free formaldehyde emissions are notable disadvantages (Siddiqui, 2013).

MF resins, developed in response to the poor resistance properties of UF resins, exhibits resistance to a wide range of conditions (Siddiqui, 2013). They are typically used for applications such as paper coating, decorative laminates, paper treating (Ferdosian, et al., 2017), and other applications requiring light-coloured adhesives. However, MF resins require moderately high curing temperatures, and are relatively expensive (Siddiqui, 2013). As a result of the latter, they are usually blended with UF resins for certain applications (Ferdosian, et al., 2017).

pMDI resins are generally used for OSB manufacture. Advantages include high versatility, fast curing rates, superior moisture and chemical resistance, no formaldehyde emissions, and small loading quantity. Additionally, pMDI is considerably less toxic than formaldehyde, the latter of which is categorized as a carcinogenic material. However, high manufacturing costs limit its use (Siddiqui, 2013; Ferdosian, et al., 2017).

PVA emulsions are commonly used in the bonding of plastic laminates, and furniture assembly. They are advantageous in that they are low cost and non-toxic. However, they exhibit poor resistance and mechanical stress properties, even when compared to UF resins. Its thermoplastic nature also limits widespread use as high temperatures and humidity significantly decreases its bonding strength. In order to improve moisture resistance, PVC emulsions have been reportedly blended or polymerized with cross-linking agents and monomers (Siddiqui, 2013).

2.2.3. Bio-Based Adhesives

Before the advent of synthetic adhesives, bio-based adhesives in the form of semi-synthetic cellulosic material were developed, however it is uncertain when they were first used as adhesives, or for what purpose they were used (Keimel, 2003). The need for wood adhesives produced from renewable and environmentally sustainable resources has revived and intensified the interest towards bio-based adhesives. Many biomass resources have been used in the research and development of such adhesives, particularly biopolymers such as lignin, starch, and plant proteins, as well as other biomass components such as tannins (Ferdosian, et al., 2017).

Starch is a promising feedstock as it has good adhesion, good film formation properties, easy accessibility, and is low cost. However, as seen from the discussion on natural adhesives, direct use of starch in adhesives is not successful due to poor bonding strength, poor moisture resistance, long drying time of the adhesive, and poor storage capabilities. Hence, starch requires some form of modification, often by chemical methods such as esterification and oxidation (Ferdosian, et al., 2017). Additionally, synthetic crosslinkers like isocyanates and hexamine, or additives like nanoparticles and nanaoclays (Hemmila, et al., 2017) may be incorporated into the formulation of starch-based adhesives to improve its bonding performance, water resistance and thermal stability (Ferdosian, et al., 2017).

Common plant proteins that have been studied for use in wood adhesives include those from soy beans, canola seeds, cotton and wheat. Direct use of plant proteins result in adhesives that have high viscosities and low water resistance. Additionally, these adhesives have short pot lives, i.e. time during which viscosity doubles, at which point it becomes difficult to handle (Ferdosian, et al., 2017). As a result, plant proteins require a denaturation step to expose hydrophilic groups for better solubility and bonding, followed by modification of the protein (Hemmila, et al., 2017). The method of modification depends on the type of plant protein used (Ferdosian, et al., 2017). Some common techniques that have been employed include enzymatic and chemical modification. Alternatively, crosslinkers like polyamides (Hemmila, et al., 2017), or additives like amino acids may be used in the adhesive formulation to improve strength and water resistance properties (Ferdosian, et al., 2017).

Lignin is an attractive candidate for adhesive application due to its high hydrophobicity, low polydispersity, low glass transition temperatures (Ferdosian, et al., 2017), and high industrial abundance. It also carries no competition to food applications, as compared to starch and plant proteins (Laurichesse & Avérous, 2014). Its phenolic structure makes it a desirable partial or total phenol substitute in PF resins (Ferdosian, et al., 2017), however its complex chemical structure greatly hinders it reactivity, especially towards formaldehyde. Consequently, these adhesives usually

possess low bonding strengths, and require long pressing times (Hemmila, et al., 2017). This has prompted research into the modification of lignin for use as a phenol substitute. Lignin-based adhesives will be further discussed in detail in Section 2.4.

Tannin is a plant component that is found in fruit, leaves, bark and wood. They already have industrial applications as corrosion inhibitors, and in the manufacture of inks and textile dyes. Like lignins, tannins are phenolic in nature, and have varying compositions that are also dependent on species, growth conditions and time of harvesting. Unlike lignin, it is highly reactive, particularly towards formaldehyde. As a result, tannin has the potential to partially or completely replace both phenol and urea in PF and UF resins, respectively. In the absence of formaldehyde, tannin can also be used with lignin or other bio-based materials to produce adhesives. Tannin-based adhesives generally display good adhesion, high moisture resistance, and low formaldehyde emissions. A downside is its short pot life due to its high reactivity. Research has shown that this can be mitigated with the use of suitable synthetic crosslinkers in the adhesive formulation, thereby prolonging pot life and decreasing viscosity for easier handling. Commercial tannin-formaldehyde adhesives exist, albeit in limited capacity due to the lack of global availability of tannins. This remains a major setback to the widespread industrial use of tannins (Hemmila, et al., 2017).

2.3. Phenol Formaldehyde Resins

Phenyl formaldehyde (PF) resins were the first synthetic polymers to be developed on a commercial scale (Pizzi, 2003), and were discovered by Dr Leo Baekeland in 1907. Following urea formaldehyde resins, they are the second most widely used and highly demanded synthetic resins used in wood products (Siddiqui, 2013), particularly in the manufacture of exterior-grade (structural) plywood panels, OSB panels, and particle boards (Ozmen, 2000). These resins are typically dark-reddish in colour, and are known for its superior bonding strength and excellent resistance properties (Siddiqui, 2013) at a relatively low cost, thus making them invaluable as adhesives (Pizzi, 2003).

PF resins are essentially the polycondensation products of the reaction between phenol and formaldehyde (Pizzi, 2003). Phenol is predominantly synthesised by the cumene process (Pfungen, 2015), which utilises petroleum-based benzene and propylene (Siddiqui, 2013). Formaldehyde is produced from the catalytic oxidation of methanol which, in turn, is derived from natural gas via steam reforming to synthesis gas (Gotro, 2013). Thus, both of these reactants are derived from fossil fuels. Since synthesis gas can also be produced from gasification of biomass, an alternative method for sustainable formaldehyde production from a renewable resource exists. However, a sustainable method to produce phenol has yet to be discovered (Gotro, 2013). As such, a lot of research is focused on the development of bio-based phenol substitutes.

2.3.1. Chemistry

PF resins are essentially formed by three stages of polymerization reactions, i.e. addition, condensation, and curing (Bhattacharjee, et al., 2014).

In the first stage, formaldehyde is added to phenol in the presence of an acidic or alkaline catalyst (Pizzi, 2003). During this addition reaction, methylolation of phenol occurs whereby formaldehyde attacks the ortho- or para- positions of the phenol ring and adds a methylol group, thereby forming mono-methylolphenols, shown in Figure 2.3. These mono-methylolphenols can react further with formaldehyde to form di- and tri-methylolphenols, shown in Figure 2.4 (Ozmen, 2000).

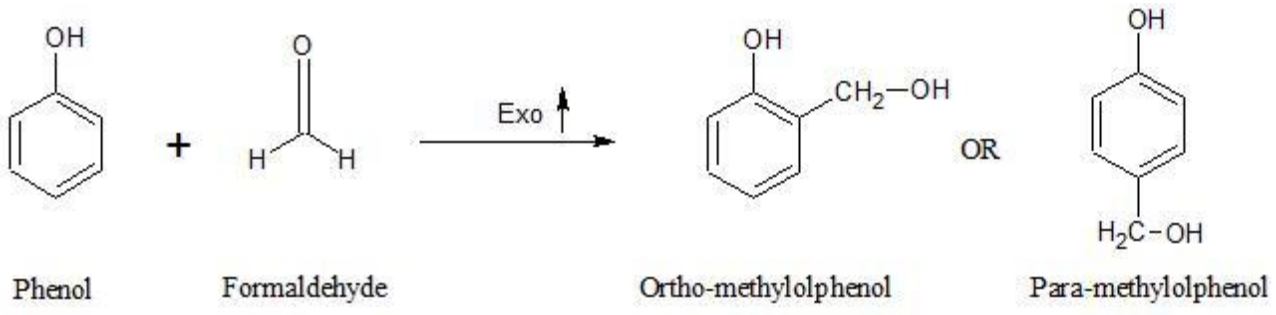

Figure 2.3: Methylolation of phenol. Redrawn from Pfungen (2015).

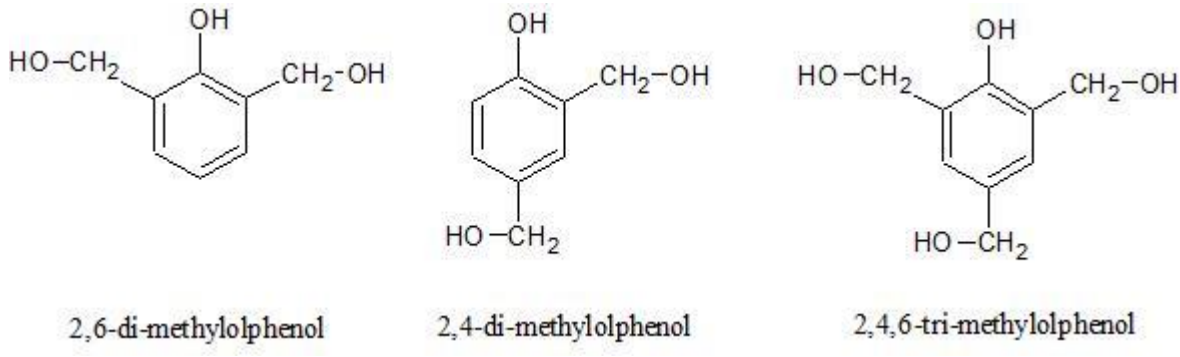

Figure 2.4: Additional methylolphenol derivatives. Redrawn from Pfungen (2015).

The second stage involves polycondensation of these methylolphenol derivatives with each other or unsubstituted phenols, thus resulting in the formation of a precondensate intermediate (Pfungen, 2015). During the reaction, methylene and dimethylene ether bridges are formed between the phenol/methylolphenol groups, and side products such as water molecules, unreacted phenols, and formaldehyde are released. The final curing reaction usually takes place upon application of the resin (Siddiqui, 2013), and is characterized by the addition of heat to initiate the final condensation of the precondensate to form a three dimensional polymer (Pfungen, 2015).

Depending on the pH of the reaction medium, and the molar ratio of phenol to formaldehyde (F/P ratio), PF resins can be classified as novolacs or resoles (Pfungen, 2015).

Novolacs are formed in the presence of an acid catalyst at F/P ratios of less than 1 (Gotro, 2013). The methylolation reaction predominantly yields mono-methylolphenols, which later condense to form dihydroxydiphenyl methane oligomers (Bhattacharjee, et al., 2014). Due to the deficiency of formaldehyde relative to phenol, and the subsequent absence of reactive hydroxymethyl groups, novolacs have no reactive functionality remaining. As such, they will not cure to form a crosslinked polymer without further addition of formaldehyde (Gotro, 2013). Instead, sole application of heat during the curing stage will result in the condensation of the oligomeric precondensate to form a relatively linear, thermoplastic polymer (Bhattacharjee, et al., 2014) that is soluble in various organic solvents (Ozmen, 2000). When curing occurs in the presence of both heat and formaldehyde, novolac oligomers cross-link to form a hard-cured, insoluble, thermosetting polymer (Pizzi, 2003). The formaldehyde is usually added in the form of paraformaldehyde or hexamethylenetetramine (Gotro, 2013), also known as hexamine.

Resoles are base-catalysed and formed at F/P ratios greater than 1 (Gotro, 2013). Methylolation results in the formation of mono-, di-, and tri-methylolphenols which condense to form a low molecular weight precondensate (Bhattacharjee, et al., 2014) that comprises of oligomeric and polymeric constituents (Pfungen, 2015). Unlike novolacs, resoles contain an excess of hydroxymethyl groups, thus they don't require additional formaldehyde to crosslink. Instead, further heating will cause sufficient cross-linking of the precondensate to form a rigid, insoluble, thermosetting polymer (Gotro, 2013). Depending on the specific end-use of the resole, it can be made in various viscosities and molecular weights (Ozmen, 2000).

2.3.2. Usage and Properties

As mentioned previously, PF resins are used as adhesives for wood construction and wood composite products. Additionally, they are also used as abrasives, binders, friction and filter materials for the automotive industry, photoresistors for the electronics industry, and moulding compounds for laminates. Their broad application range is due to its exceptional durability under mechanical stress, as well as against prolonged exposure to moisture, weathering, elevated temperatures, cleaning solutions, and acids (Gotro, 2013).

Explicitly, the advantages of PF resins include long thermal and mechanical stability, relatively low toxicity, high strength levels, excellent electrical and thermal insulation abilities (Pfungen, 2015), superior creep resistance, and a relatively straight-forward manufacturing process (Gotro, 2013). Properties of specific interest for wood applications include weather-proof characteristics, low levels

of formaldehyde release, high water resistance, and low thickness swelling of phenolic bonded boards (Pfungen, 2015). Disadvantages include toxicity problems associated with the handling of formaldehyde and phenol during manufacturing, use of fossil fuel-based materials, and fluctuating prices of phenol (Ozmen, 2000).

Resoles are preferred as wood adhesives due to its ability to form three dimensional polymers without the use of a curing agent. Its resultant structure also yields a higher tensile strength, higher modulus, higher dimensional stability and better resistance properties. Additionally, there is less cause for concern regarding wood damage as resoles are base-catalysed. However, due to the higher F/P ratios with which resoles are synthesised, the free formaldehyde content is higher compared to novolacs (Siddiqui, 2013). In general, resoles are typically used as casting and binding resins, whilst novolacs are used to make moulding compounds (Pizzi & Ibeh, 2014). Due to its relevance as a wood adhesive, phenol formaldehyde resole resins will be discussed hereafter.

2.3.3. Synthesis

Phenol formaldehyde resins are typically synthesized in jacketed, stainless steel batch reactors equipped with an agitator and reflux condenser. The production of PF resoles begins with the addition of formalin (37-42% aqueous formaldehyde) to molten phenol in the presence of an alkaline catalyst (Pizzi, 2003) at temperatures below 60°C and a pH of 8-13 (Siddiqui, 2013). Apart from catalyzing the reaction, the base serves to maintain the solubility of the reagents and resultant resin in the reaction mixture (Ozmen, 2000). Aqueous sodium hydroxide is typically used in industrial resole production, but other basic catalysts that may be used include sodium carbonate, alkaline oxides and hydroxides, and ammonia (Malutan, et al., 2008).

Upon increasing the temperature beyond 60°C, the condensation reactions begin (Siddiqui, 2013). Both the methylolation and condensation reactions are strongly exothermic (Bhattacharjee, et al., 2014), thus strict temperature control is required. Reaction temperatures are kept below 95-100°C by running cooling water through the reactor jacket. Additionally, carrying out the reactions in an aqueous system allows for easier control of the exotherm, due to the presence of water which acts as a moderator (Gelling, et al., 1983). As the condensation reaction proceeds, the molecular weight increases which, in turn, causes the viscosity to increase as well (Siddiqui, 2013). As viscosity approaches the target viscosity, the reaction mixture is cooled to a temperature that sufficiently suppresses further reactions (Gelling, et al., 1983), usually around 25-40°C (Gelling, et al., 1983; Pizzi, 2003). These target viscosities depend largely on the application. Impregnation resins have a range of 40-100 mPa.s, wood glue resins have a range of 1000-1500 mPa.s, and filling resins for fibreboard have a range of 1000-1800 mPa.s (Pfungen, 2015). Additionally, a drying stage may be

employed should the product be needed in a more concentrated form, or in a solid powder (Gelling, et al., 1983). In the latter case, the required amount of water would need to be added when applying the resin (Lorenz & Christiansen, 1995).

The final curing reaction takes place on application of the resole. During this time further condensation reactions take place, thus forming a highly branched and crosslinked polymer. Curing temperatures are around 125-150°C, but hot press temperatures can reach 200°C (Siddiqui, 2013).

2.3.4. Synthesis & Curing Parameters

The performance of PF resins are strongly influenced by chemical structure and molecular distribution of the resin, both of which are influenced by the addition, condensation and curing reactions that take place. These reactions, in turn, are influenced by synthesis and curing conditions, particularly concentration of catalyst, formaldehyde/phenol (F/P) ratios, and curing temperatures (Siddiqui, 2013).

Higher F/P ratios cause greater methylol substitution of phenol molecules. Maximum methylolation of phenol molecules is desirable as it results in a more rigid, highly crosslinked polymer. Increasing F/P ratios also increases viscosity, which is associated with decreases in gel time, as well as increases the curing rate. However, ratios that are too high run the health risk of a higher free HCHO content due to excess amounts of HCHO (Siddiqui, 2013).

Curing temperature is especially important due to the complex cross-linking reactions. Temperatures below 170°C result in the formation of methylene linkages in addition to ether bonds. Due to the instability of ether bonds, temperatures higher than 170°C can be used so that ether bridges may undergo further reaction to a more stable state. Notably, ether linkages can react further to form methylene linkages, but with loss of formaldehyde. Due to production costs, low curing temperatures are preferred (Siddiqui, 2013).

Increasing concentrations of the alkaline catalyst tends to increase the degree of condensation which increases the reactivity of the resin. This results in an increased hardening rate, as well as shorter gel and press times (Dunky, 2003). However, the Cannizzaro reaction, an undesirable side reaction, is favoured by high sodium hydroxide concentrations. This reaction consumes 3-5% of the available formaldehyde (Parker, 1981), effectively reducing the extent of methylolation of phenol. Consequently, some studies have indicated that an increase of sodium hydroxide concentration beyond 10 wt. % reduces adhesive strength (Siddiqui, 2013). Additionally, the hygroscopic nature of sodium hydroxide could cause a decrease in some mechanical properties of resoles in humid climates (Dunky, 2003). Additionally, the use of sodium hydroxide concentrations that are too low could cause unacceptable increases in free HCHO content (Ozmen, 2000).

2.4. Lignin-Phenol Formaldehyde Resins

Due to the environmental impact and long-term sustainability of fossil fuel based chemicals, the last few decades has seen an intensified interest in lignin-based adhesives, especially regarding technical lignin as a phenol substitute in phenol formaldehyde resins (PFRs). This is primarily due to structural similarities between lignin and phenol, the high availability of technical lignins in the paper and pulping industry, and the lower cost of lignin relative to phenol (Hu, et al., 2011). Additionally, lignin's natural properties, such as its thermoplastic nature and high resistance to moisture, heat and biological degradation, makes it particularly desirable for resin synthesis (Siddiqui, 2013).

However, the advancement of lignin as a phenol substitute is hindered by its chemical structure and resultant low reactivity (Hu, et al., 2011). Studies have found that lignin-phenol-formaldehyde resins (LPFRs) require higher press temperatures and longer curing times, thereby rendering them non-viable for commercial adhesive application (Matsushita, 2015). Additionally, incorporation of lignin in PFRs is limited to low phenol substitution levels. This is because LPFRs exhibit reduced adhesion strength with increasing lignin content (Ferdosian, et al., 2017). Incidentally, most studies conclude that the adhesive bonding strength of LPFRs are comparable to that of conventional PFRs up to a phenol substitution level of 50%, after which the bonding properties of the resins deteriorate (Siddiqui, 2013). As a result, direct use of lignin, i.e. unmodified lignin, is generally not seen as commercially attractive for the manufacture of bio-based PFRs (Hu, et al., 2011).

Due to difficulties with the use of unmodified lignin, modification methods were developed to enhance lignin's suitability for a specific application. For the purpose of using lignins in PFRs, most modification methods are aimed at enhancing lignin reactivity since lignin has fewer reactive sites than phenol (Hu, et al., 2014). Common modification methods include phenolation, methylolation, and demethylation. The ultimate objective would be to modify lignin such that phenol-rich compounds with high reactivity are obtained in a low cost, environmentally-sustainable manner. However, as far as is known, no method has been able to meet all three requirements (Hu, et al., 2011).

Ultimately, a wealth of research has been conducted regarding lignin-based adhesives and PFRs, with several patents having been granted as well. Unfortunately, no widespread application of these processes are known in industry today due to its inability to compete with commercial synthetic adhesives in terms of processability, economics and product quality (Pfungen, 2015). As such, there is ongoing efforts into the research and development of viable lignin-phenol-formaldehyde resins.

2.4.1. Chemistry

The reactions between lignin and formaldehyde occurs in a similar manner to that of phenol and formaldehyde. Explicitly, under alkaline conditions formaldehyde reacts with lignin by electrophilic substitution at the free ortho- positions of the phenolic nuclei via the Lederer-Manasse reaction (Matsushita, 2015). This leads to the introduction of methylol groups on the lignin ring, as shown in Figure 2.5.

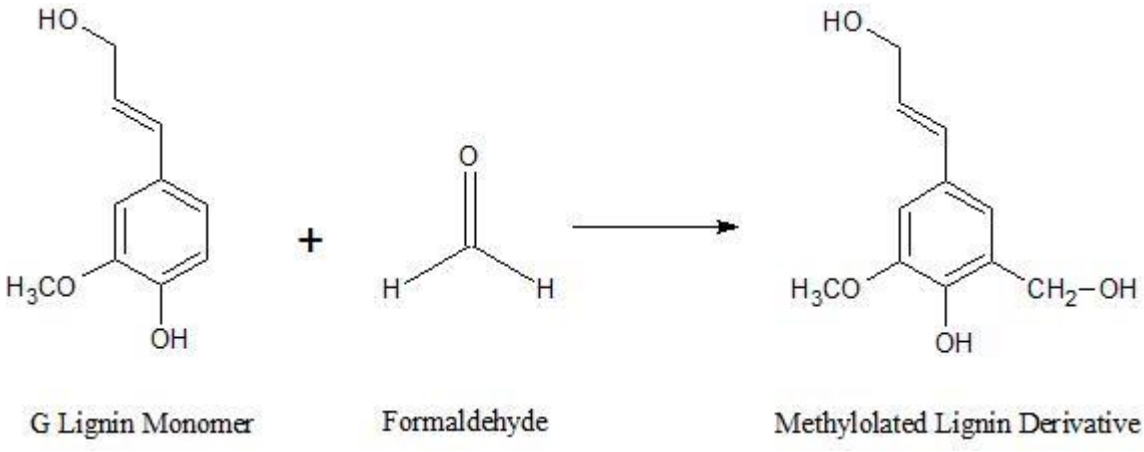

Figure 2.5: Simplistic representation of the reaction between a lignin monomer and formaldehyde. Redrawn from Hemmila et al (2017).

Thereafter, condensation reactions take place whereby the methylolated lignin derivatives react with each other, as well other available phenols and methylolphenols. This results in the initial formation of a linear polymer, and then, during the curing step, a hard cured polymer with a highly branched structure (Hemmila, et al., 2017).

Considering the position at which methylol groups are substituted onto the aromatic ring, it is worthwhile to note that lignins comprising of H and/or G monomers would be best suited for LPF resin synthesis. Both the ortho- positions of the S monomer are occupied, thus making it less reactive towards formaldehyde. Hence, it would possibly just act as a filler and not contribute to crosslinking (Pfungen, 2015). The H and G monomers, however, have both or one ortho- positions available, respectively, and are therefore more reactive. Since softwoods are predominantly composed of guaiacyl lignin, and grasses contain significant amount of H and G monomers, it follows that these may be more suitable for LPF resin production than hardwoods (Ferdosian, et al., 2017).

Similarly, lignin as a phenol substitute has less reactive aromatic sites than phenol (Figure 2.6). Compared to phenol, the ortho- positions of lignin rings are potentially occupied by methoxyl groups, whilst the para- positions of all lignin monomers are occupied by aliphatic side chains (Pfungen, 2015). This high degree of substitution causes considerable steric hindrances, thereby resulting in the low reactivity of lignin's aromatic sites. Additionally, the high stability of the phenoxyl radical during

radical coupling of monolignols, results in etherification of most phenolic hydroxyl groups within the lignin macromolecule, thus further reducing lignin's reactivity (Podschun, et al., 2015). As a result of all these factors, lignin has inferior crosslinking properties compared to phenol in PFRs. Hence, products using lignin-based adhesives usually require higher curing/press temperatures at longer heating times. Alternatively, additional cross-linking agents are required, such as epoxides, aldehydes, amines, etc. (Pizzi, 2003). This significantly deters the industrial implementation of lignin as a phenol substitute (Balgacem & Gandini, 2008).

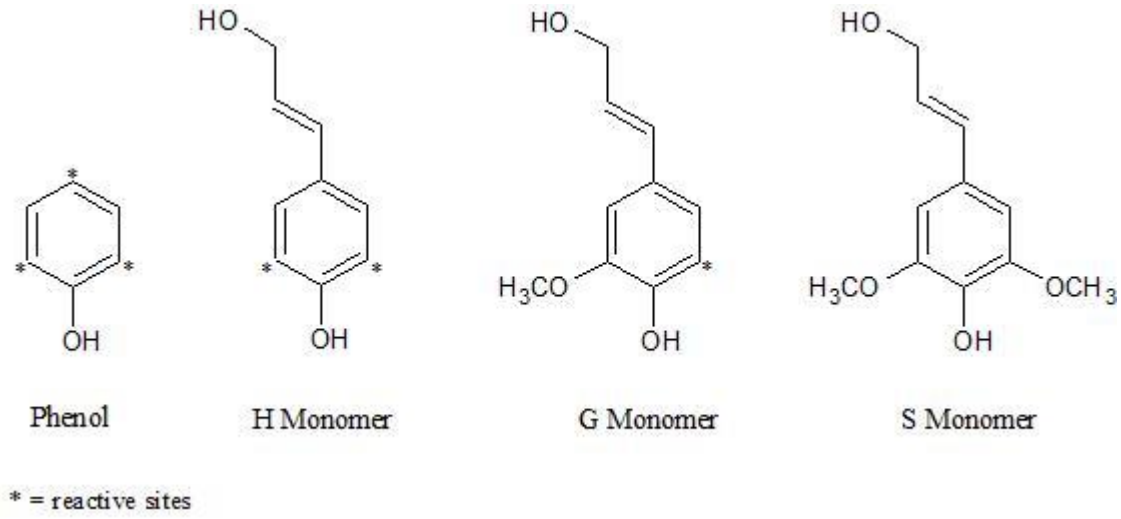

Figure 2.6: Comparison of reactivity between phenol and lignin monomers. Adapted from Hemmila et al (2017).

2.4.2. Synthesis

Most researchers have synthesised LPF resins using equipment and reaction conditions similar to that used in PF resin production.

Typically, LPF resins are formulated in three-neck round-bottom flasks equipped with condenser, thermometer, agitation, heating mantle, and a cooling system. Sodium hydroxide is usually used to catalyse the reaction, often as a 50 wt. % solution. Initially phenol and lignin are dissolved in sodium hydroxide at temperatures of 45-65°C. At a temperature of 60-65°C, formalin (37%) is slowly added to the reaction mixture in small increments and allowed to react for a period of time. In the second stage of the reaction, the mixture is heated to 80-85°C to initiate condensation reactions, and held there for 1-2 hours or until a desired target viscosity is reached. At this point, the precondensate (resin) is cooled to room temperature to stop further reactions, and often the resin is stored at temperatures below 0°C until it is used (Siddiqui, 2013; Pfungen, 2015; Ghorbani, et al., 2016). Alternatively, some studies have added the formalin and/or aqueous sodium hydroxide in steps during the course of the reaction (Zhang, et al., 2013; Yang, et al., 2014). This is most likely in an attempt to minimise

runaway reactions and ensure complete reaction of formaldehyde with the phenolic compounds. Another route to synthesise LPF resins is to copolymerize the lignin with a PF precondensate in the presence of a catalyst (Akhtar, et al., 2011). Lastly, final curing of the resin occurs upon application.

Certain reaction conditions favour undesirable side reactions during methylolation, such as the Cannizzarro reaction and the Tollens reaction. During the former, formaldehyde reacts with itself thereby reducing the amount of formaldehyde that can react with lignin, and during the latter, the aliphatic side chains are methylolated (Alonso, et al., 2001). Both of these reactions causes a reduction of aromatic methylol groups available for condensation reactions, which can lead to poor crosslinking and reduced strength. Studies investigating lignin methylolation have shown that these side reactions usually occur at increases in reaction parameters such as temperature, pH, catalyst concentration, and P/F ratios. Malutan, et al. (2008) studied the methylolation of alkali Sarkanda grass and wheat straw lignins, as well as the influence of reaction conditions. It was observed that at a pH greater than 12, and a NaOH/Lignin molar ratio of greater than 0.8, significant decreases in methylol content of the alkali lignins occurred, possibly due to consumption of formaldhyde by Cannizzarro reactions. It was concluded that a pH of 10.5, NaOH/Lignin ratio of 0.8, and reaction temperature of 50°C, were the optimum conditions to produce the best increase in methylol content for both Sarkanda grass and wheat straw lignins (Malutan, et al., 2008). Wang and Chen (2013) obtained similar results when they optimized the methylolation of steam exploded lignin. In particular, for increasing F/P mass ratios, the methylol content steadily decreases up until a ratio of 8:1, after which there is a sharp decrease. This was attributed to the fact that prior to the drop, formaldehyde exceeded the amount that lignin was capable of consuming, and afterwards there was not enough formaldehyde present for total consumption of lignin. It was suggested that this meant that only a limited amount of lignin can react with formaldehyde at any given time. This could be the reason that some studies prefer formalin addition in successive steps rather than one addition. Ultimately, it was found that a pH of 11.5, a temperature of 80°C, and a lignin to formaldehyde mass ratio of 8:1 were the optimum conditions needed to obtain the lowest free formaldehyde content, and the highest methylol content (Wang & Chen, 2013). Thus optimisation of the methylolation of a particular lignin source can provide the optimum conditions needed to obtain the highest methylol content whilst ensuring maximum consumption of formaldehyde.

Additionally, reaction parameters also influence the overall strength and curing properties of LPF resins. In a particular study, Abdelwahab and Nassar (2011) investigated the influence of F/P ratios, catalyst concentration, reaction temperatures, and reaction time on the adhesive strength and gel time of LPF resins prepared with kraft lignin. Consequently, increases in all parameters caused an increase in adhesive strength and a decrease in gel time up to a certain point, after which significant decreases

and increases were observed, respectively. From these results, it was determined that the optimum conditions for this system was at an F/P molar ratio of 10, a catalyst concentration of 10%, a reaction temperature of 80°C, and a reaction time of 4 hours (Abdelwahab & Nassar, 2011). Thus, optimising the LPFR synthesis procedure for different lignin sources is also advantageous to produce resins with satisfactory adhesive properties.

2.4.3. Unmodified Lignin

A wealth of research exists regarding the direct (unmodified) use of lignin as a phenol substitute in phenol-formaldehyde resins (PFRs). Various technical lignins have been investigated, most notably pulping- and biorefinery-based technical lignins.

Danielson and Simonson (1998) investigated the potential of using softwood kraft lignin as a phenol substitute in PFRs intended for plywood application. The kraft lignin was precipitated from black liquor using carbon dioxide at temperature of 60-70˚C, after which it was filtered and washed with water. LPF resins were then made at phenol substitution levels ranging from 0-80% (labelled LPF0-LPF80). Additionally, a commercial PFR was used for comparison. It was found that LPF resins containing up to 60% lignin produced shear strengths comparable or superior to that containing 0% lignin; above 60%, shear strength diminished significantly. Ultimately it was decided that a substitution level of 50% was ideal in order to maintain resin viscosity, storage stability and bonding ability similar to that of PFRs. However, the manufacture of plywood using LPF50 resin required a 30% increase in press time to compensate for the low curing rate, as compared to that of commercial PFRs (Danielson & Simonson, 1998). In another study, Akhtar et al. (2011) considered the use of lignosulphonate as a phenol substitute in PFRs. The lignosulphonate was precipitated from spent sulphite liquor using concentrated hydrochloric acid, and the biomass source was a mixture of grasses, i.e. bagasse, wheat straw, and kiagrass. LPF resins were synthesised at substitution levels of 0-50%, with the LPF0 resin used as a reference. While all LPFRs proved to be water resistant, it was observed that the shear strength of the LPF resins were only comparable to that of PFRs up to a 20% substitution rate. Thereafter, shear strength decreased, with a significant drop witnessed above 30% incorporation of lignin. The LPF20 resin exhibited maximum shear strength and wood failure, even when compared to the LPF0 resin (Akhtar, et al., 2011). Pfungen (2015) used sarkanda grass soda lignin to synthesise LPF resins with substitution levels of 0-40%, with the LPF0 resin used as a reference. Although the overall goal was the development of a synthesis procedure for LPF resins, an important objective was to produce LPF resins with comparable properties to that of commercial PFRs. It was ultimately found that resins with a 5% lignin substitution level exhibited the highest lap shear strength at standard climate conditions. Additionally, it was found that with increasing lignin substitution levels, the free

formaldehyde content increased, whilst curing of the resin was delayed (Pfungen, 2015). In a similar study, Ghorbani et al. (2016) also synthesised LPF resins at substitution levels of 20 and 40%, but using four different technical lignins, i.e. sarkanda grass soda lignin, wheat straw soda lignin, pine (softwood) kraft lignin, and beech (hardwood) organosolv lignin. Once again, a PFR (LPF0 resin) was synthesised to be used as a reference. The tensile shear strength of the resins were investigated as a function of hot press time, and the thermal behaviour of resins were also studied. In general, it was found that increasing the substitution rate caused a reduction in shear strength, and deferred the curing process of the LPF resins. When comparing between lignins, only the pine kraft LPF20 resin was able to achieve shear strengths similar to the LPF0 resin with the same hot press time. Its curing performance was also most comparable to that of the LPF0 resin (Ghorbani, et al., 2016).

Zhang et al. (2013) prepared LPF resins using four different biorefinery residues, i.e. ethanol residue, butanol residue, xylitol residue, and lactic acid residue. These were obtained from processes that enzymatically hydrolysed lignocellulosic biomass, thereby leaving behind a lignin-rich residue. LPF resins were synthesised at a substitution rate of 50%, with a PFR/LPF0 resin synthesised for comparison. Results revealed that the LPF50 resins all displayed lower free phenol contents than the PFR, whilst the bonding strengths were also comparable to that of the PFR. However, the overall thermal stability of the LPF50 resins were lower than that of the PFR, and its free formaldehyde content was much higher than the PFR. Amongst the different LPF50 resins, the xylitol LPFR showed the greatest thermal stability, whilst the ethanol LPFR contained the lowest free formaldehyde and phenol contents, and displayed the highest bonding strength (Zhang, et al., 2013). Qiao et al. (2016) investigated the effect of phenol substitution rate on the adhesive properties of enzymatic hydrolysis (EH) lignin. EH lignin was obtained from bioethanol residue (ER) using alkali extraction, followed by acid isolation. The residue, in turn, was acquired from a pilot plant whereby steam-exploded cornstalk material was converted to bioethanol using the SSF method. LPF resins were synthesised at substitution levels of 10-60%. A PF resin was also synthesised for comparison. Again, up to 50% phenol could be replaced, after which bonding strength of the LPF resins were adversely affected. It was also found that increasing lignin content increased free formaldehyde content, and negatively impacted the resins' thermal stability. However, it was observed that the LPFs had a slightly lower curing temperature and lower free phenol content than the PFR/LPF0 resin (Qiao, et al., 2016).

In general, it seems that most of the literature regarding LPF resins are in agreement on the direct use of technical lignins, i.e. acceptable adhesive properties are restricted to low phenol substitution levels and the curing properties of these LPF resins are inferior to conventional PFRs, thus rendering most LPF resins non-viable. However, there are a few studies that have managed to obtain acceptable LPF adhesives at high phenol substitution rates. In the study by Abdelwahab and Nassar (2011), the effect

of lignin content was also investigated in addition to the optimisation of reaction conditions. Bagasse kraft lignin was isolated from black liquor via acid precipitation, followed by filtration and washing with hot distilled water. The dried kraft lignin was then used to synthesise LPF resins with lignin contents in the range of 0-90%, with the LPF0 resin used as a reference. From the results, it was observed that increasing lignin content resulted in increased adhesive strengths and decreased gel times. A lignin content of 90% produced the highest shear strength and highest crosslinking density (lowest gel time) at optimum reaction conditions of 80°C, 4 hours, F/P molar ratio of 10, and catalyst concentration of 10%. These favourable results were attributed to the high hydroxyl content of the kraft lignin which tends to make lignin more reactive towards formaldehyde. The species and pulping process of the lignin could also be an attributing factor since grasses are known to be GH lignins, and the study mentions that kraft lignins contain a moderate number of unsubstituted 3- and 5-positions available to react with formaldehyde. Additionally, although the LPF resin had a lower thermal stability than the PF resin, the LPF resin was found to have a higher curing rate. The content of free formaldehyde and free phenol was not considered in this study (Abdelwahab & Nassar, 2011). In another study by Kalami et al. (2017), it was shown that 100% phenol replacement by unmodified lignin was possible with acceptable resin properties. The lignin sample was obtained from a cellulosic bioethanol process whereby corn stover undergoes dilute-acid pre-treatment followed by enzymatic hydrolysis. The lignin samples were purified by dissolving it in a sodium hydroxide solution so that the impurities can be filtered out. Thereafter the filtrate was heated to 80°C and the lignin was isolated using acid precipitation with sulphuric acid, after which it was filtered and washed several times with distilled water. An LPF adhesive with a phenol substitution level of 100% was then produced, and a commercial PF adhesive was obtained for comparison. Both the dry and wet shear strength of the LPF100 adhesive was similar to that of the commercial PFR, and statistical analysis showed no significant between the mean shear strength of the LPF100 adhesive and the PF adhesive. Additionally, the energy required for curing the LPF100 adhesive was half of that of the PFR, however the curing temperature, gel time, and free formaldehyde content of the LPF100 adhesive was slightly higher than that of the PF adhesive (Kalami, et al., 2017).

While a few studies have managed to successfully utilise unmodified lignin at high phenol substitution levels to produce LPF resins comparable to conventional PFRs, a large volume of research indicates that this is either not possible or not viable. From the literature we can also see that there is a high degree of variability in resin characteristics and performances, possibly due to the use of different lignin feedstocks and slight differences in isolation, purification and synthesis procedures. Incidentally, biorefinery-based technical lignins seem to produce slightly better resin properties at marginally higher phenol substitution rates. This could be due to the moderate reaction conditions of

most biorefinery processes, thus allowing lignin molecules to retain more hydroxyl groups thereby causing them to potentially be more reactive than pulping lignins (Zhang, et al., 2013). In the long run, the ability to completely replace phenol in PFRs with unmodified lignin is an ideal that would significantly relieve dependence on fossil fuels in the wood industry, and would mean complete efficiency of waste resources for pulping mills and biorefinery. Thus, there is ongoing research on the feasible utilisation of unmodified lignin as a phenol substitute.

2.4.4. Lignin Modification

In an attempt to solve the ongoing challenges associated with the direct use of lignins, various techniques have been developed over the years to functionalize lignins in such a way that new active sites or functional groups on the molecule are generated or exposed, thereby making it more suited for use in higher value applications. Although certain lignins may already have high functionality (high hydroxyl content, high phenol content, etc.), a lot of these reactive sites/groups are often sterically hindered by other functional groups or concealed within the high cross-link density of lignin. By adding or enhancing these active sites, certain properties of lignin can be improved upon, such as its reactivity, solubility, processability, and brittleness (Upton & Kasko, 2015).

Typically, lignin functionalization falls under two main categories, i.e. depolymerisation and modification (Matsushita, 2015). In the former, the three-dimensional structure of lignin is thermo-chemically broken down to oligomeric or monomeric units (Siddiqui, 2013), and these can then be re-built into functional materials (Matsushita, 2015) or aromatic chemicals (Westwood, et al., 2016). Modification involves altering the chemical structure of the lignin macromolecules, usually by chemical means, whilst retaining polymeric properties (Matsushita, 2015). Both approaches have their pros and cons, but it is reported that energy consumption may be lower in chemical modification systems (Matsushita, 2015), which may be a factor as to why this approach is more widely investigated with regards to LPF resin synthesis.

Depolymerisation techniques essentially involve the application of heat or thermal energy to the lignin sample, in the presence/absence of catalysts, solvents and/or additives. Common techniques include pyrolysis, hydrolysis, oxidation, hydrogenolysis, and liquefaction. Pyrolysis entails thermal treatment in the absence of oxygen at temperatures of 120-300°C for weaker bonds, or greater than 500°C for stronger bonds and aromatic ring cracking. Important products include solid char, lower molecular weight liquids such as monolignols and monophenols, and non-condensable gases like carbon monoxide, gaseous hydrocarbons, and carbon dioxide. Hydrolysis employs the use of sub- or supercritical water to rupture lignin's ether bonds in the presence of an acid or alkaline catalyst. The resultant products have a high phenolic hydroxyl content (Siddiqui, 2013). Hydrolysis can also be

facilitated by enzymes, which is a process widely used in the biorefinery industry for the production of biofuels, as seen from the studies discussed in section 2.4.3. Oxidation, as well as oxidative cracking, is capable of cleaving bonds and/or altering the structure of the lignin molecule depending on the type of oxidizing agent, catalyst and temperature range used. As a result, products include a variety of aromatic aldehydes as well as hydroxycinnamic acids (Hu, et al., 2011). Common oxidants for lignin include nitrobenzene, hydrogen peroxide, copper (II) oxide (Hu, et al., 2011), and laccase enzymes obtained from white rot fungi (Dunky, 2003). Hydrogenolysis, or hydrogenation, is performed in the presence of hydrogen at temperatures of 300-600°C. It is of particular interest in the production of monophenols from lignin, and the production of reformulated gasoline (Siddiqui, 2013). Ultimately, lignin valorisation via the depolymerisation route has been limited, with the only industrialised process being the production of vanillin from lignin; specifically the production of vanillin from the oxidation of spent sulphite liquor as patented and operated by Borregaard Industries Ltd (Westwood, et al., 2016).

As mentioned earlier, modification alters the chemical structure of lignin to improve reactivity, without necessarily degrading the polymeric structure or its properties. These techniques usually target two crucial reactive sites in lignin, i.e. the C_5 position on H and G monomers, and the numerous phenolic and aliphatic hydroxyl groups in the lignin macromolecule (Westwood, et al., 2016).In the case of using lignin as a phenol substitute in PF resins, chemical modification via phenolation, methylolation, and demethylation are the most widely reported modification techniques (Matsushita, 2015). Phenolation involves the thermal treatment of lignin with phenol in an acidic medium, usually in the presence of organic solvents such as methanol or ethanol (Hu, et al., 2011). This results in the incorporation of phenolic groups at aliphatic hydroxyl positions on the lignin molecules, however side reactions may cause fragmentation and reduced molecular weight. The phenolated lignin has a higher phenolic hydroxyl content which is more suited for subsequent co-polymerization reactions (Westwood, et al., 2016). Methylolation, also known as hydroxymethylation, involves the introduction of methylol/hydroxymethyl groups onto the lignin aromatic ring, specifically at the C5 position of G monomers (Westwood, et al., 2016). As discussed in previous sections, methylolation is one of the main addition reactions that occurs during the initial stages of PF resin synthesis, and details of the chemistry and reaction conditions with regard to lignin are given in sections 2.4.1, and 2.4.2. The resultant methylolated lignin has a higher content of reactive hydroxyls for ensuing condensation reactions (Westwood, et al., 2016). Demethylation involves the removal of a methyl (CH_3) group, usually by replacement with a hydrogen atom (Clayden, et al., 2001). Hence, the removal of methoxyl ($-OCH_3$) groups results in the formation of catechol moieties, which are more reactive than phenol due to the additional hydroxyl groups. Thus, catechol formation results in

increased phenolic hydroxyls and additional binding sites on the lignin molecule, which ultimately enhances lignin reactivity (Hu, et al., 2014; Li, et al., 2016). Demethylation can be achieved chemically, particularly via sulphur mediated processes, or enzymatically via oxidative degradation. Some studies have also used brown-rot fungi to demethylate lignin and partially oxidise side chains (Matsushita, 2015). Ultimately, it has been found the modification via these methods can effectively improve lignin reactivity such that resultant LPF resins have shown comparable mechanical and curing properties to that of PFRs, albeit at low phenol substitution levels (Wang & Chen, 2013; Hu, et al., 2014; Yang, et al., 2014; Li, et al., 2016).

For synthesis of LPF resins, methylolation and phenolation are industrially the most promising. Despite the success of sulphur-mediated demethylation at a research level, most of these methods have not reached industrial application, due stringent reactor requirements and harsh process conditions. Additionally, the process also requires high pressure reactors, the likes of which needs a high capital investment (Li, et al., 2016). Although fungal and bacterial demethylation have been studied for many decades (Li, et al., 2016), it has failed to attract any attention thus far (Hu, et al., 2011), possibly due to technical difficulties and high capital costs. With enzymatic demethylation, the oxidation step leads to an additional costs which are not justified as increases in lignin reactivity is not always guaranteed (Matsushita, 2015). Meanwhile phenolation of lignin can be incorporated into the manufacture of PF resins under basic or acidic conditions (Siddiqui, 2013), with both lignin and phenol contributing to the total phenol content in the reactions. An additional advantage of phenolation is that it can process raw lignin without purification. However, the use of phenol is costly, and since the objective of phenol substitution is to use less of this material, the use of it as a modification agent might hinder its practical implementation (Hu, et al., 2011). Similar to phenolation, one of the key attractions of methylolation is that the methylolated lignin can be directly added to the PF resin, and polymerize with it during the hot pressing process (Wang & Chen, 2013), or it can be added to the PF reaction mixture during the condensation stage. This makes methylolation a flexible process that can be easily integrated into the PF resin synthesis process on an industrial scale (Wang & Chen, 2013) whilst remaining relatively inexpensive to install (Perez, et al., 2007). However, there are some drawbacks to this method such as comparatively long reaction times, and limited increases in reactive sites due to the inability of methylolation to saturate available meta-positions on the aromatic ring (Hu, et al., 2014).

Ultimately, modification methods, and any other lignin functionalization process for that matter, must satisfy two requirements to be commercially viable. One, the process and any chemicals used must be of low cost, otherwise the main incentive for using lignin will be lost, i.e. low-cost feedstock compared to phenol. Second, the process should be applicable to any lignin feedstock, regardless of

biomass source or isolation process (Westwood, et al., 2016). Thus far, no method has been able to fulfil these requirements in addition to effectively enhancing lignin reactivity (Hu, et al., 2011). However, the potential of lignin cannot be ignored, thus efforts are ongoing to develop feasible modification procedures for lignin, particularly for incorporation in PFRs.

2.5. Gaps in Literature

At a global research level, several technical lignins have been studied in depth to determine its potential as a phenol substitute in phenol-formaldehyde resins (PFRs). Literature indicates that different studies have achieved varying degrees of success in this regard, although this is primarily at low phenol substitution rates. In contrast, a few studies have successfully incorporated lignin into PFRs at high substitution levels of 90-100% (Abdelwahab & Nassar, 2011; Kalami, et al., 2017). Ultimately, little to none of these findings have reached industrialization on a major scale yet. Similarly, as Ghaffar and Fan (2014) mentioned in their review, most studies in this field of work have not addressed nor investigated the problems associated with industrializing lignin-phenol formaldehyde (LPF) resins (Ghaffar & Fan, 2014).

Regarding local research on lignin and phenolic resins, available literature on this topic is not recent. Truter (1990) investigated the methylolation of hardwood kraft lignin extracted from crude black liquor, and its subsequent grafting with resorcinol to form a wood adhesive. Conradie (1990) studied the epoxidation of both pine kraft lignin and soda/AQ eucalyptus lignin with epichlorohydrin to form epoxy resins. Ysbrandy (1992) evaluated the use of autohydrolysis bagasse lignin and phenosolvan pitch for the development of binders for wood composites, specifically for moulding and laminating purposes. All of these studies concluded promising findings with recommendations for improvements (Conradie, 1990; Truter, 1990; Ysbrandy, 1992). In recent times, South African technical lignins have been characterized in detail by various researchers, but not in the context of phenol substitution in PFRs. Tyhoda (2008) characterised South African technical lignins and other ligneous residues, and investigated its use in the production of slow nitrogen release fertilisers. Namane (2016) examined the isolation and recovery of lignin from local kraft black liquor, followed by detailed lignin characterisation, and an evaluation of its valorisation via production of lignin chars and activated carbon. Naron et al. (2017) carried out a detailed characterisation of South African pulping lignins and developed a new pyrolysis-based method for determination of monomeric content in lignin (Tyhoda, 2008; Namane, 2016; Naron, et al., 2017).

To my knowledge, only Kalami et al. (2017) has, to date, managed to achieve 100% phenol substitution by lignin in PFRs with favourable results. However, it should be noted that their study involved biorefinery technical lignins (Kalami, et al., 2017). Furthermore, no study to my knowledge

has investigated the potential of South African technical lignins with specific regard to substitution of phenol in PFRs. As such, there is potential to investigate the use of South African spent pulping lignins as a total phenol replacement (100% substitution) in phenol formaldehyde resins.

2.6. Aims & Objectives

The aim of this project is to investigate the potential of using six South African pulping-based lignins as a phenol substitute in phenol-formaldehyde resins, for use as a wood adhesive in wood composites and wood construction. To achieve this goal, the following objectives were drawn up:

I. Isolation of technical lignins from spent pulping liquor, where necessary.
II. Purification of technical lignins to reduce ash content, where applicable.
III. Characterisation of technical lignins to determine important properties such as ash content, functional group content, molecular weight, and thermal behaviour.
IV. Synthesis of lignin-phenol-formaldehyde (LPF) resins at 100% phenol replacement.
V. Characterisation of LPF100 resins to determine curing properties and bonding strength.
VI. Comparisons between the different lignin-based resins, as well as between LPF resin and commercial wood adhesive (Bondite).
VII. Final conclusions and suggestions on the best suited pulping lignin(s) for use as a phenol substitute in PFRs.

Chapter 3: Characterisation of Lignin & Lignosulphonate Samples

3.1. Introduction

Lignin has great potential for use in a variety of application, as discussed in Section 2.1.6. Due to the inherent complexity of lignin, and the structural differences between species and isolation processes, different technical lignins would have different properties. Thus, it would follow that a particular application would prefer lignins with a certain set of characteristics. For polymer applications, lignins with high phenolic contents (Westwood, et al., 2016) and high thermal decomposition temperatures (Ferdosian, et al., 2017) are favoured. Other attractive qualities for adhesive applications include low glass transition temperatures (T_g), high hydrophobicity, and a low polydispersity (Ferdosian, et al., 2017). Additionally, lignins with high molecular weights supposedly possess a higher level of cross-linking (Pizzi, 2003).

To determine such properties of lignins, multiple analytical techniques exist. Some of the more established and relevant methods includes thermogravimetric analysis (TGA) for determination of thermal decomposition properties, gel permeation chromatography (GPC) for determination of molecular weights and polydispersity (Tian, et al., 2016), and spectroscopy techniques for structural analysis. In particular, Fourier transform infrared (FTIR) spectroscopy and nuclear magnetic resonance (NMR) spectroscopy are commonly used to obtain information on the structure of lignin, specifically regarding functional groups and lignin monomers. Additionally, NMR may be used to obtain information on the type of bonds that exist within the material (Lupoi, et al., 2015).

Most of these analyses require relatively pure, low-ash samples so as to not interfere with the measurements or damage equipment components. Additionally, most high-end applications prefer lignins of minimal impurities (Fatehi & Chen, 2016). As a result, lignin samples are usually purified prior to characterisation such that the ash content is $\leq$5% (Thies & Klett, 2016).

3.2. Materials & Methods

3.2.1. Experimental Approach

Experimental work started with the procurement of five lignin samples from four South African pulping mills. A sixth lignin sample was acquired from the Forestry and Wood Sciences department of Stellenbosch University, to be used as a reference sample. These lignin samples came from different biomass origins and isolation processes, thus creating a wide sample range of pulping lignins available in South Africa. Four of the five industrial lignins required sample preparation, which included sample purification. Subsequently, the samples were divided into three categories according

to plant origin or pulping process; i.e. kraft lignins, bagasse lignins, and lignosulphonates. Thereafter, various compositional, structural, and thermal analyses were performed in order to gain insight on the structure and chemistry of the different lignin samples. This study did not explore different lignin isolation techniques, nor did it focus on the optimisation of the chosen lignin isolation and purification methods. Instead, established and cost-efficient procedures were used, as outlined in the relevant literature.

3.2.2. Materials

Six lignin samples were used for experimental work, five of which were received from Sappi and MPact's pulping mills. The details of these samples are summarised in Table 3.1, along with the sample ID and group classifications that will be used henceforth. With the exception of SL-E-T and SE-SCB, the samples were received in the form of spent pulping liquor, and thus required further processing to extract the lignins and, where possible, purify them.

Table 3.1: Sources of experimental lignin samples

Biomass Origin	Pulping/Isolation Process	Mill Source	Sample ID	Group Classification
P. patula (Softwood)	Kraft	Sappi, Ngodwana	KF2-P-N	Kraft Lignins
E. grandis (Hardwood)	Kraft with prehydrolysis	Sappi, Ngodwana	KF3-E-N	
Sugarcane Bagasse (SCB)	Soda	Sappi, Stanger	S-SCB-S	Bagasse Lignins
Sugarcane Bagasse (SCB)	Steam Explosion	-	SE-SCB	
E. grandis (Hardwood)	Neutral Sulphite Semi-Chemical (NSSC)	Sappi, Tugela	SL-E-T	Lignosulphonates
Hardwood/Softwood/SCB Mix	Neutral Sulphite Semi-Chemical (NSSC)	MPact, Piet Retief	SL-M-PR	

Both the KF2-P-N and KF3-E-N lignins were extracted from spent kraft liquors obtained from Sappi's Ngodwana mill. Besides the difference in biomass origin, there was also a slight difference in the pulping process used. The KF3-E-N sample had a prehydrolysis pretreatment step whereby the wood chips were treated with steam or hot water prior to the cook stage, thus isolating some hemicelluloses and a small part of the lignin from the wood chips. This step is usually employed for the manufacture of dissolving wood pulp (Fatehi & Chen, 2016). Thus it would follow that the spent

liquor obtained from this process would contain less hemicelluloses and lignin than that obtained from a regular kraft cook.

SL-E-T was received as a ready-for-sale product from Tugela mill, whereby the spent liquor had already been concentrated and dried into a fine powder. Thus, no further processing was required for experimental purposes.

SE-SCB was purchased from Sigma-Aldrich Pty. Ltd., SA by the Department of Forestry and Wood Sciences, and was received as a purified lignin powder. As a result, this sample required no further processing. It is understood that the preparation of this lignin involved steam explosion of sugarcane bagasse, followed by alkali extraction of the lignin. Due to the nature of the steam explosion process, biopolymer fibers can be extracted with minimal degradation (Martin-Sampedro, et al., 2011). As such, it would follow that steam explosion lignins may have a higher resemblance to native lignin than other pulping lignins, especially considering the minimal use of chemicals and lack of sulphur. Thus, the SE-SCB lignin will be used as a reference sample for comparison against the commercially-available industrial lignins.

3.2.3. Preparation of Lignin Samples

Pulping liquor contains both organic and inorganic components. The former consists predominantly of lignin, in addition to extractives and derivatives from the wood/plant species used. The inorganic components consist mainly of pulping chemicals, as well as the transformation products of these pulping chemicals, and the ash components from the plant/wood species used (Tyhoda, 2008). As a result, direct application of lignin in the form of spent pulping liquor may have negative or unknown implication on the product due to the presence of other components. Hence, isolation and extraction of the lignin from pulping liquor is usually performed, specifically for higher-value applications.

The kraft lignin samples (KF2-P-N, KF3-E-N) and soda lignin sample (S-SCB-S) was received in the form of spent pulping liquor. Lignin isolation was achieved by acid precipitation with 98% sulphuric acid (H_2SO_4). As described in Naron et al. (2017), 98% H_2SO_4 was slowly added to the pulping liquor with gentle stirring until the pH dropped to 2 from an initial pH of ~12-13. Generally, it was found that the amount of acid added required to drop the pH to 2 was approximately 5mL of acid for every 200mL of liquor. Once a pH of 2 was achieved, the liquor was left to stand for a period of 24 hours. Thereafter, precipitate was recovered by centrifuging the mixture for 10 minutes at 7000 rpm. The supernatant was then discarded and the solid mass was washed with distilled water and centrifuged once again. This step was repeated twice more, after which the solid mass was placed into tinfoil trays and left to air dry overnight (Naron, et al., 2017). The dried lignin solids were then collected and

milled to a particle size of 0.5 mm using an Ultra Centrifugal Mill – ZM 200 (Retch). The lignin powders were then stored in airtight plastic bags until further use.

To ensure that the isolated kraft and soda lignins have minimal impurities, an acid purification step was employed. According to methods described in Naron et al. (2017), the isolated lignin powders were suspended in a 1N sulphuric acid solution based on a proportion of 200mL of acid solution for every 1g of dried lignin. This suspension was allowed to stir for a period of 24 hours, after which the lignin was recovered by centrifuging the mixture for 10 minutes at 7000 rpm. The solid mass was then washed with distilled water and centrifuged for another 10 minutes at 7000 rpm; this step was repeated twice more. Thereafter, the solids were placed into tinfoil trays and left to air dry overnight (Naron, et al., 2017). The yield of purified lignin was generally found to be 60-70%, i.e. for every 50g of isolated lignin, ~30-35g of purified lignin was obtained. The dried, purified lignin powders were then sub-sampled to ensure a uniform sample, after which they were stored in airtight plastic bags until further use.

MPact's sodium lignosulphonate (SL-M-PR) was received in the form of a spent pulping liquor. Since lignosulphonates are soluble in water and acid solutions, recovering and purifying the lignin solids by acid precipitation and acid purification were not suitable. Instead, the pulping liquor was poured into tinfoil trays (approximately 1L per 32 x 26.5 x 6cm tray), and allowed to dry for 3-4 weeks in a nursery which had a relative humidity of 40-54% and a temperature of 30-50 ˚C. Thereafter, the tinfoil trays were put into a 40˚C oven for approximately 2 more weeks. The dried solids were then collected and immediately sealed in an airtight plastic bag since lignosulphonates are highly hydrophilic. Then, using a Ring and Puck Pulverizer, the lignosulphonate solids were milled into a fine powder, and then immediately stored in airtight plastic bags until further use. Sub-sampling was not possible due to the rapid absorbance of moisture.

3.2.4. Characterisation Methods

Proximate analyses, such as moisture and ash content, were determined according to methods adapted from the NREL/TP-510-42621 and NREL/TP-510-42622 standards, respectively. For determination of moisture content, clean watch glasses were pre-dried in a 105˚C oven for 4 hours, after which they were removed and allowed to cool in a desiccator. Thereafter, the weight of the watch glasses were recorded, and 2g of each sample was weighed and loaded onto a watch glass. The watch glasses containing the samples were then placed in the 105 ˚C oven for 24 hours. Subsequently, the watch glasses were removed from the oven and allowed to cool to room temperature in a desiccator, after which the weight was recorded. The watch glasses were then placed back in the oven for 1 hour to ensure a constant dry weight. Thereafter, the watch glasses were removed from the oven and placed

in the desiccator to cool to room temperature. The oven dry weight (ODW) of each sample was recorded and moisture content was calculated according to Equation 3.1. All samples were analysed in duplicate. For determination of ash content, clean crucibles were pre-dried in a 105˚C oven for 24 hours, after which they were cooled in a desiccator. The weight of each crucible was then recorded, after which 1.5g of each oven dried sample was weighed and loaded onto a crucible. The crucibles containing the kraft and bagasse lignin samples were then loaded into a muffle furnace, which was gradually heated to 575˚C, over a period of 30-45 minutes. Thereafter, the temperature was held at 575˚C for four hours, after which the crucibles were removed from the furnace and allowed to cool for 1 hour in a desiccator. The weight of the crucibles containing the ash samples were then recorded, and ash content was calculated according to Equation 3.2. The lignosulphonate samples were ashed in a similar way with the exception of the furnace temperature. Since lignosulphonates are not purified, the high inorganic content requires a higher ashing temperature to obtain an accurate representation of the samples' ash contents. Thus, the crucibles containing the lignosulphonate samples were loaded into a muffle furnace equipped with a ramping program. The furnace was then heated to 250˚C over a period of 25 minutes, and then held at that temperature for 30 minutes. Thereafter, the furnace was heated to 800˚C over a 40 minute period, and held at that temperature for 16 hours. Finally, the furnace was cooled to 200˚C at which point the crucibles were removed and left to cool for 1 hour in a desiccator. The weight of the crucibles containing the ash samples were then recorded and the ash content was calculated according to Equation 3.1.

$$\% \text{ Moisture} = 100 - \left(\frac{(Weight\ dry\ watch\ glass + sample - Weight\ of\ dry\ watch\ glass)}{Weight\ of\ sample}\ x\ 100\right)$$

Equation 3.1

$$\% \text{ Ash} = \frac{(Weight\ crucible + ash - Weight\ of\ crucible)}{ODW\ of\ sample}\ x\ 100$$

Equation 3.2

Elemental analysis of organic components in the lignin samples were conducted at the Central Analytical Facilities (CAF) of Stellenbosch University. A Vario EL Cube Elemental Analyser was used to determine the composition of carbon (C), hydrogen (H), nitrogen (N) and sulphur (S).

Total sugar content was determined at the Sappi Technology Centre using a Thermo Scientific High Performance Anion Exchange Chromatography system equipped with Pulsed Amperometric Detection (HPAE-PAD). Only the kraft and bagasse lignins were analysed; lignosulphonates were not suitable for HPLC analysis as the impurities in the samples would damage the column and

interfere with the separation process. A 10% solids solution was made with the kraft and bagasse lignin samples using HPLC-grade water. The aqueous samples were stirred well and 5mL of each aqueous sample was quickly pipetted into a glass serum bottle, before the lignin could settle out of solution. Thereafter, 8.4mL of HPLC-grade water, and 1mL of 72% sulphuric acid was pipetted into each serum bottle. The serum bottles were sealed with metal caps and autoclaved for 1 hour at 100˚C. The bottles were then allowed to cool to room temperature, after which 5mL of each autoclaved sample was filtered into a 15mL plastic vial using disposable syringes equipped with micro filters. Next, 1mL of the filtered sample and 9mL of HPLC-grade water was pipetted into another 15mL plastic vial and mixed on a vortex machine. Subsequently, 1mL of the diluted sample was pipetted into a HPLC glass vial which was then capped. All the prepared samples were then loaded onto the HPAE-PAD system, after which the total content of glucose, galactose, mannose, xylose, arabinose, and rhamnose was determined.

Molecular weight was determined by Gel Permeation Chromatography (GPC). Lignosulphonates could not be analysed due to the high ash content that would damage the column, thus only the purified lignins were analysed. Prior to analysis, the bagasse and kraft lignins had to be acetylated, and this was done according to the method described in Naron, et al. (2017). First, 0.5g of each lignin sample was weighed into conical flasks. A pyridine-acetic anhydride solution was made using the volumetric ratio of 1:1, after which 20mL of the pyridine-acetic anhydride solution was added to each flask. The flasks were then placed in a shaking oven set to 25˚C and 120 rpm for 24 hours. Thereafter, 100mL of 0.1M hydrochloric acid was added to each flask, and the mixture was then qualitatively transferred to centrifugation bottles. The acetylated samples were then centrifuged for 5 minutes at 8000 rpm, and the supernatant was discarded. The precipitates were then washed twice with distilled water, and after each wash the mixture was centrifuged for 5 minutes at 8000 rpm. The acetylated lignin samples were then placed in tinfoil trays and left to air dry overnight (Naron, et al., 2017). The acetylated samples were then prepared for analysis; approximately 4mg of each sample was dissolved in 2mL of HPLC-grade tetrahydrofuran (THF) stabilised with 0.125% butylated hydroxytoluene (BHT). The mixture was then left to stand for 24 hours to check if the lignin samples re-precipitate. All lignin samples except the S-SCB-S sample remained dissolved in solution. The dissolved samples were then filtered in GPC vials using a syringe filter. The samples were then run on the GPC system to determine the average molecular weight (M_W), the number average (M_N), and the polydispersity (M_W/M_N). The GPC system consisted of a Waters 1515 isocratic HPLC pump, a Waters 717_{plus} auto-sampler, a Waters 600E system controller (run by Breeze Version 3.30 SPA), a Waters in-line Degasser AF, a Waters 2414 differential refractometer was used at 30°C, and a Waters 2487 dual wavelength absorbance UV/Vis detector operating at variable wavelengths. THF stabilized with

0.125% BHT was used as the mobile phase at a flowrate of 1 mL/min. An injection volume of 100µL was used, and the column oven was maintained at 30°C. Columns used included two PLgel (Agilent Technologies) 5µm Mixed-C (300 x 7.5mm i.d.) columns and a pre-column, PLgel 5µm Guard (50 x 7.5 i.d.). Calibration using narrow polystyrene standards ranging from 580 to $2x10^6$ g/mol. The S-SCB-S sample was re-acetylated and then dissolved in THF once more, however it was unsuccessful once again. Thus, it was also not analysed as re-precipitation in the column would damage the column and interfere with the analysis.

Fourier Transformed Infra-Red (FTIR) Spectroscopy was performed using a Thermo Scientific Nicolet iS10 Spectrometer (Thermo Scientific, Waltham, MA) equipped with a Smart iTR ATR accessory, with a diamond crystal. Spectra were obtained in Attenuated Total Reflectance (ATR) mode at a resolution of 4 cm^{-1}, 64 scans per sample, and within the absorption bands in the 4000-600 cm^{-1} region. Collection and processing of data was done with Thermo Scientific OMNIC software. Spectra was baselined corrected, and assignment of absorption bands were based on relevant literature. Principal Component Analysis (PCA) was performed using Statistica software (Version 13.2) to determine any spectral differences in chemical structure and composition. The PCA focused on the spectral region of 1800-600 cm^{-1} since this a complex band region containing most of the relevant information pertaining to lignin.

As described in Yang et al. (2016), quantitative ^{13}C NMR spectroscopy was performed using a Bruker AVIII 400 MHz spectrometer at 25 ˚C, using DMSO-d_6 as the solvent. About 125 mg of the lignin was dissolved in 0.5 mL of DMSO-d_6. Spectra was then recorded in FT mode at 100.6 MHz. Inverse-gated decoupling sequence was used at a pulse angle of 90˚, an acquisition time of 1.4s, a relaxation delay of 2s, 64 000 data points, and 30 000 scans. To provide complete relaxation of nuclei, chromium (III) acetylacetonate (0.01 M) was added to the lignin solution.

To observe the thermal decomposition behaviour of the lignin samples, Thermogravimetric Analysis (TGA) was performed using a TGA Q50 thermogravimetric apparatus. Approximately 5 ± 0.5 mg of sample was placed into an aluminium crucible which was then loaded onto the TGA pan. Using a heating rate of 10˚C/min, the analysis was conducted under argon atmosphere from 20-30 ˚C up to 595 ˚C. The resultant data was used to construct weight loss versus temperature curves, from which degradation curves (dTG) where produced to determine the temperature at which maximum degradation occurs.

3.3. Results & Discussion

3.3.1. Compositional Analyses

Results from the proximate, elemental and sugar analyses are summarised in Table 3.2. The ash content of the purified lignins, i.e. the kraft and bagasse lignins, are well below the recommended level of ≤ 5% (Thies & Klett, 2016). Additionally, they agree with literature in that the ash content of woody lignins are usually below 1%, whilst grasses generally possess ash contents in the range of 2-5% (Chen, 2014). In contrast, the lignosulphonates have ash contents in the range of 28-43%. This is expected as the lignosulphonates could not undergo acid purification due to its high solubility in water and acid solutions. As a result, the lignosulphonate samples were not suitable for subsequent analyses such as HPLC and GPC.

Table 3.2: Proximate analysis, elemental analysis, and sugar analysis of lignosulphonate and purified lignin samples (wt. %, dry basis).

Sample ID	Moisture Content	Ash Content	C	H	N	S	Total Sugars
KF2-P-N	8.6	0.3	58.8	6.4	0.2	3.8	0.01
KF3-E-N	7.5	0.4	58.1	5.9	0.2	4.0	0.00
S-SCB-S	18.6	2.0	51.7	6.7	0.3	1.1	0.25
SE-SCB	4.8	1.9	62.1	6.4	0.7	0.5	0.00
SL-E-T	10.2	28.6	35.1	4.1	0.2	3.9	ND
SL-M-PR	11.3	43.2	24.0	4.0	0.1	9.0	ND

ND: Not Determined due to unsuitability of Lignosulphonates for HPLC analysis

The total sugars content of the purified lignins reveal that the kraft and SE-SCB lignins have negligible sugar contents, whilst the S-SCB-S lignin sample had a total sugar content of 0.25%. Literature often reports that lignins from sugarcane bagasse often have a significant sugar content, as non-woody species possess lignin-carbohydrate complexes that can be difficult to separate during isolations processes (Naron, et al., 2017). Whilst the bagasse steam explosion sample (SE-SCB) had a negligible sugar content, the bagasse soda lignin (S-SCB-S) showed a comparatively higher sugar content indicating that the soda process was not completely successful in breaking lignin-carbohydrate bonds. Ultimately, the sugar content of both the bagasse and kraft lignins are well below

0.5 wt. %. As such, it was concluded that this amount is not significant enough to interfere in any proceeding analyses, neither is it significant enough to negatively impact resin properties. Lignosulphonate samples could not be analysed to due to the high impurity content.

Results from the elemental analysis of organic elements were consistent with ranges reported in literature (Mousavioun & Doherty, 2010; Zhou, et al., 2016; Naron, et al., 2017; Kröhnke, et al., 2019). All samples had negligible amounts of nitrogen (≤1%), which most likely originated form the biomass sources. The amount of elemental sulphur in the kraft and lignosulphonate samples were in the range of 3-9%, most of which would have originated from the isolation, precipitation and/or purification processes that were employed. In contrast, the bagasse lignins had sulphur contents of <1%, which possibly originated from the biomass source, and, in the case of S-SCB-S lignin, the precipitation and purification steps. The amount of carbon and hydrogen in the purified lignin samples (50-63%, 5-7% respectively) are higher than that of the lignosulphonates (24-35%, ~4% respectively), which is expected given the high ash content and the undetermined sugar content of the lignosulphonates.

3.3.2. Structural Analyses

Results from the FTIR analysis were used to obtain information on the chemical structure of the lignin samples. These spectral results are presented in Figure 3.1. The peak assignments of important functional bands are listed in Table 3.3.

The broad peaks observed in the region of 3440-3430 cm^{-1} are attributed to the stretching of aromatic and aliphatic hydroxyl (O-H) groups. The KF2-P-N and S-SCB-S lignins registered the highest absorbances, thereby indicating a higher content of hydroxyl groups. As discussed in previous sections, lignin reactivity is based on the type of substitution at its aromatic rings. Additionally, the presence of hydroxyl groups also affects lignin's reactivity. Phenolic hydroxyl groups in particular are the most reactive functional group, and can significantly affect the reactivity of lignin (Laurichesse & Avérous, 2014). Bands at 1220-1210 cm^{-1} are typically assigned to the stretching of phenolic hydroxyl groups, specifically C-O stretching of phenolic C-OH and phenolic C-O (Ar) groups of G and S units. The kraft and bagasse lignin samples showed distinctive peaks in this region, with the KF3-E-N lignin showing the lowest intensity, and the SE-SCB lignin recording the highest intensity. Meanwhile, the lignosulphonates showed no peaks at this region. However, all lignins did have distinctive peaks in the region of 1044-1030 cm^{-1}, assigned to stretching of primary aliphatic hydroxyls, specifically C-O stretching. This could suggest that while aliphatic hydroxyls are present in the lignosulphonates, there is minimal/trace amounts of phenolic hydroxyls. Another possibility is that the high impurity content of the lignosulphonates may have shifted the position of the C-O bands.

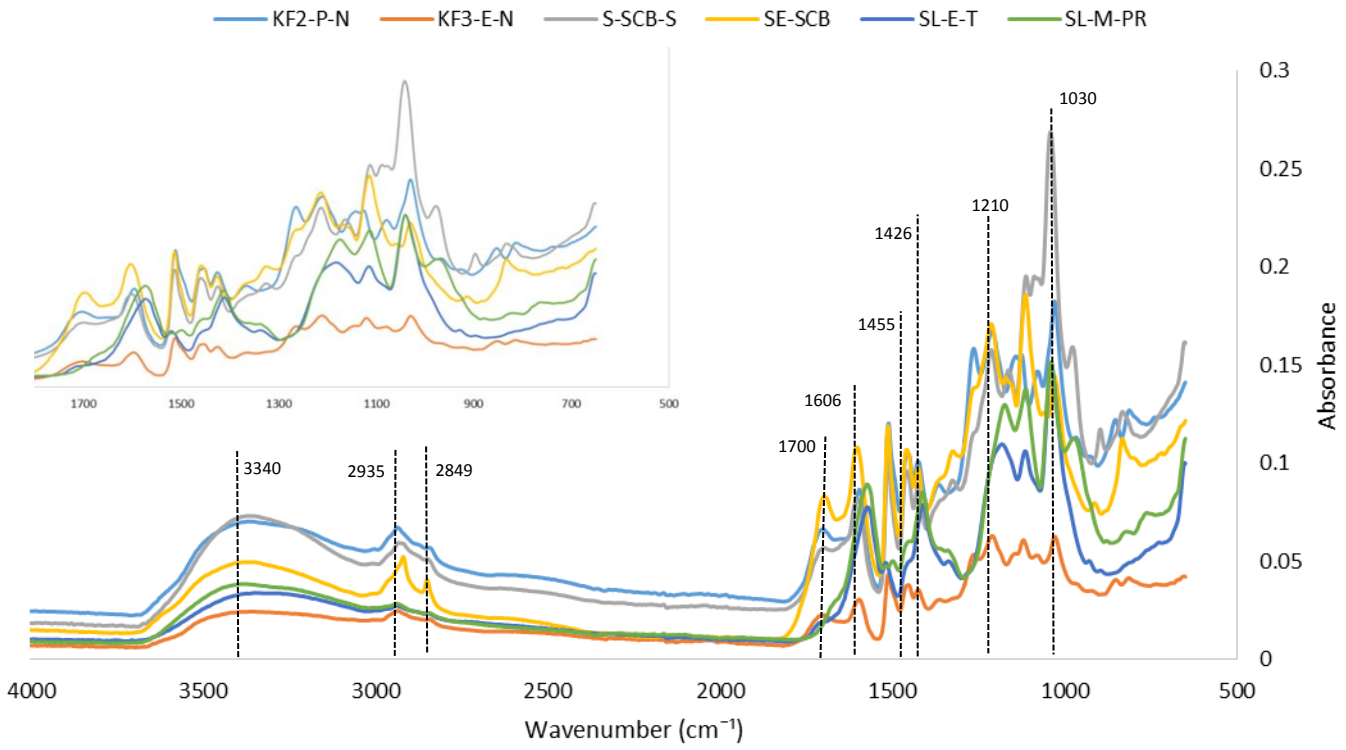

Figure 3.1: FTIR spectra of lignin samples

Table 3.3: Peak assignment of important FTIR bands of lignin

Peaks (cm^{-1})	Assignment	References
3430-3440, 3400	Aromatic and aliphatic O-H stretching	(Li, et al., 2016)(Lupoi, et al., 2015) (Hergert,
2935	C-H stretching of methyl and methylene groups	(Lisperguer, et al., 2009)
2849	C-H vibration of $–OCH_3$ groups	(Li, et al., 2016)
1702-1712	Unconjugated ketone and aldehyde groups	(Naron, et al., 2017)
1606-1510, 1500	Aromatic skeletal vibrations	(Naron, et al., 2017) (Tian, et al., 2016)
1457	C-H bending of methoxyl groups	(Hu, et al., 2014)
1424-1426	Ring stretching coupled with C-H in-plane deformation	(Naron, et al., 2017)

1264	C=O stretching of G units	(Hu, et al., 2014)
1220	Stretching of phenolic hydroxyl groups	(Hu, et al., 2014)
1210	G & S ring breathing with C-O stretching of phenolic C-OH and phenolic C-O(Ar)	(Li, et al., 2016)
1190	Sulphonic acids/sulphonate groups in lignosulphonates	(Hergert, 1971)
1141	C-H bending G units	(Hu, et al., 2014)
1030	Stretching of primary aliphatic OH	(Hu, et al., 2014)
1030-1044	C-O stretching of primary alcohols	(Naron, et al., 2017)
914-813	C-H bending of G & S units	(Naron, et al., 2017)
854	C-H out-of-plane deformation typical of guaiacyl aromatic ring structure	(Naron, et al., 2017)
832	C-H stretching of p-hydroxyphenylpropane	(Yang, et al., 2016)

Peaks at 2849 cm^{-1}, representing C-H vibration of methoxyl groups, registered relatively weak intensities for all samples except the bagasse steam explosion lignin (SE-SCB), which showed a distinctive peak in that region. However, this confirms the presence of methoxyl groups in the lignin sample structures. The bagasse and kraft lignin samples also showed sharp absorbances at 1461-1451 cm^{-1}, which are characteristic of C-H bending in methoxyl groups. This would suggest that whilst all the bagasse and kraft lignin samples contain distinctive amounts of methoxyl groups, the SE-SCB lignin sample may contain the highest amount given the strong absorbances at both 2849 cm^{-1} and 1458 cm^{-1}.However, something worth noting is that the general spectra of the SE-SCB lignin seems to have higher intensities for certain functional groups, compared to the other samples. This could be due to the steam explosion process itself, which allows extraction of biopolymers with minimal degradation (Martin-Sampedro, et al., 2011). Thus, there may be a greater extent of preservation of the structure, thus the SE-SCB lignin contains higher contents of certain functional groups. Meanwhile, the lignosulphonate samples showed an absence of peaks in the region of 1461-1451 cm^{1}. This could mean that the lignosulphonates have a lower content of methoxyl groups than the bagasse and kraft lignins. Alternatively, the lack of peaks at 1461-1451 cm^{-1} could possibly be the result of a band shift due to the presence of impurities in the lignosulphonate samples (Hergert, 1971). Incidentally, the appearance of sharp bands at 1412/1411 cm^{-1} appears only for the lignosulphonate

spectra, but these peak assignments are not recorded in available literature. Finally, the appearance of sharp peaks at1180-1175 cm^{-1} in the lignosulphonates' spectra are typical of sulphonate groups.

The remaining bands are assigned to functional groups commonly found within the lignin structure. Bands at 2935 cm^{-1} are typical of C-H stretching, whilst bands at 1712-1702 cm^{-1} are characteristic of conjugated ketones and aldehydes. The presence of peaks within 1606-1510 cm^{-1} are attributed to aromatic skeletal vibration, and peaks within 1426-1424 cm^{-1} indicates ring stretching coupled with C-H in-plane deformations.

The bands within the region 914-813 cm^{-1} are assigned to C-H bending of G and S units. Peaks at 854 cm^{-1} are specifically assigned to C-H out-of-plane deformation of guaiacyl rings. The pine kraft lignin (KF2-P-N) shows distinctive peaks at 1264 cm^{-1}, 1141 cm^{-1}, and 854 cm^{-1}, which are all typical of vibrations associated with G units. This is expected given that softwoods are predominantly composed of G monomers (see Section 2.1.2.). Bagasse lignins also showed absorptions at 832cm^{-1} which is characteristic of C-H stretching of H monomers. This is explained by the fact that grasses are HGS lignins, containing appreciable amounts of three monomeric units (see Section 2.1.2.).

Due to the spectral similarities of the lignin samples, principal component analysis (PCA) was performed to determine any differences in chemical structure or composition between the samples. PCA is a mathematical technique that provides a visual representation of the degree of correlation that occurs in multivariable data. When applied to FTIR data, it is able to assess minor and major differences between spectra, thus converting the multivariable data into a new dataset that is dependent on 2 to 4 variables or principle components. The first component is typically associated with the majority of variability in the spectra, and successive components thereafter are associated with decreasing proportions of variability. Contributing wavenumbers are directly related to a set of loadings, which in turn is associated with a principle component. The spectra are then individually scored according to their degree of correlation with the loadings of each component, and this can then be visually depicted on score scatter plots. On scatter plots, spectra with similar scores are clustered together, thus indicating similarity in spectral features, and thus possessing similar compositions and structures (Kline, et al., 2010).

The score plot for the six lignin spectra as a function of two principle components is shown in Fig 3.2. Interestingly, all lignin samples are located on the positive side of PC1, with three distinctive clusters observed. This could indicate that on PC1, no significant contribution to groupings based on biomass origin or pulping method was observed. Meanwhile, on PC2, key differences contributing to the groupings based on chemical features were observed. On PC2, clusters 1 and 2 had positive

loadings, with cluster 2 having a near zero loading, while cluster 3 had a negative loading. Looking more closely at the clusters, cluster 1 comprises of the lignosulphonates, cluster 2 is the soda bagasse lignin (S-SCB-S), and cluster 3 is the kraft lignins and steam explosion bagasse lignin (SE-SCB). Cluster three is unexpected as all three lignins come from different biomass sources, and the isolation method of SE-SCB differs from the kraft lignins. A more expected grouping would have been S-SCB-S lignin with the kraft lignins due to similar pulping processes and sample preparation methods, or S-SCB-S with SE-SCB due to biomass sources. The difference between clusters 2 and 3 may be attributed to the bands at 2935 cm^{-1} and 2849 cm^{-1}, which indicate C-H stretching of methyl and methylene groups and unconjugated ketone and aldehyde groups, respectively. Similarities between cluster 1 (lignosulphonates) and cluster 2 (soda bagasse lignin) lie at bands 2935 cm^{-1} and 2949 cm^{-1} which are attributed to C-H stretching of methyl and methylene groups and C-H vibrations of methoxyl groups, respectively. Cluster 1 differs from both cluster 2 and 3 at bands 1700 cm^{-1} and 1455 cm^{-1}, which is characteristic of unconjugated ketone and aldehyde groups and C-H bending of methyl and methylene groups, respectively. At these bands, the lignosulphonates show an absence of peaks in comparison to the bagasse and kraft lignins.

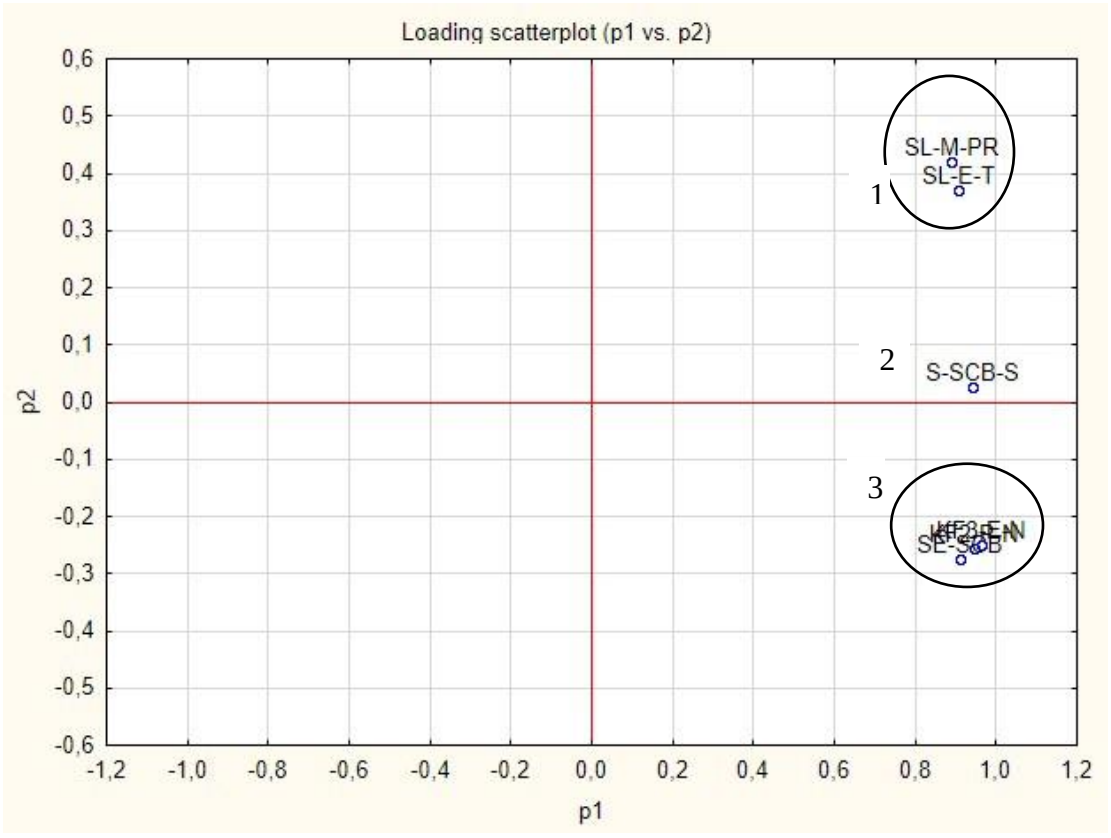

Figure 3.2: PCA score plot (PC1 vs. PC2) showing variation in lignin FTIR spectra

The NMR spectra for the individual lignin samples is presented in Appendix A. The peak assignments for important ^{13}C NMR chemical shifts of lignin are presented in Table 3.4. The SL-M-PR lignin could not undergo analysis due to unsuitability. Thus, only 5 samples were analysed. The NMR spectra of all samples were fairly similar, indicating that the lignin samples share a similar molecular structure, thus agreeing with the FTIR spectra.

Table 3.4: Peak assignment for important chemical shifts of ^{13}C NMR lignin spectra

Range of Chemical Shift (ppm)	Assignment	Reference
178.0-167.5	Unconjugated $-CO_2H$	(Tian, et al., 2016)
167.5-162.5	Conjugated $-CO_2H$	(Tian, et al., 2016)
154.0-140.0	C_3, C_4 aromatic ether or hydroxyl groups	
152.8	Etherified aromatic C_3/ C_5 in S units	(Podschun, et al., 2015)(Yang, et al., 2016)
148.3	Etherified aromatic C_3 in G units	(Podschun, et al., 2015)(Yang, et al., 2016)
140-124	Aromatic condensed C-C bonds	(Yang, et al., 2014)
133.6	Aromatic C_1 in S units	(Yang, et al., 2016)
128.6	Aromatic $C_{2/}$ C_6 in H units	(Yang, et al., 2016)
127.0-123.0	C_5 aromatic C-C bond	(Tian, et al., 2016)
117.0-114.0	C_5 aromatic C-H bond	(Tian, et al., 2016)
104	Aromatic C_2/ C_6 in S units	(Podschun, et al., 2015)
79.0-67.0	aliphatic C-O bonds, with C_α in the β-O-4	(Tian, et al., 2016)
72.8	C_α in the β-O-4	(Yang, et al., 2016)
71.1	C_γ in the β- β	(Yang, et al., 2016)
65.0-61.5	Aliphatic COR	(Tian, et al., 2016)
61.5-57.5	aliphatic C-O-C_γ in β-O-4	(Tian, et al., 2016)
60.7	C_γ in the β-O-4	(Yang, et al., 2016)
57.5-54.0	Methoxyl $-OCH_3$	(Tian, et al., 2016) (Yang, et al., 2016)
49-0	Aliphatic C-C bond	(Tian, et al., 2016)

All samples except for the KF3-E-N lignin showed signals at 178-173ppm, which are assigned to unconjugated carboxylic groups. All samples except for the KF3-E-N and SL-E-T lignins showed signals at 167-162ppm, which is typical of conjugated carboxyl groups. This indicates that the eucalyptus kraft (KF3-E-N) sample contains no carboxylic groups.

Signals at 154-140ppm were present in all samples, and these were assigned to C_3, C_4 aromatic ether or hydroxyl groups. Explicitly, all samples showed signals at 148ppm assigned to etherified C_3 on the aromatic rings of G units. The KF3-E-N lignin sample, a hardwood lignin (GS lignins), surprisingly showed no signals at 152ppm which is typical of etherified aromatic C_3/ C_5 in S units. It

did, however, show a weak signal at 133ppm, characteristic of aromatic C_1 in S units, and a weak signal at 128ppm, which is attributed to aromatic C_2/ C_6 in H units. Additionally, there was a number of signals in the range of 104-100ppm, attributed to aromatic C_2/ C_6 in S units. The presence of appreciable amounts of G and S units and trace amounts of H units is in line with monomeric distribution of hardwoods (Gellerstedt & Henriksson, 2008). Meanwhile, both bagasse lignins showed signals at 152ppm, 148ppm, 133ppm, and 128ppm, indicating the presence of all three monomeric units which is expected of grass lignins (Gellerstedt & Henriksson, 2008). The signal intensities of the bagasse soda lignin (S-SCB-S) indicated appreciable amounts of G and S units, but trace amounts of H units, with G units having the highest signal intensity. The signal intensities of bagasse steam explosion lignin indicated almost equal amounts of H, G, and S units, with G units having only a slightly higher intensity than the rest. The eucalyptus lignosulphonate (SL-E-T), also of hardwood origin, showed signals at 152ppm, 148ppm, 133ppm, 128ppm, and 104-100ppm, also indicating the presence of all three monomeric units. Intensities of the signals were almost equal, with the signal at 148ppm being slightly higher, indicating a slightly higher amount of G units. This is mildly unexpected for hardwoods as they are not generally known to have significant amounts of H units (Gellerstedt & Henriksson, 2008). The significant amount of H units, and comparatively smaller amount of S units, could be a result of the NSSC pulping conditions which possibly reduced methoxyl groups at the ortho positions on the aromatic ring. Finally, the pine kraft lignin showed a medium intensity signal at 148ppm, and weaker signals at 133ppm and 104-100ppm, indicating appreciable amounts of G units and smaller amounts of S units. This is in line with monomeric distribution in softwoods (Gellerstedt & Henriksson, 2008).

All samples except KF3-E-N, showed signals in the region of 117-114ppm, indicating the presence of C_5 aromatic C-H bonds, which are indicative of the presence of G units. Similarly, all samples except the lignosulphonate sample (SL-E-T) showed a number of signals in the range 140-124ppm, which is assigned to condensed aromatic C-C bonds, specifically of the C_5 carbon. Condensed C-C bonds usually possess relatively high bond energies, and are thus a significant amount of these linkages would add to the mechanical stability of the bond line LPF adhesives (Yang, et al., 2014).

The pine kraft (KF2-P-N) and bagasse soda (S-SCB-S) lignins also showed weak signals at 67ppm and 61ppm, the former indicating aliphatic C-O bonds, with C_α in the β-O-4 ether bond. The latter indicates aliphatic carbonyl groups. SL-E-T also showed signals within regions ascribed to aliphatic C-O bonds, with C_α in the β-O-4 ether bond (79-67 ppm), aliphatic carbonyl groups (65-61 ppm), and aliphatic C-O-C_γ in β-O-4 bonds (61-57 ppm).

All samples except bagasse soda lignin (S-SCB-S) showed signals at 57-54ppm, assigned to methoxyl groups.

All spectra show dominant signals at 40ppm, which falls within the region ascribed to aliphatic C-C bonds. This could indicate that the lignin molecules present in the different lignin samples are still quite complex, and have not been completely broken down to monomeric units.

In general, the NMR spectra agrees with the information supplied by the FTIR spectra, and also provides some insight on the C-C and ether bonds present within the lignin samples.

3.3.3. Molecular Weight Analysis

The results obtained from GPC analysis are listed in Table 3.5. Lignosulphonates could not be analysed due to the high ash content. The S-SCB-S lignin could not be acetylated to an acceptable extent, thus it was not run to prevent possible damage to the GPC column.

Table 3.5: GPC results of molecular weights of lignin samples

Sample ID	Mw (g/mol)	M_N (g/mol)	Polydispersity
KF2-P-N	4666	1848	2.52
KF3-E-N	3071	1696	1.81
S-SCB-S	NA	NA	NA
SE-SCB	6335	2263	2.80
SL-E-T	NA	NA	NA
SL-M-PR	NA	NA	NA

Looking at the kraft lignins, KF2-P-N, the pine kraft lignin, possesses a higher weighted average molecular weight (Mw) and polydispersity than KF3-E-N, the eucalyptus kraft lignin. This is consistent with literature (Naron, et al., 2017), and is most likely due to the difference in guaiacyl content between softwood and hardwood lignins. From FTIR spectra in Figure 3.1, bands at 854 cm^{-1} and 813 cm^{-1} are characteristic of C-H out-of-plane deformation of G aromatic structure and C-H bending of G & S units, respectively. For both these regions, the peaks of KF2-P-N lignin has a higher intensity than that of the KF3-E-N lignin, alluding that the pine kraft lignin contains a higher content of G units. G units are known to have very stable structure; in particular the C-C linkages formed at the C_5 position of the guaiacyl ring is difficult to cleave during isolation processes (Naron, et al., 2017). Additionally, the β–aryl ether bonds present in sinapyl units of hardwoods are easily broken and have a lower tendency of re-polymerisation compared to the β-aryl ether bonds of the coniferyl units of softwoods (Naron, et al., 2017).

The SE-SCB, a steam explosion bagasse lignin, has a considerably higher Mw and polydispersity than both kraft lignins. Naron et al. (2017) characterised soda bagasse lignin and found the Mw to be ~7779 and the PD to be 3.10 (Naron, et al., 2017). Hence, bagasse lignins seem to possess higher molecular weights whilst being polydisperse.

3.3.4. Thermal Analysis

Results from thermogravimetric analysis were used to construct TG curves that depicts weight loss with increasing temperature, as seen in Figure 3.3.

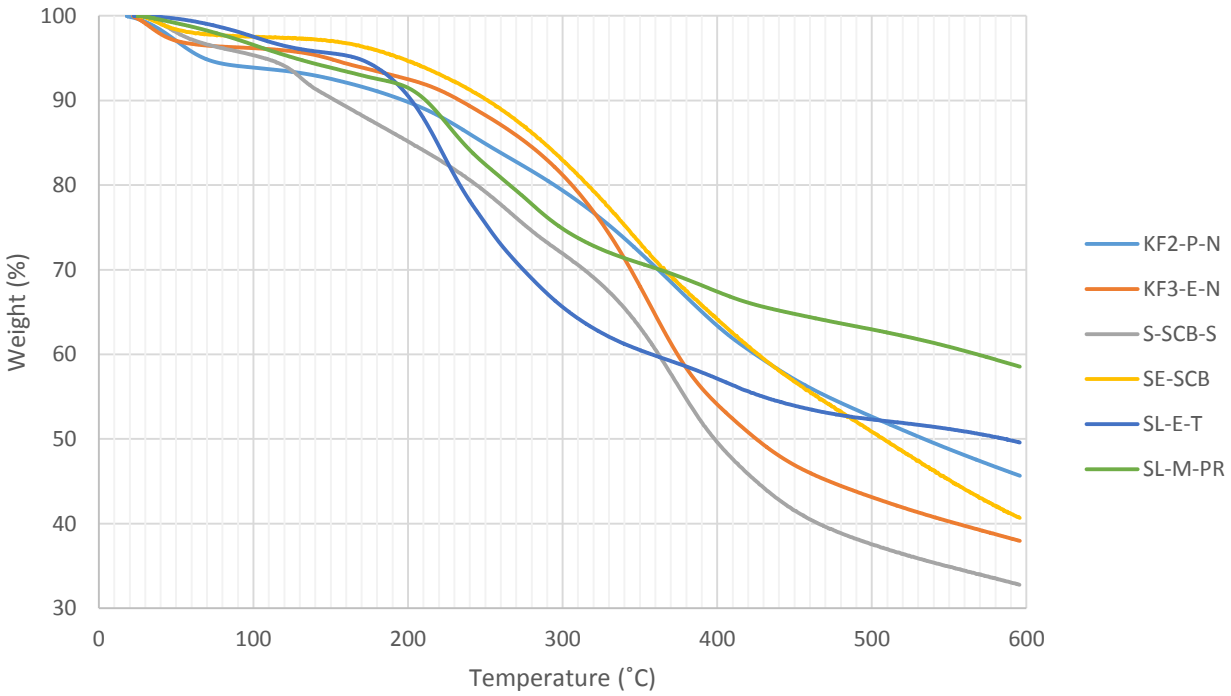

Figure 3.3: TGA curve of lignin samples

No noticeable degradation occurs from 0-100°C, with all lignin samples retaining 93-97% of their initial mass. Between 100-200°C, slow degradation is evident in the KF2-P-N, S-SCB-S, and SL-E T samples with these lignins retaining only 85-89% of their initial mass. In comparison, the KF3-E-N, SE-SCB, and SL-M-PR samples still retain 91-94% of their mass. This degradation continues between 200-300°C, with the S-SCB-S and SL-E-T samples degrading slightly faster than the others, thus consequently losing approximately 29% and 35% of their initial mass, respectively. This slight increase in degradation could be due to the dehydration of hydroxyl groups located on benzyl groups, as well the cleavage of α- and β-aryl-alkyl-ether bonds (Laurichesse & Avérous, 2014). Between 300-400°C the rate of degradation seems to increase, with the KF3-E-N and S-SCB-S lignins losing as

much as 50% of their initial mass. This could be attributed to the splitting of aliphatic side chains from aromatic rings, and the cleavage of C-C bonds (Laurichesse & Avérous, 2014). Degradation of the samples seems to stabilise between 400-500°C, with the exception of the S-SCB-S lignin which only retains 37.35% of its initial mass. Lastly, the weight residue at 595°C is given in Table 3. 6. The SL-M-PR and S-SCB-S samples show the highest (58.58%) and lowest weight residues (32.79%), respectively. Interestingly, the lignosulphonate had higher weight residues than the purified lignin resins. This could be a result of the high ash content present in the lignosulphonates, especially since these impurities degrade at temperatures higher than 600°C, as evidenced by need to ash the lignosulphonate samples at a higher temperature than the purified lignin samples (see section 3.2.4). Overall, the weight residues of all samples are in agreement with that of literature, i.e. 30-50% weight residue (Laurichesse & Avérous, 2014).

Table 3.6: Weight loss (%) of lignin samples at varying temperature intervals

Sample	Weight at 100°C	Weight at 200°C	Weight at 300°C	Weight at 400°C	Weight at 500°C	Weight Residue at 595°C
KF2-P-N	93.85	89.63	78.99	63.09	52.40	45.69
KF3-E-N	96.15	92.35	80.96	53.92	42.96	37.99
S-SCB-S	95.29	84.76	71.68	49.26	37.35	32.79
SE-SCB	97.55	94.52	82.60	63.88	50.59	40.73
SL-E-T	97.41	89.91	65.25	57.00	52.25	49.63
SL-M-PR	96.31	91.35	74.47	67.15	62.92	58.58

The first derivative curves (DTG) of the TG curves are presented in Figure 3.4. These curves are referred to as degradation curves, whereby the maxima of the curve represents the maximum degradation rate of the sample at a particular temperature.

Looking at Figure 3.4, it is observed that the kraft and bagasse lignins experience their maximum degradation rates within the temperature range of 360-380˚C, as reported in literature. It also seems that the KF2-P-N (Pine kraft) lignin is the most thermally stable, since it experiences its maximum degradation rate at a higher temperature compared to the rest of the lignin samples. The high thermal stability of the KF2-P-N lignin could be due to the high guaiacyl composition of softwoods that have condensed C-C bonds, thereby making it very thermally stable (Naron, et al., 2017).

The lignosulphonates experience their maximum degradation at a temperature of approximately 220/230˚C. This agrees with what is reported in literature, whereby the significant inorganic matter has a catalytic effect (Naron, et al., 2017) thereby causing them to degrade at lower temperatures.

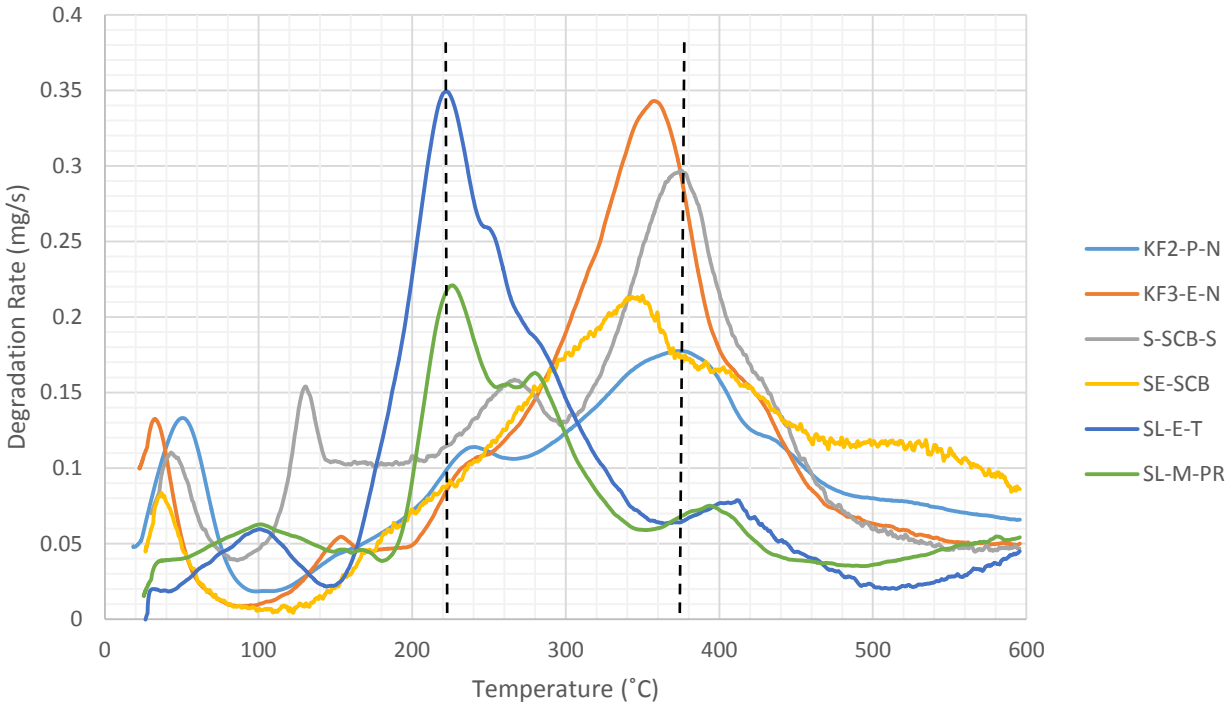

Figure 3.4: DTG curve of lignin samples

Chapter 4: Synthesis & Characterization of Lignin-Phenol-Formaldehyde Resins at 100% Phenol Substitution Level

4.1. Introduction

As discussed in Chapter 2, phenolic resins are excellent wood adhesives for a variety of reasons, specifically its high bonding strengths. Lignin-based phenolic resins aim to replicate these qualities, though there is still much work to be done in that regard. The synthesis of lignin phenol formaldehyde resins are very similar to that of phenol formaldehyde resins, and both these processes are described in detail in Chapter 2.

Wood adhesives are typically comprised of its base material, usually a natural or synthetic resin, in addition to a number of other additives, depending on the specifications required of the adhesive. These additives include catalysts or hardeners, fillers, cross-linking agents, retarders, plasticizers, surfactants, wetting agents, stabilizers, and so forth. The selection of additives depend on factors pertaining to required end-use properties of the adhesives, processing requirements, as well as the target cost of the adhesive (Alawode, 2019). Cross-linking agents and hardeners in particular are quite important as they promote polycondensation and crosslinking of the adhesive during curing (Uner & Olgun, 2017). A variety of crosslinkers exist, such as epoxides, polyols, amines, melamine, aldehydes, etc. (Pizzi, 2003). One commonly used crosslinker is hexamethylenetetramine, also known as hexamine. A number of hardeners may be used, but a highly effective agent used widely in industry is epichlorohydrin (Kishi & Fujita, 2008). Epichlorohydrin is a colourless liquid with an epoxide ring and chlorine atom in its structure. Due to its structural nature, it is able to undergo many chemical reactions, and is used for a wide variety of applications (Sulaiman, et al., 2013). A major disadvantage of epichlorohydrin is its highly toxic nature, for which products using it must comply with emission standards (Kishi & Fujita, 2008). On the other hand, another hardener that can be used is glyoxal, which is biodegradable and non-toxic. It is also typically used with lignin-based resins (Xi, et al., 2017).

Some important requirements of wood adhesives include high bonding strengths, easy application, high gluing quality, environmental resistance, and little to no chemical emissions during the production of wood products and during their use. Additionally, relatively cheap raw materials, as well as short press times and low press temperatures are also important to minimize production costs (Dunky, 2003). As a result, a number of tests have been developed to test structural and end-use properties of adhesives, specifically their resins, in order to determine if they meet the necessary requirements.

Chemical tests such as Fourier Transformed Infra-Red (FTIR) Spectroscopy can be used to determine the chemical structure of the resins/adhesives. More importantly, thermal techniques such as differential thermal analysis (DTA) and differential scanning calorimetry (DSC) are preferred methods to determine curing behavior and thermal stability (Hon, 2003), in addition to thermogravimetric analysis (TGA). A major physical property of adhesives is mechanical strength. Tests to determine adhesive strength generally falls under three categories, i.e. tensile, peel and shear. The most common tests fall under the last category and results are reported as load at failure divided by area of overlap, thus giving the shear bonding strength of the adhesive. Advantages of this method is that samples are relatively easy to prepare, and the geometry of these samples closely resembles that of many practical joints (DeVries & Borgmeier, 2003).

4.2. Materials & Methods

4.2.1. Experimental Approach

Experimental work started with the synthesis of lignin phenol formaldehyde resins using each of the six lignin samples described in Section 3.2.2. The synthesis procedure is adapted primarily from Kalami et al. (2017), since this is the only study, in recent times, to successfully synthesise LPF resins at 100% phenol replacement. Each lignin was used as a phenol substitute in the resin synthesis process, essentially producing six different lignin-based PF resins at 100% phenol substitution (6 x LPF100 resins). These resins were then categorised into three groups according to the biomass origin and isolation method of its lignin, i.e. kraft LPF100 resins, bagasse LPF100 resins, and lignosulphonate LPF100 resins.

Thereafter, the LPF100 resins were characterised according to chemical structure and curing behaviour. Each LPF100 resin was then used directly as an adhesive in the preparation of plywood samples for shear bonding strength testing. This batch of LPF100 adhesives, essentially consisting of just the LPF100 resins, was termed to be ‘unmodified’ adhesives (R_0). Based on the results of the (R_0) shear bonding strength tests, it was decided that ‘modification’ of the LPF100 adhesives were required to improve its strength properties.

The LPF100 adhesives were ‘modified’ by the addition of a hardener and crosslinker in its adhesive formulation. Hexamine was chosen as a crosslinker. Two different hardeners were chosen, to see which would ultimately perform best in conjunction with the lignin-based resin and hexamine. Glyoxal (R_1) was chosen due to its biodegradability, keeping in mind that the ultimate goal is to move onto completely bio-based adhesives. Epichlorohydrin (R_2) was also chosen due to its high efficiency and common use in industry, since the potential performance of the LPF100 resins in an industrial

setting is of interest. Each LPF100 resin was used together with hexamine and the relevant hardener to produce R_1 and R_2 adhesives. These adhesives were subsequently used to prepare plywood samples for shear bonding strength tests. Based on all these results, a conclusion was made on which resin(s) were best suited as a phenol substitute in PF resins.

Due to time constraints, limited resin samples were produced, since the drying stage of the resins was time-consuming. As a result, adhesives and plywood boards were not prepared in replicate. Furthermore, this study did not consider optimisation of the resin synthesis process, neither did it focus on the optimisation of adhesive formulation or the procedure for preparation of plywood boards. Instead, established methods were used based on available resources, finances, and time constraints. The detailed interactions of the additives in the adhesive formulae were also not considered. The study merely aims to assess the potential of the lignins characterised in Chapter 3 as total phenol substitutes for LPF resins, with a cursory look at its performance in an industrial context in terms of adhesive modification.

4.2.2. Materials

For the synthesis of the LPF100 resins, 37% formaldehyde and 98% NaOH was purchased from ScienceWorld. The 98% NaOH was used to make 1M solution of NaOH. The synthesis process will be discussed explicitly in Section 4.2.3. The synthesized resins were then named with the same sample ID as their lignin sources, as seen in Table 3.1 in Chapter 3 (i.e. KF2-P-N resin).

For the formulation of the lignin-based adhesives, Glyoxal solution (40 wt. % in H_2O), Analytical grade Epichlorohydrin (≥ 99%), and Hexamine were purchased from Sigma-Aldrich Pty. Ltd., SA. For the preparation of plywood samples, Douglas Fir veneers was supplied by a local wood mill, and Bondite 345, a commercial tannin-based wood resin, was supplied by Bondite* (Pty) Ltd, South Africa. Adhesive formulation and plywood preparation will be discussed further in Section 4.2.4 and 4.2.5, respectively.

4.2.3. Synthesis of 100% LPF Resins

The synthesis procedure was adapted primarily from Kalami et al. (2017), whilst synthesis parameter such as Formaldehyde/Phenol (2.5) and NaOH/Phenol (0.3) molar ratios were determined after consulting various relevant literature sources (Siddiqui, 2013; Pfungen, 2015; Ghorbani, et al., 2016; Kalami, et al., 2017), and were based on the amount of lignin/phenol used for each resin batch.

The set-up for resin synthesis makes use of a round-bottom reaction flask fitted with a flat flange, a 5-port flange lid, flange clamp, heating mantle, a laboratory-scale overhead stirrer, a reflux condenser, dropping funnel, thermometer, and a water bath. This apparatus is seen in Figure 4.1.

Before connecting the apparatus together, 20g of the relevant lignin sample was weighed and added into a beaker. Two thirds of the required 1M NaOH (~ 86 mL) was added, and stirred gently until lignin had completely dissolved into NaOH solution. Thereafter, the mixture was poured into the reaction flask, and the set-up was connected. The stirrer and water for the condenser were then switched on. After a minute of stirring, the required amount of 37% formaldehyde (31.5 mL) was added to the reaction mixture, drop-wise, using the dropping funnel. Once that was completed, the mixture was allowed to stir for a few minutes. Thereafter, the mixture was gradually heated to 65 ˚C whilst continuously stirring at 160 rpm. Once the temperature of 65˚C had been attained, the reaction mixture was held at that temperature for 10 minutes, whilst the stirring continued. Subsequently, the last amount of NaOH (45 mL) was added drop-wise to the mixture, after which it was heated to a temperature of 85 ˚C. Once at that temperature, the reaction was held at 85 ˚C for 1 hour. Finally, the heating mantle was switched off and the mixture was allowed to cool to room temperature. The liquid resins were then placed in Schott bottles and stored in the fridge at a temperature of ~13 ˚C.

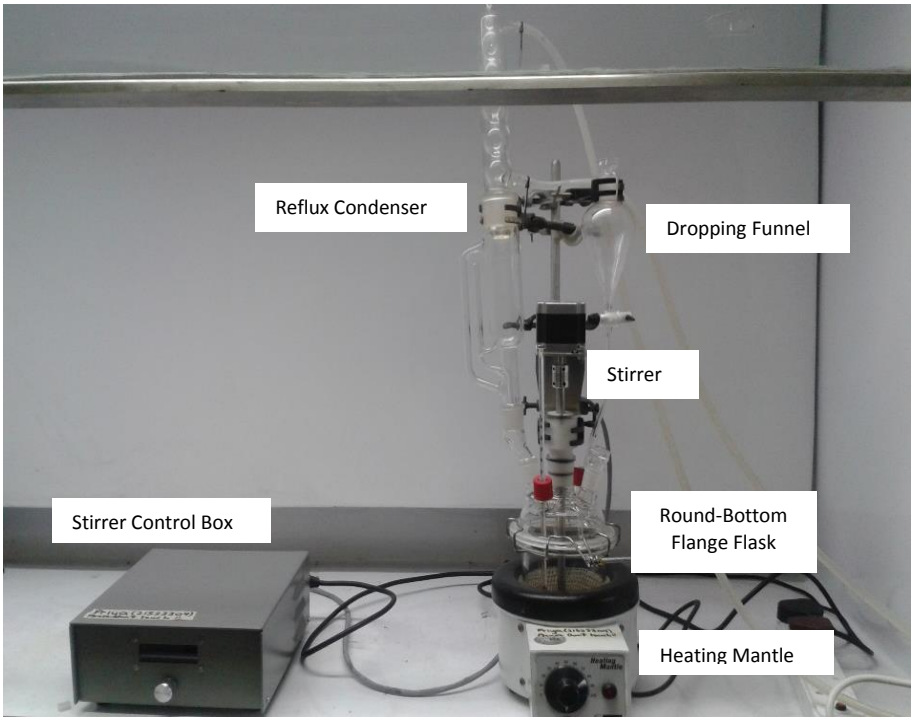

Figure 4.1: Overview of experimental set-up for resin synthesis

At a later stage, each LPF100 resins was poured into separate foil trays and dried in a 40 ˚C vacuum oven. The oven was continuously purged with nitrogen to avoid build-up of any trace amounts of unreacted formaldehyde. The bagasse and kraft resins required approximately 24 hours to completely dry, whilst the lignosulphonates had to be dried for 5-7 days. Once dried, an Ultra Centrifugal Mill – ZM 200 (Retch) was used to mill the resins into powders with a particle size of 0.5mm. These resin powders were then stored in airtight plastic bags until further use.

4.2.4. Adhesive Formulation

R_0 adhesives were not produced according to typical adhesive formulae, and was simply made to gauge the strength of the LPF100 resins on their own. Alongside, an adhesive produced from a commercial wood resin, Bondite 345, was made. For each LPF100 resin, 8g of resin was mixed with water at a water/resin mass ratio of 1. The commercial adhesive was prepared using Bondite 345 and Hexamine, as recommended by the manufacturers. Adapted from Alawode et al. (2019), 10g of Bondite 345 and 2g of hexamine were mixed together to form a well-mixed powdered mixture. Subsequently, the mixture was dissolved in 15-20mL of distilled water (Alawode, et al., 2019). These adhesives were then used for plywood preparation and subsequent testing.

The R_1 and R_2 adhesives are produced according to the more general formulae used for adhesive production. Both R_1 and R_2 adhesives use the respective LPF100 resin together with hexamine as a crosslinker. The difference lies in the hardener used; Glyoxal for R_1 adhesives and Epichlorohydrin for R_2 adhesives. This information is tabulated in Table 4.1. Using the amount of resin as a basis, the mass ratios of crosslinker/resin and hardener/resin was adapted from Alawode et al. (2019). The hexamine/resin was 0.2, Glyoxal/resin was 0.45, and epichlorohydrin/resin was 0.39. Distilled water was added to each adhesive at a water/resin mass ratio of 1.87. Essentially, the dry powders were mixed together, after which the water was added in increments, until the powders had completely dissolved in the water (Alawode, et al., 2019).

Table 4.1: Adhesive formulations for plywood boards

R_0	Resin + Water
R_1	Resin + Water + Hexamine (crosslinker) + Glyoxal(hardener)
R_2	Resin + Water + Hexamine (crosslinker) + Epichlorohydrin(hardener)
Commercial	Bondite Resin + Hexamine (crosslinker) [as recommended for industrial use]

4.2.5. Plywood Preparation

Three-layer plywood boards were made using the different LPF100 adhesive samples. Specification relating to the board, press, and conditioning are listed in Table 4.2. These specifications were adapted from literature as well as trial and error (Imman, et al., 2001; Alawode, et al., 2019).

Table 4.2: Board, press, and conditioning specifications of plywood boards

Veneer Dimensions (mm)	Spread Rate (g/m²)	Press Temp. (˚C)	Press Time (min)	Cond. Time (days)	Cond. Temp. (˚C)	Cond. RH (%)
100x100x4	350	150	10	7	20-23	60

As described in literature, a three-layered plywood sample of 9mm thickness was prepared using 100x100x4mm Douglas Fir veneers. The middle layer was coated with 350 g/m² of adhesive on either side, and then left exposed to air for 5 minutes to evaporate excessive moisture. The veneers were then arranged in such a way that the middle layer was perpendicular to the outer layers. The glued veneers were then hot pressed for 10 minutes at 150 ˚C. This was repeated for each adhesive. The boards were then left to cure in a conditioning room for 7 days, at a temperature of 20-23 ˚C and a relative humidity of 60% (Alawode, et al., 2019).

4.2.6. Resin Characterisation Methods

Fourier Transformed Infra-Red (FTIR) Spectroscopy was performed to determine the chemical structure of the LPF100 resins. A Thermo Scientific Nicolet iS10 Spectrometer (Thermo Scientific, Waltham, MA) equipped with a Smart iTR ATR accessory, with a diamond crystal was used. Spectra was obtained in Attenuated Total Reflectance (ATR) mode at a resolution of 8 cm^{-1}, 32 scans per sample, and within the absorption bands in the 4000-500 cm^{-1} region. Collection and processing of data was done with Thermo Scientific OMNIC software. Spectra was baselined corrected, and assignment of absorption bands were based on relevant literature. Principal Component Analysis (PCA) was performed using Statistica software (Version 13.2) to determine any spectral differences in chemical structure and composition. The PCA focused on the spectral region of 1700-500 cm^{-1} since this a complex band region containing most of the relevant information pertaining to the LPF100 resins.

To observe the thermal behaviour of the LPF100 resin samples, Thermogravimetric Analysis (TGA) was performed using a TGA Q50 thermogravimetric apparatus. Approximately 5 ± 0.5 mg of sample was placed into an aluminium crucible which was then loaded onto the TGA pan. Using a heating rate of 10 ˚C/min, the analysis was conducted from room temperature up to 600 ˚C, under nitrogen atmosphere. The resultant data was used to construct weight loss versus temperature curves, from which degradation curves (dTG) where produced to determine the temperature at which maximum degradation occurs.

The curing behaviour of the LPF100 resins was observed by Differential Scanning Calorimetry (DSC) using a TA Instrument Q100 calorimeter. Calibration of the instrument was done using an indium metal standard according to standard procedure. Approximately 4mg of LPF100 resin was weighed into an aluminium pan and loaded onto the calorimeter; an empty aluminium pan was also loaded on as a reference. The samples were heated up at a rate of 10 ˚C /min over a temperature range of 0 ˚C to 250 ˚C, under nitrogen atmosphere.

Bonding strength was tested according to the ASTM D906-98 (2011) standard for Shear Strength of Plywood Samples by Tension Loading. The plywood board specimens were cut according to the dimensions listed in the standard (25.4x82.5mm), as shown in Figure 4.2. Three replicates of each board sample was obtained. Thereafter, the test specimens of each board sample was tested in a Zwicks Testing Machine. A test load was applied at a crosshead speed of 5mm/min.

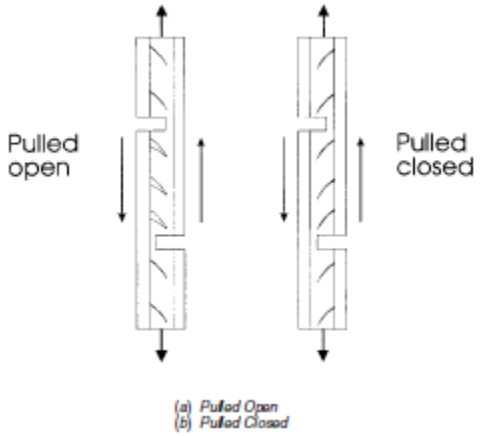

Figure 4.2: Lathe and notch orientation for testing, ASTM D906-98 (2011)

4.3. Results & Discussion

4.3.1. FTIR Analysis

The results generated by FTIR analysis provided information on the chemical structure of the LPF100 resins. The spectra are presented in Figure 4.3, and peak assignments for LPF resins are listed in Table 4.3.

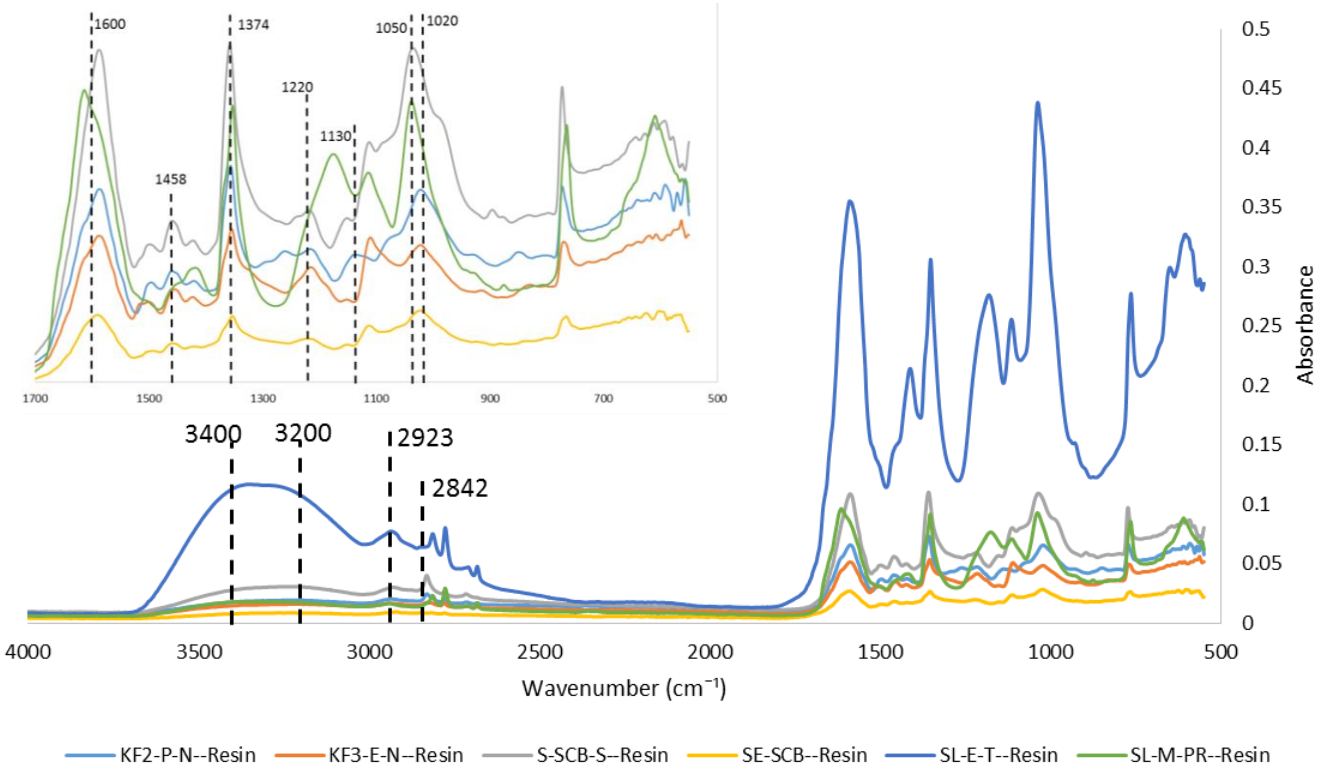

Figure 4.3: FTIR spectra of LPF100 resins

All resins exhibit a broad peak in the region of 3400-3200 cm^{-1}, which is assigned to the stretching of OH groups. With particular respect to phenolic OH groups, all resins showed bands around 1374 cm^{-1} which is characteristic of phenolic OH vibrations.

Bands at 2923 cm^{-1} and 2842 cm^{-1} are attributed to out-of-plane bending of aliphatic C-H groups and symmetric stretching of CH_2 groups, respectively. Whilst the former band is present in all resin spectra, the latter only appears in the kraft and bagasse resin spectra.

All resins exhibit peaks at 1600 cm^{-1}, assigned to C=C stretching of the aromatic ring. Additionally, bands at 1114 cm^{-1}, typical of aromatic C-H vibrations, appear in all resin spectra except that of the KF2-P-N resin.

Table 4.3: Peak assignments of important FTIR bands of LPF resins

Peaks (cm^{-1})	Assignment	References
3400	OH stretching	(Khan & Ashraf, 2006)
2923	Out-of-plane deformation of aliphatic C-H	(Abdelwahab & Nassar, 2011)
2842	Symmetric stretching of CH_2 groups	(Khan & Ashraf, 2006)
1600/1500/1450	C=C stretching of aromatic ring	(Li, et al., 2016)
1458	C-H deformation in CH_2 group	(Khan & Ashraf, 2006)
1374	Phenolic OH groups	(Abdelwahab & Nassar, 2011)
1250	C-O stretching of phenolic OH	(Li, et al., 2016)
1230	C-O stretching of syringyl phenolic OH	(Khan & Ashraf, 2006)
1205	Phenolic C-O vibrations	(Abdelwahab & Nassar, 2011)
1130	Stretching of ether linkages	(Khan & Ashraf, 2006)
1114	Aromatic C-H groups	(Abdelwahab & Nassar, 2011)
1050	C-O stretch of methylol groups	(Khan & Ashraf, 2006)
1020	C-O stretching of Al C-OH, Al C-O(Ar),methylol C-OH	(Li, et al., 2016) (Qiao, et al., 2016)

With the exception of the lignosulphonate resins, weak peaks appear at 1458 cm-1 characteristic of C - H bending in CH_2 groups. This band is of particular interest, as it indicates the presence of methylene bridges in the resin structure. As discussed in Sections 2.3 and 2.4, formaldehyde and phenol groups react to form methylolphenols which then condense together, forming methylene or dimethylene ether bridges between them (Siddiqui, 2013). Thus, the existence of these bridges gives a rough indication of the reaction between formaldehyde and the phenol moieties in lignin, as well as the condensation between the methylolphenols into some sort of prepolymer. This was further confirmed by the medium intensity absorption band at 1020 cm^{-1} in the kraft and SE-SCB resin spectra, which is characteristic of C-O stretching of methylol C-OH, aliphatic C-OH, and aliphatic C-O (Ar). Additionally, the KF2-P-N resin showed a weak absorption peak at 1130 cm^{-1}, which is attributed to the stretching of ether linkages, thus possibly alluding to dimethylene ether linkages. Although these peaks were absent in the lignosulphonate resin spectra, the lignosulphonate resins, along with the S-SCB-S resin, showed absorption peaks near 1050 cm^{-1}, which are assigned to the C-O stretching of methylol groups. This may signify that while there was some reaction between the formaldehyde and phenol moieties in the lignosulphonates, the resultant methylolphenols did not successfully condense into a prepolymeric structure.

The remaining bands are related to C-O vibrations. The kraft and bagasse resin exhibit peaks between the regions of 1230 and 1205, assigned to phenolic C-O stretching in syringyl groups and phenolic C-O vibrations, respectively. In addition, the KF2-P-N resin experienced an absorption band at 1250 cm^{-1}, typical of C-O stretching of phenolic OH groups.

Interestingly, all LPF100 resins showed very small peaks near the 2724 band, which an overtone band assigned to C-H bending in formaldehyde (Poljanšek & Krajnc, 2005). This may indicate that there was still small amounts of formaldehyde that did not take part in the resin synthesis reactions, possibly due to the well documented limitations of the lignin molecule.

Similar to the spectral results of the lignins, the FTIR spectra of the LPF100 resins are similar in structure, however the absorption bands of the SL-E-T resin are markedly higher than the rest. This could indeed indicate a higher content of the relevant functional groups, or perhaps the there was some interference during analysis, thereby resulting in an intensification of peaks. Should the former be true, it should reflect accordingly in the bonding strength and thermal analysis results of the SL-E-T resin.

Due to the spectral similarities of the LPF100 resins, principal component analysis (PCA) was once again performed to assess possible differences in chemical structure or composition. The score plot for the spectra of the LPF100 resins as a function of two principle components (PC) is shown in Figure 4.4.

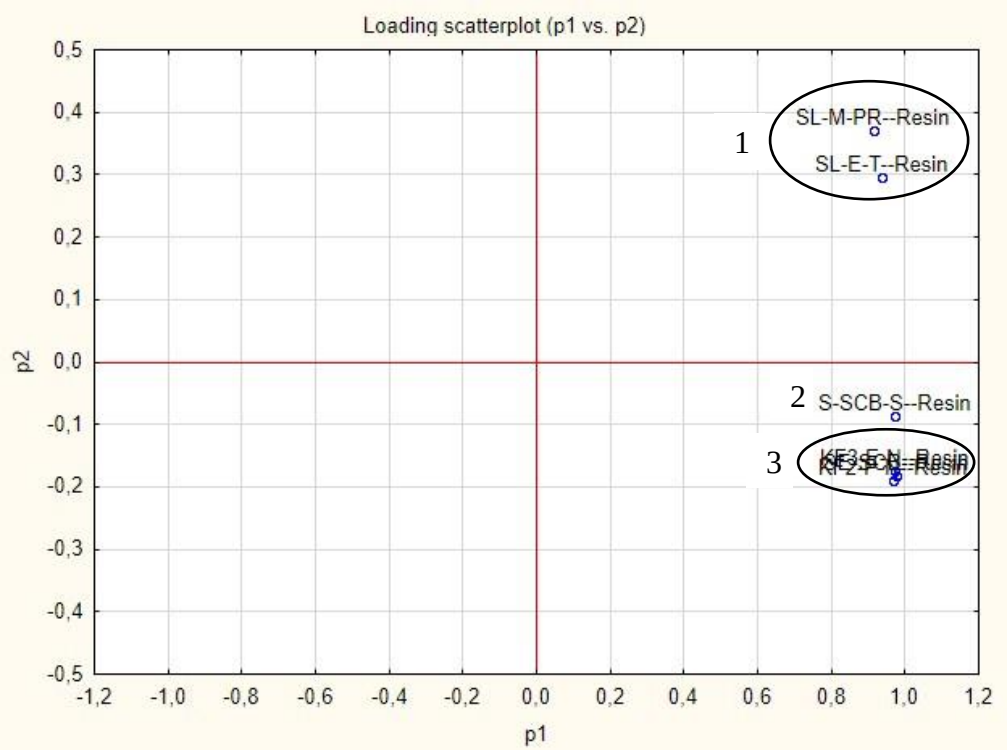

Figure 4.4: PCA score plot (PC1 vs. PC2) showing variation in LPF100 resin FTIR spectra

Similar to the PCA analysis of the lignins, all samples lie on the positive side of PC1. The samples can be categorized into roughly three clusters. The lignosulphonate resins forming cluster 1, S-SCB-S resin forming cluster 2, and the kraft and SE-SCB resins forming cluster 3. This time on PC2,

cluster 1 had a positive loading, whilst clusters 2 and 3 had negative loadings. The difference between cluster 1 and clusters 2 and 3 are attributed to the spectral bands 2842 cm^{-1} and 1458 cm^{-1}, which are characteristic of symmetric stretching of methylene groups and C-H deformations of methylene groups, respectively. These bands were present in the kraft and bagasse resins, but absent in the lignosulphonate resins. The difference between clusters 2 and 3 lies in the bands at 1020 cm^{-1}, assigned to C-O stretching of methylol C-OH, aliphatic C-OH, and aliphatic C-O (Ar). Whilst these peaks are present in cluster 3 resins, they are absent in the S-SCB-S resin. Similarly, at 1050 cm^{-1}, peaks attributed to the C-O stretch of methylol groups are absent in cluster 3 resins, but present in cluster 1 and 2 resins, thus showing a slight similarity between the lignosulphonate and S-SCB-S resins.

4.3.2. Thermal Analyses

Thermogravimetric analysis (TGA) was performed to determine thermal stability of the LPF100 resins. The TGA curves are presented in Figure 4.5 below.

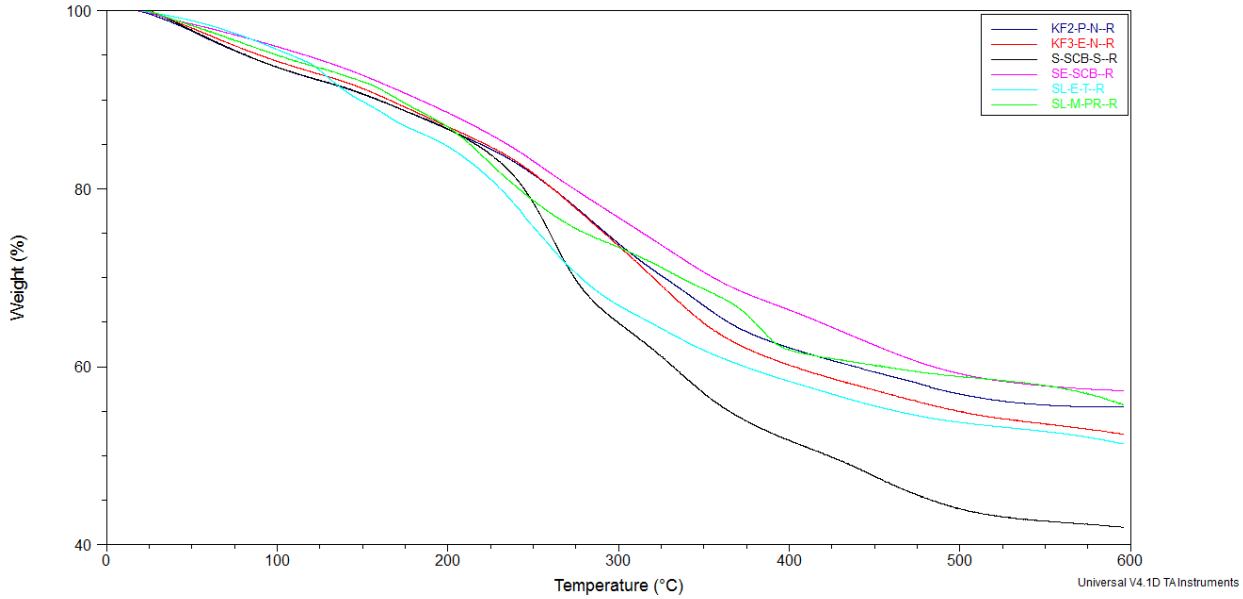

Figure 4.5: TGA curves of LPF100 resins

From 0-100°C, barely any degradation occurs, with all resins retaining 93-95% of their initial mass. Between 100-200°C, all resins undergo slow degradation, losing approximately 15% of their initial mass at this point. Between 200-300°C, the resins start to exhibit different thermal behaviours. The kraft, SE-SCB and SL-M-PR resins continue to slowly degrade, retaining roughly 75% of their initial mass. Meanwhile the S-SCB-S and SL-E-T resins degrade at a slightly faster pace, retaining 65% of their initial mass. Between 300-500°C, all resins continue to slowly degrade at approximately the

same pace, with the kraft and lignosulphonate resins showing slightly better thermal stability than the bagasse resins. The weight residues of the resins are given in Table 4.4, with the S-SCB-S and SE-SCB resins showing the lowest and highest thermal stability, respectively. Once more, the SL-M-PR resin has a higher weight residue than the resins with purified lignin feedstocks. The SL-E-T resin also has a weight residue similar to those of the kraft resins. This could yet again be explained by the high ash content present in the lignosulphonate samples, which degrade at higher temperatures of 800°C.

Table 4.4: Weight loss (%) of LPF100 resins at varying temperature intervals

Sample	Weight at 100°C	Weight at 200°C	Weight at 300°C	Weight at 400°C	Weight at 500°C	Weight Residue at 595°C
KF2-P-N--R	93.66	86.68	73.85	62.13	56.92	55.47
KF3-E-N--R	94.34	86.95	73.59	60.18	54.94	52.43
S-SCB-S--R	93.67	86.74	64.93	51.69	44.03	41.96
SE-SCB--R	95.98	88.55	76.77	66.38	59.21	57.30
SL-E-T--R	95.66	84.74	66.91	58.36	53.74	51.32
SL-M-PR--R	95.06	86.99	73.42	61.91	58.87	55.74

Differential scanning calorimetry (DSC) was performed to observe the curing behaviour of the resins. The thermograms are displayed in figure 4.6.

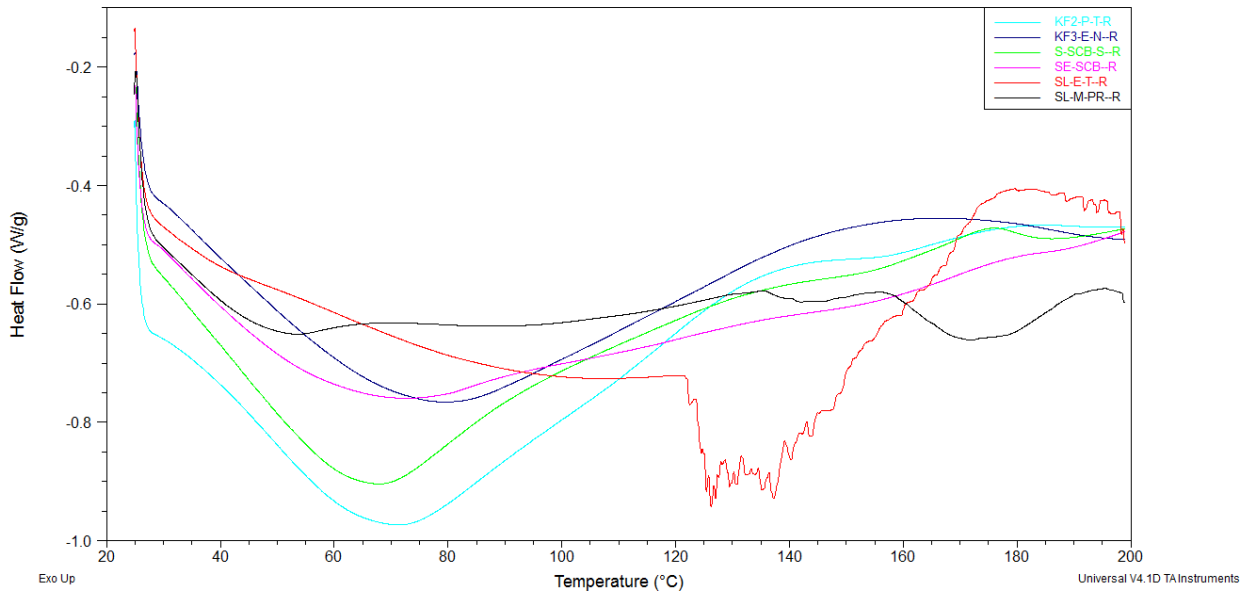

Figure 4.6: DSC curves of LPF100 resins

A distinctive endotherm is observed for all resins, which is an indication of resin curing (Abdelwahab & Nassar, 2011). Table 4.5 lists the T_p, T_o, and ΔT values for the different resins. T_o is the onset temperature which marks the start of curing of the resin, whilst T_p is the peak temperature. The difference of these two values, ΔT, is the rate of curing, whereby a high ΔT indicates a low rate of curing and vice versa (Abdelwahab & Nassar, 2011).

Table 4.5: Summary of LPF100 resin curing properties

Sample	T_o (°C)	T_p (°C)	ΔT (°C)
KF2-P-N--R	27	71	44
KF3-E-N--R	28	80	52
S-SCB-S--R	27	68	40
SE-SCB--R	27	73	45
SL-E-T--R	27	126	99
SL-M-PR--R	28	172	144

As seen from Table 4.5, all resins have their onset temperatures at about 27/28°C. Peak temperatures of the bagasse and kraft resins are in the range of 70-80°C, with the S-SCB-S resin curing at the lowest temperature, 68°C. Meanwhile, the lignosulphonate seem to cure at a much higher temperature, with SL-M-PR resin curing at the highest temperature, 172°C. Correspondingly, the S-SCB-S resin has the highest cure rate with a ΔT value of 40°C, and the SL-M-PR resin has the lowest cure rate at 144°C.

Additionally, the lignosulphonate resins experience additional exotherms and endotherms not observed in the other lignins. Looking at the DSC curve of the SL-E-T resin, it can be seen that the curve becomes quite noisy after a temperature of 120°C has been reached. Its maximum endotherm, attributed to the curing of the resin, is experienced at 126°C, however it also has another distinctive endotherm at 137°C. This may be due to other reaction mechanisms (Ghorbani, et al., 2016) influenced by the sulphonate groups in the lignosulphonates, or even the inorganic content in the material. Similarly, the SL-M-PR resin experiences two distinctive endotherms, as well as two exotherms. The first endotherm, experienced at 54°C, may be related to other reaction mechanism, or sterical hindrances within the resin structure (Ghorbani, et al., 2016). The resin then experiences two minor exotherms, 136°C and 156°C, before reaching its curing temperature at 172°C. The first endotherm occurs at the same temperature at which the SL-E-T resin experienced a second endotherm, 136/137°C. This could allude to a similar reaction occurring in both lignosulphonate resins, but with a different temperature requirements.

4.3.3. Shear Bonding Strength Tests

The bonding performance of the LPF100 adhesives and the commercial adhesive were evaluated according to the ASTM D906-98 (2011) standard for Shear Strength of Plywood Samples by Tension Loading. These results are presented in Figure 4.7, and were assessed against the Chinese Grade A plywood standard (GB/T 17657-2013), whereby bonding strength should be ≥0.7MPa for commercial use. The blue dotted line on Figure 4.7 represents the GB/T 17657-2013 standard. The maroon dotted line represents the shear bonding strength of the Bondite adhesive.

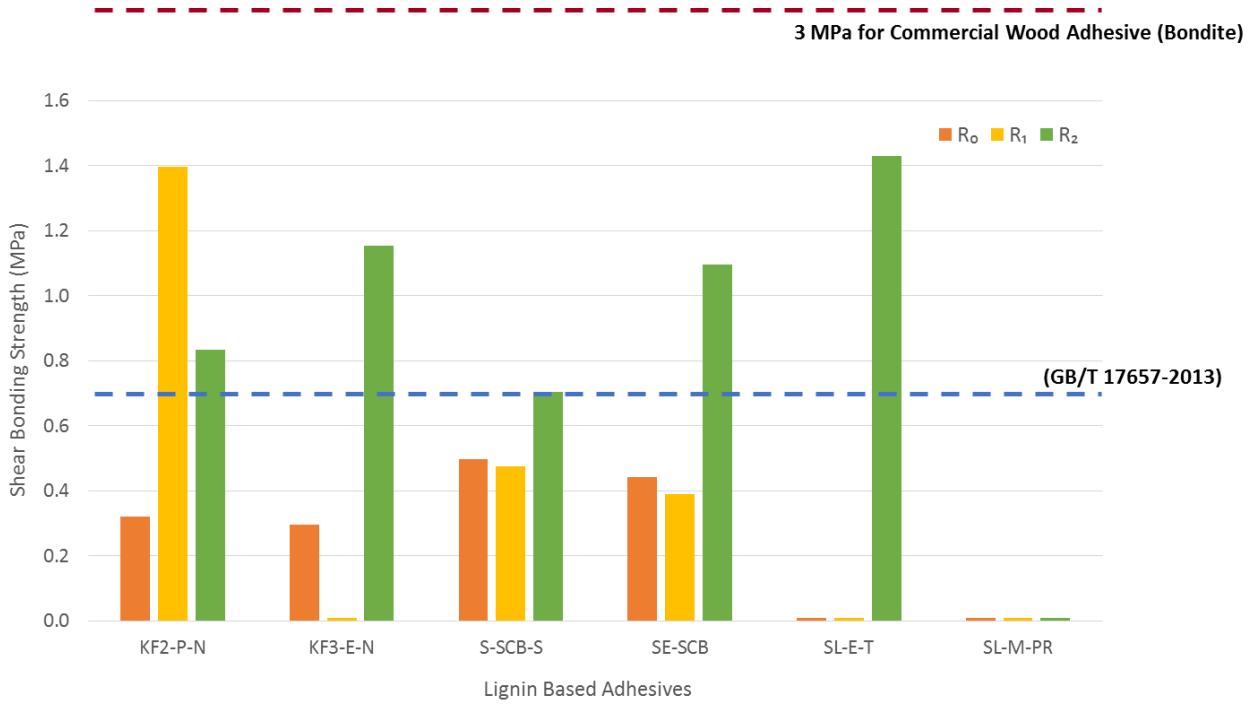

Figure 4.7: Shear bonding strength of unmodified LPF100 adhesives (R_0) and modified LPF100 adhesives (R_1 & R_2)

Looking at the LPF100 adhesives (R_0), none of them were able to meet the standard of ≥ 0.7 MPa. In contrast, the commercial Bondite adhesive exceeded the standard, recording a shear bonding strength of 3 MPa. This performance of Bondite is consistent with another study that used Bondite as a reference adhesive, whereby Bondite 345 produced a shear strength of 4.7 MPa (Alawode, et al., 2019). It should be noted though that the Bondite adhesive consists of both Bondite 345 and hexamine, without which Bondite 345 cannot be used as a resin (as specified by the manufacturers).

Comparing the R_0 LPF100 adhesives to each other, it can be seen that the bagasse soda lignin (S-SCB-S) recorded the highest bonding strength of 0.5 MPa, and the two kraft lignins recording 0.3 MPa each. The bagasse steam explosion lignin was in the middle with 0.4 MPa. The fact that these four LPF100 adhesives were able to effectively glue the wood veneers together and register a substantial bonding strength, speaks to their potential as wood glues which was very well supported by the FTIR results obtained in both Chapter 3 and 4.

FTIR spectroscopy of the lignin samples (Chapter 3) revealed that both KF2-P-N and S-SCB-S lignins recorded the highest intensities in the region 3340-3330 cm^{-1}, attributed to total hydroxyl content. Further to that, the SE-SCB and KF2-P-N lignins showed the highest absorbances in the region of 1220-1210 cm^{-1}, attributed to stretching of phenolic hydroxyl groups. This holds significance due to the reactive nature of hydroxyl groups, particularly phenolic hydroxyl groups during resin synthesis (Siddiqui, 2013). Additionally, the pine kraft lignin (KF2-P-N) showed distinctive peaks at 1264 cm^{-1}, 1141 cm^{-1}, and 854 cm^{-1}, which are all typical of vibrations associated with G units. Both the bagasse lignins also showed absorptions at 832cm^{-1} which is characteristic of C-H stretching of H monomers. Since H and G monomers are less substituted at the aromatic ring, it follows that more reactive sites may be available during resin synthesis (Pfungen, 2015). This corresponded well with the FTIR results from the resins samples (Chapter 4). The bagasse and kraft lignins showed absorption bands at 1458cm^{-1}, indicating the presence of methylene bridges that are formed when methylolphenols (lignin/phenol-formaldehyde derivatives) condense with each other during the second stage of resin synthesis. Furthermore, the KF2-P-N resin showed a weak absorption at 1130cm^{-1}, attributed to stretching of ether linkages, possibly alluding to the dimethylene ether linkages formed during methylolphenol condensation. The presence of these bands confirms that a reaction between formaldehyde and the respective kraft and bagasse lignins did indeed take place, which is reflected by the adhesions displayed by each of these LPF100 adhesives.

It was anticipated, however, that the pine kraft (KF2-P-N) lignin would perform at least marginally better than the eucalyptus kraft (KF3-E-N) lignin for the abovementioned reasons. Further to that, the ^{13}C NMR analysis showed that all samples except the lignosulphonate sample (SL-E-T) showed a number of signals in the range 140-124ppm, which is assigned to condensed aromatic C-C bonds, specifically of the C_5 carbon. This corresponded to GPC analysis of lignins, whereby it was found that KF2-P-N has a higher molecular weight than KF3-E-N due to guaiacyl difference between soft and hardwoods. Guaiacyl units are known to have stable structure due to C-C linkages at C_5. Additionally, beta-aryl bonds in syringyl units in hardwood are easily broken. The content of C-C linkages and it stability agreed with results obtained from TGA analysis of lignins, where KF2-P-N lignin was revealed to be the most thermally stable. Condensed C-C bonds usually possess relatively

high bond energies, and thus a significant amount of these linkages would normally add to the mechanical stability of the bond line in LPF adhesives (Yang, et al., 2014). However, this was not reflected in the bonding strength results. FTIR of the lignins did allude to a relatively higher content of phenolic hydroxyls in SE-SCB and KF2-P-N lignins. Although many agree that phenolic hydroxyl groups are important for lignin's reactivity during resin synthesis, particularly by activating free ring positions to increase reactivity towards formaldehyde, some researcher have found that there might be disadvantages to this. Some studies have found that very large quantities of phenolic hydroxyls could promote higher non-covalent interactions between lignin units, thus resulting in a 'crowded' stiff macromolecule, which would ultimately hinder the final properties of adhesives made with it (Zhang, et al., 2013). This may be a reason why the KF2-P-N lignin, and even the SE-SCB lignin, could not match the bonding performance of the S-SCB-S lignin, despite having a higher phenolic hydroxyl content.

Looking at the two lignosulphonate adhesives, they registered no strength. This was because when preparing to cut these boards into specimens for testing, the layers delaminated and unglued from each other. This was equated to the lignosulphonate adhesives having zero shear bonding strength. Once again, this poor performance of the lignosulphonates could be predicated from characterization analyses of the lignin samples. ^{13} C NMR analysis (of which the SL-M-PR lignin was unsuitable for analysis) showed that the SL-E-T lignin showed no signals in the range 140-124ppm, which is assigned to condensed aromatic C-C bonds, specifically of the C_5 carbon, which are linkages thought to provide mechanical stability in adhesive applications (Yang, et al., 2014). Additionally, the lignosulphonate samples were not able to undergo purification, and as result they had high ash contents in the range of 28-43 wt. %. It is often thought that such impurities, especially at high quantities, often impede reactivity during resin synthesis, acting as fillers and potentially hindering board properties (Effendi, et al., 2008). Furthermore, Khan& Ashraf (2006) stated that high shear strengths result from high degrees of polycondensation (during synthesis) and crosslinking (during synthesis and curing). A high rate of polycondensation and crosslinking is, in return, due to the large availability of phenol groups in lignin molecules (Khan & Ashraf, 2006). Considering the high impurity content of the lignosulphonates and its structural chemistry revealed in FTIR analysis, it can be deduced that these lignin samples did not have enough accessible phenol groups to sufficiently react with formaldehyde and condense thereafter.

When comparing the R_0 LPF100 adhesives to literature, it is evident that the LPF100 bonding performances were comparatively lower. Kalami et al. (2017) synthesized LPF resins at a 100% phenol substitution using biorefinery corn stover lignin. The dry shear bonding strength the obtained was 3.4 MPa. However, it should be noted that their adhesive formulation included additives like

wheat flour, alder bark modal, and sodium hydroxide, presumably as a binder, filler, and catalyst respectively. Meanwhile, the curing temperature of the corn stover resins were markedly higher at 203°C, whereas the kraft and bagasse LPF100 resins had curing temperatures in the range of 68-80°C, and the lignosulphonate LPF100 resins a range of 126-172°C. These curing temperatures of the LPF100 resins were incidentally lower than the commercial PF resin prepared by Kalami et al. (2017) which recorded a curing temperature of 195°C (Kalami, et al., 2017). Similarly, Yang et al. (2015) synthesized LPF resins at a 50% phenol substitution rate using four different biorefinery lignins. Bonding strengths of these LPF50 resins were above the GB/T 17657-2013 Chinese plywood standard, in the range of 1.18-0.95 MPa. Curing temperatures of the LPF50 resins were in the range of 124-130°C (Yang, et al., 2015). Thus, by this preliminary comparison, it would seem that whilst pulping-based lignins give below-standard shear bonding strengths compared to biorefinery lignins, the curing properties of the pulping lignins are superior.

Ultimately, given the below-standard performance of the R_0 LPF100 adhesives, and the obvious potential of the LPF100 resins, specifically the bagasse and kraft LPF100 resins, it was decided that modification of the R_0 LPF100 adhesives would be carried out to try and improve strength properties. This 'modification' would be carried out by addition of selected additives to the adhesive formulation to improve bonding performances. The choice to modify the adhesive rather than the lignin sample was taken with the idea of practical industrial implementation in mind. Whilst there are a number of reasons to turn away from the use of petroleum-derived adhesives, lignin still needs to compete with these adhesives in terms of economic viability (Gandini & Belgacem, 2008). If lignin as a feedstock is accompanied with the requirement of modification, of which a no process to date has been able to successfully incorporate economic and environmental viability with efficient modification, it would significantly impede industrialization, as it does now (Hu, et al., 2011). Thus, modification of the adhesive was chosen, especially since the addition of required additives is already industrially practiced (Alawode, 2019).

As discussed in Section 4.2.1, a crosslinker and two different hardeners were chosen in order to improve crosslinking of the adhesive during curing. Hexamine was chosen as a crosslinker, and glyoxal and epichlorohydrin were chosen as hardeners. Adhesives using composed of hexamine and glyoxal (in addition to the LPF100 resin) is labelled as R_1 LPF100 adhesives. Adhesives composed of epichlorohydrin and hexamine (as well as LPF100 resin) is labelled as R_2 LPF100 adhesive.

The shear bonding strength results of the R_1 and R_2 LPF100 adhesives are presented in Figure 4.7 as well. Looking at the R_1 LPF100 adhesives, the best performing adhesive is the KF2-P-N adhesive with a shear bond strength of 1.4 MPa. This exceeds the GB/T 17657-2013 Chinese plywood standard. Bagasse LPF100 adhesives showed no improvement in bonding strength, still registering

shear strengths of 0.5 and 0.4 MPa for S-SCB-S and SE-SCB, respectively. Meanwhile, the KF3-E-N and lignosulphonate LPF100 adhesives could not undergo testing as the veneers in the respective boards delaminated, qualitatively indicating poor bonding performance.

Considering the R_2 LPF100 adhesives, the overall bonding performances showed great improvement, with all LPF100 adhesives, except SL-M-PR, meeting or exceeding the standard of 0.7 MPa. Unfortunately, the SL-M-PR LPF100 adhesive delaminated prior to testing, once again qualitatively showing poor bonding performance. The best performing adhesive was the SL-E-T LPF100 adhesive with 1.4 MPa. However, considering that both the R_0 and R_1 SL-E-T adhesives delaminated prior to testing, it is likely that the exceptional performance of the R_2 SL-E-T adhesive is due to the hexamine and epichlorohydrin.

In general it would seem that R_1 adhesives using glyoxal, did not enable improvement of bonding strength, with the exception of the KF2-P-N LPF100 adhesive. On the other hand, R_2 adhesives using epichlorohydrin showed significant improvements, with the bagasse, kraft and SL-E-T LPF100 adhesives meeting standard. To try and understand the variability in results across R_1 and R_2 test results, it is necessary to understand the reaction mechanism between the lignin-based resins, the wood and the additives. Hexamine acts as a crosslinker via the trans-esterfication reaction of its methoxyl groups with the hydroxyl groups present in the LPF100 resins, wood veneers, Glyoxal ($C_2H_2O_2$), and epichlorohydrin (C_3H_5ClO). Its effectiveness as a crosslinker comes from the presence of six methoxyl methyl groups within its structure, thus providing a sufficient network of crosslinks by which hydroxyl groups in the LPF100 resin, wood and hardeners can react with (Imman, et al., 2001; Alawode, 2019). Since the hexamine reacts with hydroxyl groups, it follows from Section 3.3.2, that the KF2-P-N and S-SCB-S adhesives would form a more extensive and stable crosslinked network with hexamine, due to the higher availability if phenolic hydroxyl groups. However, there is a difference in bonding strengths of R_1 S-SCB-S and R_2 S-SCB-S which comes from the difference of hardener used. Similar results were reflected in the KF3-E-N, SE-SCB, and SL-E-T LPF100 adhesives, whereby improvements in bonding performance from R_0 tests were only achieved in R_2 tests using epichlorohydrin. This could be attributed to presence of ester groups within epichlorohydrin which are more susceptible to reacting with the hexamine, since trans-esterification usually occurs between ester and alcohol groups. Meanwhile, glyoxal is a dialdehyde with carbonyl groups in its structure. This could also explain why the R_2 SL-E-T adhesive performed so well, whilst the R_0 and R_1 SL-E-T adhesives delaminated prior to testing. In contrast, KF2-P-N LPF100 adhesives were the only adhesive to show improvements with the use of both R_1 and R_2 formulations, but with greater performance reflecting in R_1 tests. Thus, there could be an interaction between glyoxal and the particular functional groups within the KF2-P-N resin that allows for effective crosslinking and

curing. In the same vein, SL-M-PR LPF100 adhesive did not show an improvement in performance for either R_1 or R_2 tests. As discussed previously, FTIR showed an absence of phenolic hydroxyl groups, which would hinder sufficient crosslinking with hexamine. However, SL-M-PR lignin did show presence of aliphatic hydroxyls, so its underperformance indicates that impurities in the lignosulphonate possible impeded interactions of aliphatic hydroxyls with hexamine, the wood surface and either hardener.

Ultimately, looking at the modified LPF100 adhesives, the best performing were the R_1 KF2-P-N LPF100 adhesive and the R_2 SL-E-T LPF100 adhesive, both recording 1.4 MPa of shear strength, thus exceeding the GB/T 17567-2013 plywood standard of $\geq$0.7 MPa. The curing temperature of these two resins are 71°C and 126°C, respectively. Thus, considering both curing and bonding properties, KF2-P-N lignin is a more promising phenol substitute. However, the S-SCB-S resin was a consistent performer, even recording the highest shear strength from the unmodified adhesives (0.5 MPa). Additionally, the S-SCB-S resin had the highest curing rate form all resins samples, and the lowest curing temperature of 68°C. Thus, it also shows great potential as a phenol substitute.

Chapter 5: General Conclusions & Recommendations

This study conducts research based on the topic of lignin as a phenol substitute in phenol formaldehyde resins (PFRs). However, within a South African context, it looks at using lignins derived from industrial spent pulping liquor as a phenol substitute in PFRs, thus providing insight on a research avenue in this field of work that is not commonly explored. The intention of this study is to provide a screening of which available South African pulping lignins show the greatest potential as a phenol substitute, thus enabling further research on specific points to ultimately reach a stage of industrialization. As such, an extreme case of 100% phenol substitution was chosen, thus this study attempts total phenol replacement with local pulping-based lignins. To my knowledge, only one study has successfully attempted this, but with use of biorefinery technical lignin (Kalami, et al., 2017). The use of lignin as a phenol substitute would greatly relieve the reliance on petroleum based adhesives and environmental burdens, whilst simultaneously increasing waste efficiency in the South African paper and pulp industry. The rest of this chapter discusses conclusions from this study, and suggests recommendations for future research.

5.1. Conclusions

The overall aim of this project was to investigate the potential of using six South African pulping-based lignins as a phenol substitute in phenol-formaldehyde resins, for use as a wood adhesive in wood composites and wood construction.

Based on the results of lignin characterisation carried out in Chapter 3, the following conclusions can be drawn:

From compositional analyses it was found that the kraft and bagasse lignins boasted ash and sugar contents of $\leq 5\%$ and $\leq 0.5\%$, respectively. This is largely attributed to the purification step carried out prior to characterization. Meanwhile, the ash contents of the lignosulphonates were in the range of 28-43%, which was expected as purification could not be carried out due to the solubility of lignosulphonates in water and acid solutions. However, this foreshadows poor reactivity and resin properties due to the high quantity of impurities. Additionally, the sugar content of lignosulphonates could not be determined due its high unsuitability for HPLC analysis.

From Structural analyses like FTIR and ^{13}C NMR spectroscopy, it can be concluded that KF2-P-N (pine kraft), S-SCB-S (bagasse soda) SE-SCB (bagasse steam explosion) lignins have the highest reactivity to due high contents of phenolic hydroxyls. Explicitly referring to FTIR results, all samples showed broad bands in the region 3340-3330 cm^{-1}, attributed to total hydroxyl content, with the pine kraft (KF2-P-N) and bagasse soda (S-SCB-S) lignins recording the highest intensities. Bagasse steam

explosion (SE-SCB) and KF2-P-N lignins showed high absorbances in the region of 1220-1210 cm^{-1}, attributed to stretching of phenolic hydroxyl groups. This is significant since hydroxyl groups, specifically the phenolic hydroxyl groups which are known to be highly reactive, is known to have a great effect on lignin's reactivity. Ideally, a high content of phenolic hydroxyl would indicate high reactivity of that lignin (Laurichesse & Avérous, 2014). Furthermore, the SL-E-T and SL-M-PR (lignosulphonate) samples registered no peaks in this region, likely indicating a shift in the positions of these bands due to a high impurity content. All samples showed distinctive peaks at 1044-1030 cm^{-1}, typical of stretching of aliphatic hydroxyl groups. All samples registered weak bands at 2849 cm^{-1} indicating the presence of methoxyl groups, which are known to hinder reactivity due to steric hindrances at the aromatic ring. Additionally, bagasse and kraft lignins showed sharp peaks at 1461-1451 cm^{-1}, which is characteristic C-H bending in methoxyl groups, possibly indicating that these samples contain a significant amount of methoxyl groups within its structure. Regarding ^{13}C NMR results, all samples except KF3-E-N, showed signals in the region of 117-114ppm, indicating the presence of C_5 aromatic C-H bonds, which are indicative of the presence of G units. Similarly, all samples except the lignosulphonate sample (SL-E-T) showed a number of signals in the range 140-124ppm, which is assigned to condensed aromatic C-C bonds, specifically of the C_5 carbon. Condensed C-C bonds usually possess relatively high bond energies, and are thus a significant amount of these linkages would add to the mechanical stability of the bond line LPF adhesives (Yang, et al., 2014). All samples except bagasse soda lignin (S-SCB-S) showed signals at 57-54ppm, assigned to methoxyl groups.

From GPC analysis, KF2-P-N lignin had a higher Mw and PDI than KF3-E-N lignin, due to guaiacyl difference between soft and hardwoods. Compared to both, SE-SCB lignin had the highest Mw and PDI of 6335 g/mol and 2.80, respectively. The soda bagasse lignin and lignosulphonates were not suitable for analysis. Furthermore, lignins with high molecular weights supposedly possess a higher level of cross-linking (Pizzi, 2003), thus high strength properties can be expected.

Based on TGA results, the KF2-P-N was determined to be the most thermally stable, followed by the bagasse lignins, registering maximum degradation temperatures in the range of 380°C. The high thermal stability of the KF2-P-N and SE-SCB lignins can be attributed to its comparatively higher G monomer content. G monomers are known to have highly stable structures due to condensed C-C bonds that are not easily cleaved during isolation processes (Naron, et al., 2017). Similar behaviour was observed for the TGA of resins samples; all resins showed gradual degradation over a 600°C with SE-SB and KF2-P-N resins ending off with the highest weight residues at 57 and 55%, respectively.

Ultimately, from the lignin characterisation analyses in Chapter 3, it can be deduced that the KF2-P-N (pine kraft) and S-SCB-S (soda bagasse) lignins would most likely perform best as a phenol substitute in PF resins, followed closely by the SE-SCB (steam explosion bagasse) lignin.

Based on the results of resin characterisation carried out in Chapter 4, the following conclusions can be drawn:

Similar to Chapter 3, FTIR analysis of LPF100 resins concluded that KF2-P-N, S-SCB-S, and SE-SCB LPF100 resins would most likely produce the best bonding performances. With the exception of the lignosulphonate resins, weak peaks appear at 1458 cm-1 characteristic of C - H bending in CH_2 groups. This band is of particular interest, as it indicates the presence of methylene bridges in the resin structure, thus giving a rough indication of the reaction between formaldehyde and the phenol moieties in lignin, as well as the condensation of these groups into a prepolymer (Siddiqui, 2013). This was further confirmed by the medium intensity absorption band at 1020 cm^{-1} in the kraft and SE-SCB resin spectra, which is characteristic of C-O stretching of methylol C-OH, aliphatic C-OH, and aliphatic C-O (Ar). Additionally, the KF2-P-N and S-SCB-S resins showed absorption peaks at 1130 cm^{-1} and 1050 cm^{-1}, alluding to ether linkages between methylol groups.

Finally, differential scanning calorimetry (DSC) provided information of the curing behaviour of the resins. Once again, the S-SCB-S and KF2-P-N resins showed the best curing qualities, possessing both low curing temperatures (68°C and 71°C respectively) and high curing rates.

With regards to shear bonding strength, when looking at the R_0 (unmodified) LPF100 adhesives, none of them were able to meet the Chinese plywood standard of $\geq$ 0.7 MPa (GB/T 17657-2013). In contrast, the commercial Bondite adhesive exceeded the standard, recording a shear bonding strength of 3 MPa. It should be noted though that the Bondite adhesive consists of both Bondite 345 and hexamine, without which Bondite 345 cannot be used as a resin (as specified by the manufacturers).

Comparing the R_0 LPF100 adhesives to each other, it can be seen that the bagasse soda lignin (S-SCB-S) recorded the highest bonding strength of 0.5 MPa, and the two kraft lignins recording 0.3 MPa each. The bagasse steam explosion lignin was in the middle with 0.4 MPa. The fact that these four LPF100 adhesives were able to effectively glue the wood veneers together and register a substantial bonding strength, speaks to their potential as wood glues which was very well supported by the FTIR results obtained in both Chapter 3 and 4.

It was anticipated, however, that the pine kraft (KF2-P-N) resin would perform at least marginally better than the eucalyptus kraft (KF3-E-N) resin. Further to that, the ^{13}C NMR analysis showed that all samples except the lignosulphonate sample (SL-E-T) showed a number of signals in the range 140-124ppm, which is assigned to condensed aromatic C-C bonds, specifically of the C_5 carbon.

Condensed C-C bonds usually possess relatively high bond energies, and are thus a significant amount of these linkages would normally add to the mechanical stability of the bond line LPF adhesives (Yang, et al., 2014). This corresponded to both GPC and TGA analyses on the lignin samples. However, this was not reflected in the bonding strength results. FTIR of the lignins did allude to a relatively higher content of phenolic hydroxyls in SE-SCB and KF2-P-N lignins. Some studies have found that very large quantities of phenolic hydroxyls could promote higher non-covalent interactions between lignin units, thus resulting in a stiff macromolecule, which would ultimately hinder the final properties of adhesives made with it (Zhang, et al., 2013). This may be a reason why the KF2-P-N lignin, and even the SE-SCB lignin, could not match the bonding performance of the S-SCB-S lignin, despite having a higher phenolic hydroxyl content.

Looking at the two lignosulphonate adhesives, they registered no strength, and this was because when preparing to cut these boards into specimens for testing, the layers delaminated and unglued from each other. Once again, this poor performance of the lignosulphonates could be predicated form characterization analyses of the lignin samples.

Looking at the R_1 LPF100 adhesives, the best performing adhesive is the KF2-P-N adhesive with a shear bond strength of 1.4 MPa. This exceeds the GB/T 17657-2013 Chinese plywood standard. Bagasse LPF100 adhesives showed no improvement in bonding strength, still registering shear strengths of 0.5 and 0.4 MPa for S-SCB-S and SE-SCB, respectively. Meanwhile, the KF3-E-N and lignosulphonate LPF100 adhesives could not undergo testing as the veneers in the respective boards delaminated, qualitatively indicating poor bonding performance.

Considering the R_2 LPF100 adhesives, the overall bonding performances showed great improvement, with all LPF100 adhesives, except SL-M-PR, meeting or exceeding the standard of 0.7 MPa. Unfortunately, the SL-M-PR LPF100 adhesive delaminated prior to testing, once again qualitatively showing poor bonding performance. The best performing adhesive was the SL-E-T LPF100 adhesive with 1.4 MPa.

Ultimately, looking at the modified LPF100 adhesives, the best performing were the R_1 KF2-P-N LPF100 adhesive and the R_2 SL-E-T LPF100 adhesive, both recording 1.4 MPa of shear strength, thus exceeding the GB/T 17567-2013 plywood standard of $\geq$0.7 MPa. The curing temperature of these two resins are 71°C and 126°C, respectively. Thus, considering both curing and bonding properties, KF2-P-N lignin is a more promising phenol substitute. However, the S-SCB-S resin was a consistent performer, even recording the highest shear strength from the unmodified adhesives (0.5 MPa). Additionally, the S-SCB-S resin had the highest curing rate from all resins samples, and the lowest curing temperature of 68°C. Thus, it also shows great potential as a phenol substitute.

5.2. Recommendations

The aim of this study was to investigate the potential of spent pulping lignins as total phenol replacements in phenol formaldehyde resins. In that regard, it is recommended that the S-SBC-S and KF2-P-N lignins be further studied, as LPF100 resins made from these lignins produced consistent and favourable resin properties. With regards to the different adhesive formulations, it is recommended that further work be done using the R_1 formulation (resin, hexamine as crosslinker, and glyoxal as hardener) for KF2-P-N LPF100 resin, and R_2 formulation (resin, hexamine as crosslinker, and epichlorohydrin as hardener) for S-SCB-S LPF100 resin.

It is recommended that future work be focused on resin synthesis and resin characterisation, as the S-SCB-S and KF2-P-N resins were able to perform well without modification to the lignins themselves. Explicitly, optimisation of the resin synthesis process could be studied, looking particularly at the effect of Formaldehyde/Phenol (F/P) and catalyst molar ratios on bonding strength or curing temperature. With regards to the bonding strength tests, it would be worthwhile optimising the board making process, particularly the hot pressing of the plywood samples. Variables such as hot press temperature and hot press time could be investigated in relation to the bonding strengths of the resins.

For improved results that is perhaps more industrially favourable, different phenol substitution levels could also be investigated (LPF50, LPF75 resins, etc.), and depending on the corresponding strength of the lignins, less crosslinker and hardener could be used since a higher rate of condensation during synthesis requires less enhancement of crosslinking during the curing process.

Additionally, for a greater understanding of the chemistry and bonding capability of lignosulphonates, it is recommended that future work look into desulphonation of lignosulphonate. This might allow extraction and purification of the lignin, which in turn would allow for better characterisation of the lignin samples. An improvement in the resultant resins may also be observed.

Finally, another possibility for future work would be investigating crude spent pulping lignins as a phenol substitute, i.e. unpurified spent pulping lignins. In this study, purified lignins were studied to get a base case idea of the capabilities of the lignins themselves. However, the actual implementation of lignin as a phenol replacement in PF resins will only reach commercialisation with minimum added processing steps for both the pulping mills and resin manufacturing plants. Thus, the final goal would be using unpurified pulping lignins, if not crude pulping liquor itself.

Ultimately, from the six lignin studied, the S-SCB-S (soda bagasse) and KF2-P-N (pine kraft) lignins showed the most favourable results, and it is recommended that they be further investigated as a phenol replacement in PF resins.

References

Abdelwahab, N. & Nassar, M., 2011. Preparation, optimisation and characterisation of lignin phenol formaldehyde resin as wood adhesive. *Pigment & Resin Technology,* 40(3), pp. 169 - 174.

Akhtar, T., Lutfullah, G. & Zahoorullah, 2011. Lignonsulfonate-phenolformaldehyrde Adhesive: A Potenstial Binder for Wood Panel Industries. *Journal of the Chemical Society of Pakistan,* 33(4), pp. 535-538.

Alawode, A. et al., 2019. Properties and characteristics of novel formaldehyde-free wood adhesives prepared from Irvingia gabonensis and Irvingia wombolu seed kernel extracts. *International Journal of Adhesion and Adhesives,* Volume 95, p. 102423.

Alawode, A. O., 2019. *Properties and potential use of Irvingia gabonensis and Irvingia wombolu kernel extract as an eco-friendly wood adhesive,* Stellenbosch: Forestry and Wood Sciences Department, Stellenbosch University.

Alonso, M. et al., 2005. Modification of ammonium lignosulfonate by phenolation for use in phenolic resins. *Bioresource Technology,* Volume 96, p. 1013–1018.

Alonso, M. V. et al., 2001. Characterization and Structural Modification of Ammonic Lignosulfonate by Methylolation. *Journal of Applied Polymer Science,* Volume 82, pp. 2661-2668.

Argyropoulos, D. S. & Menachem, S. B., 1997. Lignin. In: *Advances in Biochemical Engineering/Biotechnology.* Montreal: s.n., pp. 128 - 158.

Atkins, P. & Paula, J. d., 2006. *Atkins' Physical Chemistry.* 8th ed. New York: W. H. Freeman and Company.

Balgacem, M. N. & Gandini, A., 2008. Lignins as Components of Macromolecular Materials. In: M. N. Balgacem & A. Gandini, eds. *Monomers, Polymers and Composites from Renewable Resources.* s.l.:Elsevier, pp. 243-271.

Bhattacharjee, G., Neogi, S. & Das, S. K., 2014. Phenol–formaldehyde runaway reaction: a case study. *International Journal of Industrial Chemistry,* 5(2).

Chen, H., 2014. Chapter 2 Chemical Composition and Structure of Natural Lignocellulose. In: H. Chen, ed. *Biotechnology of Lignocellulose: Theory and Practice.* Beijing: Springer, pp. 25 - 71.

Clayden, J., Greeves, N., Warren, S. & Wothers, P., 2001. *Organic Chemistry.* Oxford: Oxford University Press.

Conradie, D., 1990. *Lignin-Based Epoxides,* Stellenbosch: University of Stellenbosch.

DeVries, K. L. & Borgmeier, P. R., 2003. Testing of Adhesives. In: A. Pizzi & K. L. Mittal, eds. *Handbook of Adhesive Technology.* Utah: Marcel Dekker, Inc., p. Chapter 11.

Dunky, M., 2003. Adhesives in the Wood Industry. In: A. Pizzi & K. L. Mittal, eds. *Handbook of Adhesive Technology.* Austria: Marcel Dekker, Inc., p. Chapter 47.

Dunky, M., 2003. Adhesives in the Wood Industry. In: A. Pizzi & K. L. Mittal, eds. *Handbook of Adhesive Technology.* Austria: Marcel Dekker, Inc., p. Chapetr 47.

Effendi, A., Gerhauser, H. & Bridgwater, A., 2008. Production of renewable phenolic resins by thermochemical conversion of biomass: A review. *Renewable and Sustainable Energy Reviews,* Volume 12, pp. 2092-2116.

Fatehi, P. & Chen, J., 2016. Extraction of Technical Lignins from Pulping Spent Liquors, Challenges and Opportunities. In: Z. Fang & J. Richard L. Smith, eds. *Production of Biofuels and Chemicals from Lignin, Biofuels and Biorefineries.* s.l.:Springer Science+Business Media Singapore, pp. 35-54.

Ferdosian, F., Pan, Z., Gao, G. & Zhao, B., 2017. Bio-Based Adhesives and Evaluation for Wood Composites Application. *Polymers,* 9(70).

Gandini, A. & Belgacem, M. N., 2008. Lignins as Components of Macromolecular Materials. In: A. Gandini & M. N. Belgacem, eds. *Monomers, Polymers and Composites from Renewable Resources.* s.l.:Elsevier, pp. 243-271.

Gellerstedt, G. & Henriksson, G., 2008. Lignins: Major Sources, Structure and Properties. In: M. N. Balgacem & A. Gandini, eds. *Monomers, Polymers and Composites from Renewable Resources.* UK: Elsevier, pp. 201 - 272.

Gelling, P. J., Hunt, J. E. B. & Marshman, J. D., 1983. *Continuous Production of Phenol-Formaldehyde Resin and Laminates Produced Therefrom.* United States of America, Patent No. 4413113.

Ghaffar, S. H. & Fan, M., 2014. Lignin in Straw and its Applications as an Adhesive. *International Journal of Adhesion & Adhesives,* Volume 48, pp. 92-101.

Ghorbani, M. et al., 2016. Lignin Phenol Formaldehyde Resoles: The Impact of Lignin Type on Adhesive Properties. *BioResources,* 11(3), pp. 6727-6741.

Goring, D., 1971. Polymer Properties of Lignin and Lignin Derivatives. In: K. Sarkanen & C. Ludwig, eds. *Lignins Occurence, Formation, Structure and Reactions.* USA: John Wiley & Sons, Inc., pp. 695-768.

Gotro, J., 2013. *The Winding Road to Renewable Thermoset Polymers Part 4: Phenolic Resins.* [Online] Available at: https://polymerinnovationblog.com/the-winding-road-to-renewable-thermoset-

polymers-part-4-phenolic-resins/
[Accessed 20 February 2017].

Gravitis, J. et al., 2010. Substitution of Phenolic Components by Steam-Exploded Lignin in Plywood and Self-binding Boards with Account of Energy Vecessary for Steam Explosion Treatment. *Scientific Journal of Riga Technical University*, Volume 21, pp. 7-11.

Haygreen, J. & Bowyer, J., 2007. 3. Composition and Structure of Wood Cells. In: *Forest Products and Wood Science: An Introduction.* s.l.:s.n., pp. 45 - 61.

Hemmila, V., Adamopoulos, S., Karlssonb, O. & Kumar, A., 2017. Development of sustainable bio-adhesives for engineered wood panels – A Review. *RSC Advances,* 7(61), pp. 38604-38630.

Hergert, H. L., 1971. Infrared Spectra. In: K. Sarkanen & C. Ludwig, eds. *Lignins Occurence, Formation, Structure and Reactions.* USA: John Wiley & Sons, Inc., pp. 267-297.

Hon, D. N.-S., 2003. Analysis of Adhesives. In: K. L. M. A Pizzi, ed. *Handbook of Adhesive Technology.* South Carolina: Marcel Dekker, Inc. , p. Chapter 14.

Hu, L. et al., 2014. Chemical Groups and Structural Characterization of Lignin via Thiol-Mediated Demethylation. *Journal of Wood Chemistry and Technology,* 2(34), pp. 122-134.

Hu, L., Pan, H., Zhou, Y. & Zhang, M., 2011. *Methods to Improve Lignin's Reactivity as a Phenol Substitute and as Replacement for Other Phenolic Compounds: A Brief Review,* Nanjing: BioResources.

Imman, S. H., Gordon, S. H., Mao, L. & Chen, L., 2001. Environmentally friendly wood adhesive from renewable plant ploymer: characteristics and optimization. *Polymer Degradation and stability,* Volume 73, pp. 529-533.

Kalami, S., Arefmanesh, M., Master, E. & Nejad, M., 2017. Replacing 100% of phenol in phenolic adhesive formulations with lignin. *Journal of Polymer Science,* p. 45124.

Keimel, F. A., 2003. Historical Development of Adhesives and Adhesive Bonding. In: A. Pizzi & K. L. Mittal, eds. *Handbook of Adhesive Technology.* New Jersey: Marcel Dekker, Inc., p. Chapter 1.

Khan, M. A. & Ashraf, S. M., 2006. Development and characterization of groundnut shell lignin modified phenol formaldehyde wood adhesive. *Indian Journal of Chemical Technology,* Volume 13, pp. 347-352.

Kishi, H. & Fujita, A., 2008. Wood-Based Epoxy Resins and the Ramie Fiber Reinforced Composites. *Environmental Engineering and Management Journal,* 7(5), pp. 517-523.

Kline, L. M., Hayes, D. G., Womac, A. R. & Labbe, N., 2010. Simplified Determination of Lignin Content in Hard and Softwoods via UV-Spectrophotometric Analysis of Biomass Dissolved in Ionic Liquids. *BioResources*, 5(3), pp. 1366-1383.

Kröhnke, J. et al., 2019. Comparison of Four Technical Lignins as a Resource for Electrically Conductive Carbon Particles. *BioResources*, 14(1), pp. 1091-1109.

Laurichesse, S. & Avérous, L., 2014. Chemical Modification of Lignins: Towards Biobased Polymers. *Progress in Polymer Science,* Volume 39, pp. 1266-1290.

Li, J. et al., 2016. Preparation and characterization of lignin demethylated at atmospheric pressure and its application in fast curing biobased phenolic resins. *RSC Advances*, 6(71), p. 67435–67443.

Li, J. et al., 2017. Fast Curing Bio-Based Phenolic Resins via Lignin Demethylated under Mild Reaction Condition. *Polymers*, Volume 9, p. 428.

Lisperguer, J., Perez, P. & Urizar, S., 2009. Structure and Thermal Properties of Lignins: Characterization by Infrared Spectroscopy and Differential Scanning Calorimetry. *Chile Chemistry Society*, 54(4), pp. 460-463.

Lora, J., 2008. Chapter 10 - Industrial Commercial Lignins: Sources, Properties and Applications. In: M. N. Belgacem & A. Gandini, eds. *Monomers, Polymers and Composites from Renewable Resources.* Amsterdam: Elsevier, pp. 225 - 242.

Lorenz, L. F. & Christiansen, A. W., 1995. Interactions of Phenolic Resin Alkalinity, Moisture Content, and Cure Behavior. *Industrial & Engineering Chemistry Research*, 34(12), pp. 4520-4523.

Lupoi, J. S. et al., 2015. Recent innovations in analytical methods for qualitative and quantitative assessment of lignin. *Renewable and Sustainable Energy Reviews,* Volume 49, pp. 871-906.

Malutan, T., Nicu, R. & Popa, V. I., 2008. Contribution to the Study of Hydroxymethylation Reaction of Alkali Lignin. *BioResources*, 3(1), pp. 13-20.

Martin-Sampedro, R. et al., 2011. Integration of kraft pulping on a forest biorefinery by the addition of a steam explosion pretreatment. *BioResources,* 6(1), pp. 513-528.

Martone, P. T. et al., 2009. *Discovery of Lignin in Seaweed Reveals Convergent Evolution of Cell-Wall Architecture,* USA: Elsevier Ltd.

Mathias, L., 2016. *Molecular Weight.* [Online]
Available at: http://www.pslc.ws/macrog/weight.htm
[Accessed 2017].

Matsushita, Y., 2015. Conversion of technical lignins to functional materials with retained polymeric properties. *The Japan Wood Research Society*, Volume 61, pp. 230-250.

Mousavioun, P. & Doherty, W., 2010. Chemical and Thermal Properties of Bagasse Soda Lignin. *Industrial Crops and Products,* 31(1), pp. 52-58.

Namane, M., 2016. *Precipitation and Valorisation of Lignin Obtained from South African Kraft Mill Black Liquor,* Cape Town: University fo Cape Town.

Naron, D. R., F-X, C., Tyhoda, L. & Gorgens, J., 2017. Characterisation of lignins from different sources by appropriate analytical methods: Introducing thermogravimetric analysis-thermal desorption-gas chromatography-mass spectroscopy. *Industrial Crops and Products*, Volume 101, pp. 61-74.

Ozmen, N., 2000. *Lignin Based Adhesives for Particleboard Production,* Bangor: University of Wales Bangor .

PAMSA, 2018. *Production Statistics.* [Online]
Available at: https://www.thepaperstory.co.za/the-economic-story/production-statistics/
[Accessed 2019].

PAMSA, 2019. *The Economic Story.* [Online]
Available at: https://www.thepaperstory.co.za/the-economic-story/
[Accessed 2019].

PAMSA, 2019. *The Sustainability Story.* [Online]
Available at: https://www.thepaperstory.co.za/the-sustainability-story/
[Accessed 2019].

Parker, R. J., 1981. *The Effect of Synthsis Variables on Composition and Reactivity of Phenol-Formaldehyde Resins,* Oregon: Oregon State University .

Perez, J. M. et al., 2007. Characterisation of a novolac resin substituting phenol by ammonium lignosulfonate as filler or extender. *BioResources,* 2(2), pp. 270-283.

Pfungen, L., 2015. *Lignin Phenol Formaldehyde Wood Adhesives,* Vienna: University of Natural Resources and Life Sciences.

Pizzi, A., 2003. Natural Phenolic Adhesives II: Lignin. In: A. Pizzi & K. L. Mittal, eds. *Handbook of Adhesive Technology.* s.l.:Marcel Dekker, Inc., p. Chapter 28.

Pizzi, A., 2003. Phenolic Resin Adhesive. In: A. Pizzi & K. L. Mittal, eds. *Handbook of Adhesive Technology.* France: Marcel Dekker; Inc., p. Chapter 26.

Pizzi, A. & Ibeh, C., 2014. Phenol-Formaldehydes . In: H. Dodiuk & S. H. Goodman, eds. *Handbook of Thermoset Plastics.* s.l.:s.n., pp. 13-44.

Podschun, J., Saake, B. & Lehnen, R., 2015. Reactivity enhancement of organosolv lignin by phenolation for improved bio-based thermosets. *European Polymer Journal,* Volume 67, pp. 1-11.

Poljanšek, I. & Krajnc, M., 2005. Characterization of Phenol-Formaldehyde Prepolymer Resins by In Line FT-IR Spectroscopy. *Acta Chimica Slovenica,* Volume 52, pp. 238-244.

Qiao, W., Li, S. & Xu, F., 2016. Preparation and Characterization of a Phenol-formaldehyde Resin Adhesive Obtained From Bio-ethanol Production Residue. *Polymers and Polymer Composites,* 24(2), pp. 99-106.

Rodríguez-Lucena, P., Lucena, J. J. & Hernández-Apaolaza, L., 2009. *Relationship between the structure of Fe-Lignosulfonate complexes determined by FTIR spectroscopy and their reduction by the leaf Fe reductase.* Calafornia, The Proceedings of the International Plant Nutrition Colloquium XVI, Department of Plant Sciences, UC Davis.

Sappi Ltd, 2019. *Lignin.* [Online]
Available at: https://www.sappi.com/lignin
[Accessed 2019].

Siddiqui, H., 2013. *Production of Lignin-Based Phenolic Resins Using De-Polymerized Kraft Lignin and Process Optimization,* Ontario: The University of Western Ontario.

Song, Y. et al., 2016. Demethylation of Wheat Straw Alkali Lignin for Application in Phenol Formaldehyde Adhesives. *Polymers,* Volume 8, p. 209.

Strydom, C., MthomboI, T., Bunt, J. & Neomagus, H., 2018. Some physical and chemical characteristics of calcium lignosulphonate-bound coal fines. *Journal of the Southern African Institute of Mining and Metallurgy*, 118(2).

Sulaiman, N. S. et al., 2013. Evaluation of the Properties of Particleboard Made Using Oil Palm Starch Modified with Epichlorohydrin. *BioResources,* 8(1), pp. 283-301.

Thies, M. C. & Klett, A. S., 2016. Recovery of Low-Ash and Ultrapure Lignins from Alkaline Liquor By-Product Streams. In: Z. Fang & J. Richard L. Smith, eds. *Production of Biofuels and Chemicals from Lignin, Biofuels and Biorefineries.* s.l.:Springer Science+Business Media Singapore, pp. 55-78.

Tian, X., Fang, Z., Richard L. Smith, J. & Wu, Z., 2016. Properties, Chemical Characteristics and Application of Lignin and Its Derivatives. In: Z. Fang & J. Richard L. Smith, eds. *Production of Biofules and Chemicals form Lignin.* s.l.:Springer Science+Business Media Singapore, pp. 3-33.

Truter, P.-A., 1990. *Hydroxymethylation of Hardwood Kraft Lignin*, Stellenbosch: University of Stellenbosch.

Tyhoda, L., 2008. *Synthesis, characterisation and evaluation of slow nitrogen release organic soil conditioners from South African technical lignins*, Stellenbosch: Stellenbosch University.

Uner, B. & Olgun, C., 2017. The Effect of Hardener on Adhesive and Fiberboard Properties. *Wood Research*, 62(1), pp. 27-36.

Upton, B. M. & Kasko, A. M., 2015. Strategies for the Conversion of Lignin to High-Value Polymeric Materials: Review and Perspective. *Chemical Reviews*, 116(4), p. 2275−2306.

Vinardell, M. P. & Mitjans, M., 2017. Lignins and Their Derivatives with Beneficial Effects on Human Health. *International Journal of Molecular Sciences*, 18(6), p. 1219.

Wang, G. & Chen, H., 2013. Carbohydrate elimination of alkaline-extracted lignin liquor by steam explosion and its methylolation for substitution of phenolic adhesive. *Industrial Crops and Products*, Issue 53, pp. 93-101.

Welker, C. M. et al., 2015. *Engineering Plant Biomass Lignin Content and Composition for Biofuels and Bioproducts*, USA: Energies.

Westwood, N. J., Panovic, I. & Lancefield, C. S., 2016. Chemical Modification of Lignin for Renewable Polymers or Chemicals. In: Z. Fang & J. Richard L. Smith, eds. *Production of Biofuels and Chemicals from Lignin, Biofuels and Biorefineries.* s.l.:Springer Science+Business Media Singapore, pp. 183-216.

Xi, X., Pizzi, A. & Amirou, S., 2017. Melamine–Glyoxal–Glutaraldehyde Wood Panel Adhesives without Formaldehyde. *Polymers*, 22(10), p. 18.

Xu, C., Arancon, R. A. D., Labidid, J. & Luque, R., 2014. Lignin depolymerisation strategies: towards valuable chemicals and fuels. *Royal Society of Chemistry*, 43(22), pp. 7485-7500.

Yang, H. et al., 2016. Comparative study of lignin characteristic from wheat straw obtained by soda-AQ or kraft pretreatment and effect on the following enzymatic hydrolysis process. *Bioresource Technology*, Volume 207, pp. 361-369.

Yang, S., Wen, J.-L., Yuan, T.-Q. & Sun, R.-C., 2014. Characterization and phenolation of biorefinery technical lignins for lignin-phenol-formaldehyde resin adhesive synthesis. *Royal Society of Chemistry*, Volume 4, pp. 57996-58004.

Yang, S., Zhang, Y., Yuan, T.-Q. & Sun, R.-C., 2015. Lignin-phenol-formaldehyde resin adhesives prepared with biorefinery technical lignins. *Journal of Applied Polymer Science*, p. 42493.

Ysbrandy, R. E., 1992. *Adhesives Derived from Bagasse Autohydrolysis Lignin and Waste Phenolics from Binding of Wood Products*, Stellenbosch: University of Stellenbosch.

Zhang, W. et al., 2013. Preparation and properties of lignin-phenol-formaldehyde resins based on different residues of agricultural biomass. *Industrial Crops and Products*, Volume 43, pp. 326-333.

Zhang, W. et al., 2013. Preparation and properties of lignin-phenol-formaldehyde resins based on different residues of agricultural biomass. *Industrial Crops and Products*, Volume 43, pp. 326-333.

Zhou, H., Yang, D. & Zhu2, J. Y., 2016. Molecular Structure of Sodium Lignosulfonate from Different Sources and their Properties as Dispersant of TiO2 Slurry. *Journal of Dispersion Science Technology*, Volume 37, pp. 296-303.

Appendices

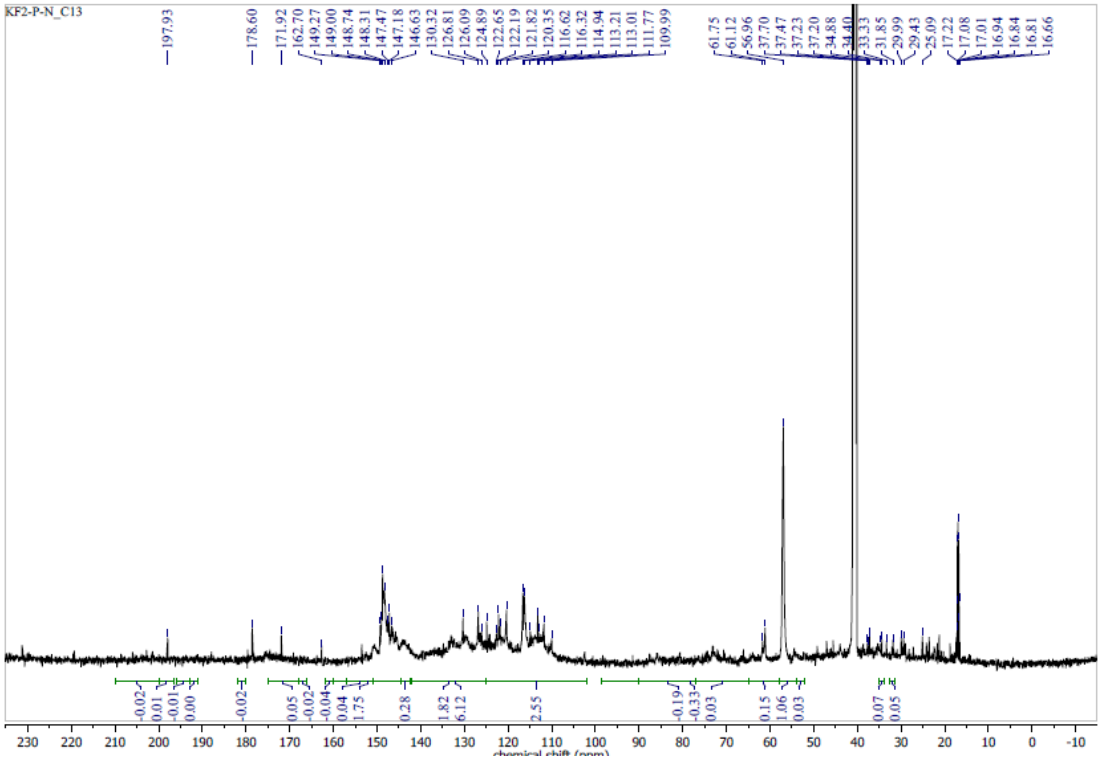

Figure A1: ^{13}C NMR Spectra of KF2-P-N lignin

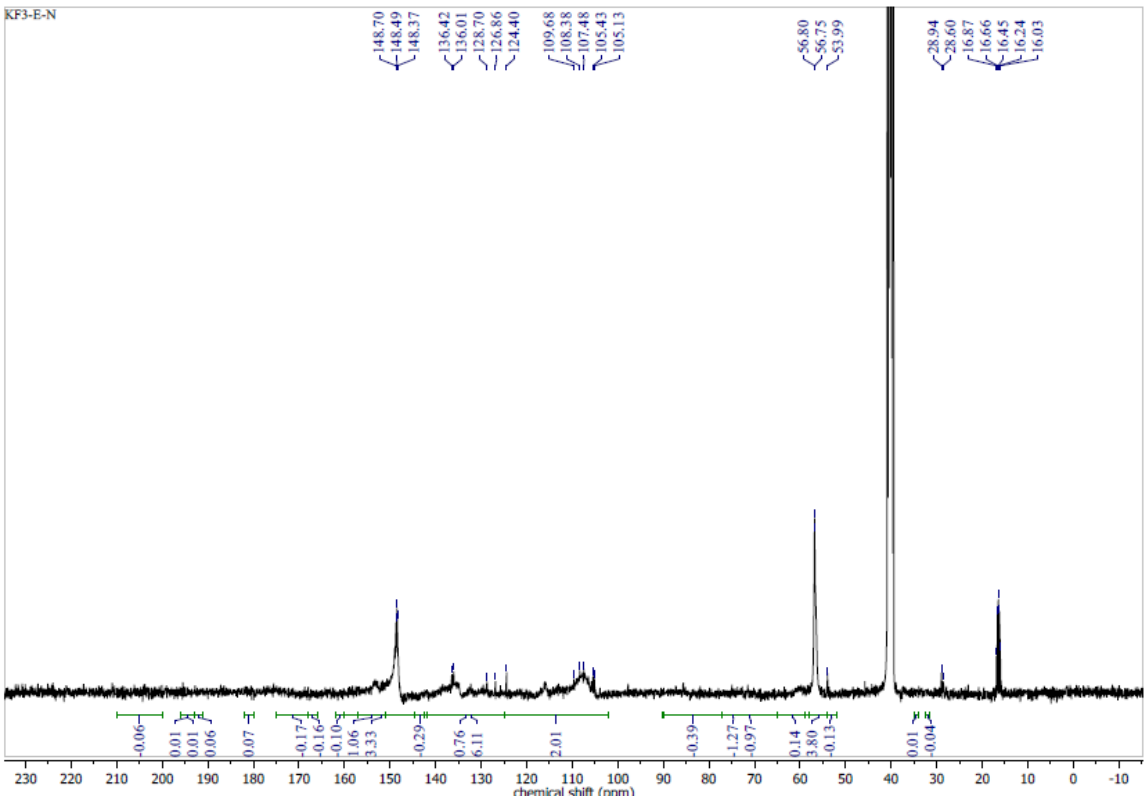

Figure A2: ^{13}C NMR Spectra of KF3-E-N lignin

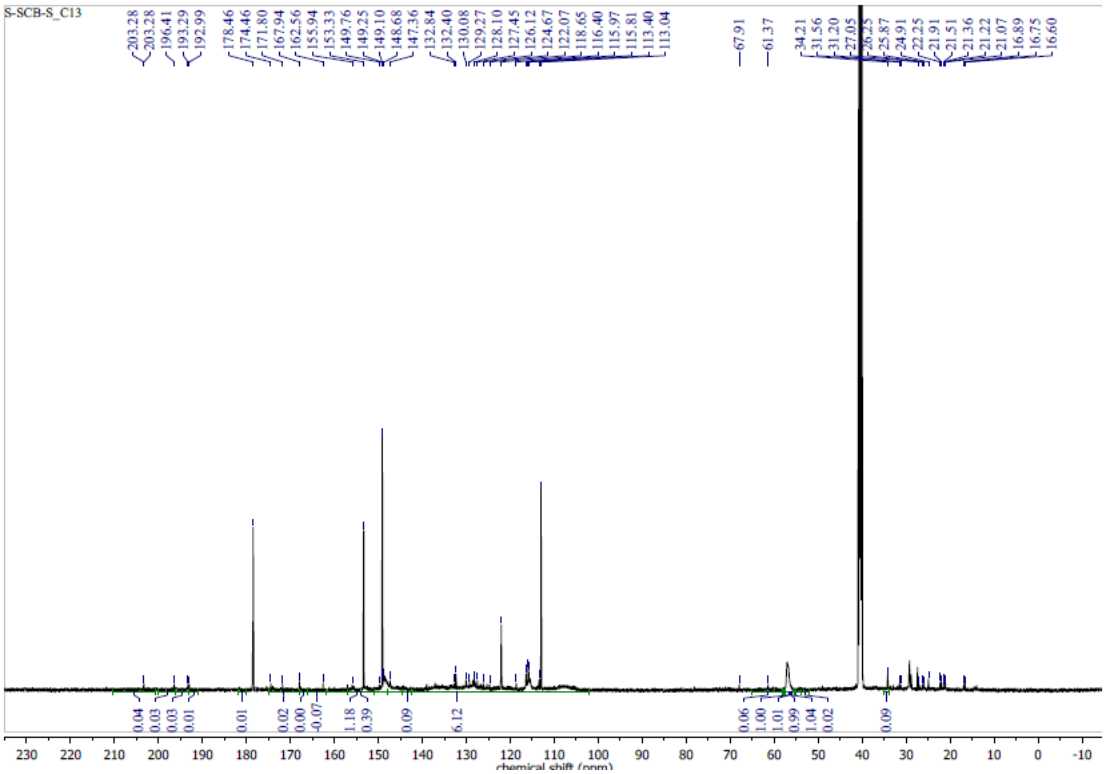

Figure A3: ^{13}C NMR Spectra of S-SCB-S lignin

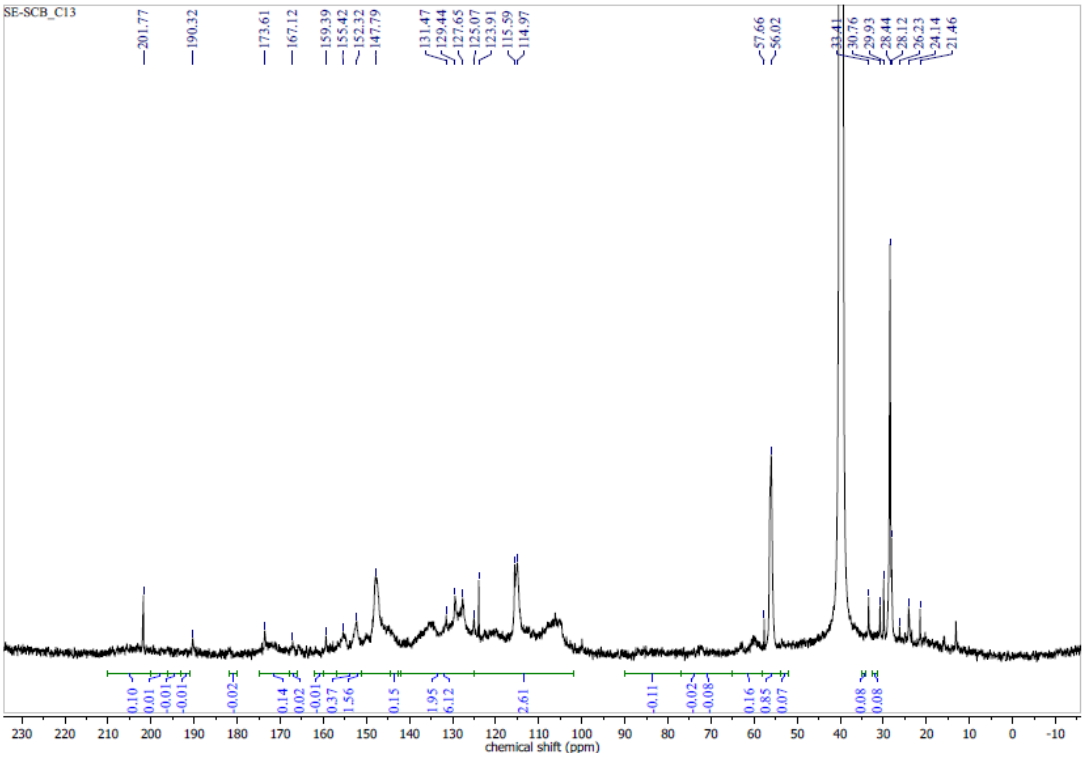

Figure A4: ^{13}C NMR Spectra of SE-SCB lignin

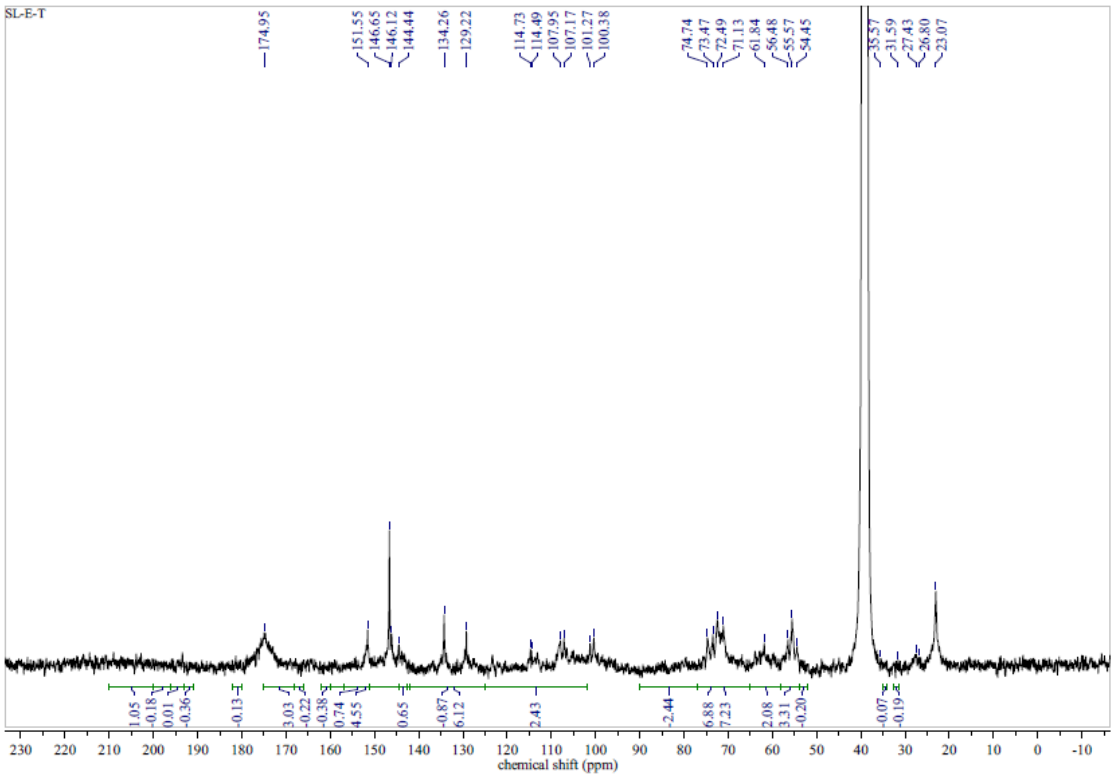

Figure A5: ^{13}C NMR Spectra of SL-E-T lignin